

**UNCLASSIFIED**

**AD 4 2 4 3 7 5**

**DEFENSE DOCUMENTATION CENTER**

**FOR**

**SCIENTIFIC AND TECHNICAL INFORMATION**

**CAMERON STATION, ALEXANDRIA, VIRGINIA**



**UNCLASSIFIED**

NOTICE: When government or other drawings, specifications or other data are used for any purpose other than in connection with a definitely related government procurement operation, the U. S. Government thereby incurs no responsibility, nor any obligation whatsoever; and the fact that the Government may have formulated, furnished, or in any way supplied the said drawings, specifications, or other data is not to be regarded by implication or otherwise as in any manner licensing the holder or any other person or corporation, or conveying any rights or permission to manufacture, use or sell any patented invention that may in any way be related thereto.

CATALOGED BY DDC 424375

ASD-TDR-63-597

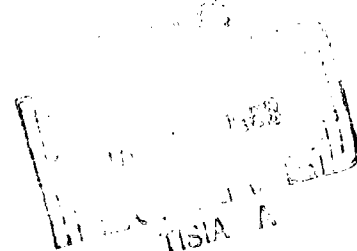
AS AD No. \_\_\_\_\_

# Thermal Properties of Refractory Alloys

TECHNICAL DOCUMENTARY REPORT NO. ASD-TDR-63-597  
June 1963

AF Materials Laboratory  
Aeronautical Systems Division  
Air Force Systems Command  
Wright-Patterson Air Force Base, Ohio

Project No. 7360, Task No. 736004



(Prepared under Contract No. AF 33(657)-8810 by the IIT Research  
Institute, Chicago, Illinois, J. C. Hedge, C. Kostenko, and  
J. I. Lang, Authors)

## NOTICES

When Government drawings, specifications, or other data are used for any purpose other than in connection with a definitely related Government procurement operation, the United States Government thereby incurs no responsibility nor any obligation whatsoever; and the fact that the Government may have formulated, furnished, or in any way supplied the said drawings, specifications, or other data, is not to be regarded by implication or otherwise as in any manner licensing the holder or any other person or corporation, or conveying any rights or permission to manufacture, use, or sell any patented invention that may in any way be related thereto.

Qualified requesters may obtain copies of this report from the Armed Services Technical Information Agency, (ASTIA), Arlington Hall Station, Arlington 12, Virginia.

This report has been released to the Office of Technical Services, U.S. Department of Commerce, Washington 25, D.C., in stock quantities for sale to the general public.

Copies of this report should not be returned to the Aeronautical Systems Division unless return is required by security considerations, contractual obligations, or notice on a specific document.

## FOREWORD

This report was prepared by the Heat and Mass Transfer Section of the Physics Division of the IIT Research Institute (formerly Armour Research Foundation) under USAF Contract No. AF 33(657)-8810. The contract was initiated under Project No. 7360, "The Chemistry and Physics of Materials", Task No. 736004, "Physical Properties of Materials". The work was administered under the direction of the AF Materials Laboratory, Aeronautical Systems Division, Wright-Patterson Air Force Base, Ohio, with Mr. Hyman Marcus as project engineer.

This report covers work conducted from May 1, 1962 to May 31, 1963. Contributions to this project were made by J. C. Hedge, J. W. Kopec, C. Kostenko and J. I. Lang.

## ABSTRACT

The objective of this program was the determination of the thermal properties of fifteen selected refractory materials. The materials investigated were boron carbide, zirconium nitride, spinel, beryllium oxide, six columbium alloys, three tantalum alloys, and two molybdenum alloys. The thermal conductivity, specific heat, and linear thermal expansion were measured from room temperature to the melting point, or 5000°F, whichever was lower.

This technical documentary report has been reviewed and is approved.



ROBERT E. BROCKLEHURST  
Assistant Director  
Materials Physics Division  
AF Materials Laboratory

# TABLE OF CONTENTS

	<u>Page</u>
I. INTRODUCTION	1
II. LINEAR THERMAL EXPANSION	4
A. Description of Equipment	4
B. Experimental Procedure	4
C. Test Results	8
D. Experimental Accuracy	8
III. SPECIFIC HEAT	39
A. Description of Equipment	39
B. Experimental Procedure	42
C. Test Results	43
D. Experimental Accuracy	74
IV. THERMAL CONDUCTIVITY	82
A. Thermal Conductivity - Room Temperature to 1500°F	82
1. Description of Equipment	82
2. Experimental Procedure	82
3. Test Results	85
4. Experimental Accuracy	85
B. Thermal Diffusivity	85
1. Introduction	85
2. Discussion of the Mathematical Formulation	86
a. Statement of Problem	86
b. Mathematical Formulation	86
3. Description of Apparatus	88
a. Description of Furnace	88
b. Description of Instrumentation	94
4. Measurement Technique	95
5. Calculation of Thermal Diffusivity	96

# LIST OF ILLUSTRATIONS

Figure		Page
1	Apparatus for Measuring Linear Thermal Expansion to 3000°F . . . . .	5
2	Linear Thermal Expansion Apparatus for Use to 3000°F . .	6
3	Linear Thermal Expansion Apparatus for Use From 3000 to 5000°F . . . . .	7
4	Linear Thermal Expansion of Boron Carbide . . . . .	24
5	Linear Thermal Expansion of Spinel . . . . .	25
6	Linear Thermal Expansion of Zirconium Nitride . . . . .	26
7	Linear Thermal Expansion of Beryllium Oxide . . . . .	27
8	Linear Thermal Expansion of Cb-10W-1Zr-0.1C Alloy. . .	28
9	Linear Thermal Expansion of Cb-5Mo-5V-1Zr Alloy. . . .	29
10	Linear Thermal Expansion of Cb-10W-5Zr Alloy. . . . .	30
11	Linear Thermal Expansion of Cb-10Ti-5Zr Alloy. . . . .	31
12	Linear Thermal Expansion of Cb-15W-5Mo-1Zr-0.05C Alloy . . . . .	32
13	Linear Thermal Expansion of Cb-27Ta-12W-0.5Zr Alloy. .	33
14	Linear Thermal Expansion of Mo-0.5Ti-0.08Zr Alloy . . .	34
15	Linear Thermal Expansion of Mo-29.83W-0.07Zr-0.012C Alloy . . . . .	35
16	Linear Thermal Expansion of Ta-10W Alloy . . . . .	36
17	Linear Thermal Expansion of Ta-8W-2Hf Alloy. . . . .	37
18	Linear Thermal Expansion of Ta-30Cb-7.5V Alloy. . . . .	38
19	Schematic Diagram of Apparatus for Measuring Specific Heat. . . . .	40
20	Parr Calorimeter for Heat Capacity Measurements . . . .	41
21	Enthalpy of Boron Carbide. . . . .	59
22	Enthalpy of Spinel . . . . .	60

# LIST OF ILLUSTRATIONS (Continued)

Figure		Page
23	Enthalpy of Zirconium Nitride . . . . .	61
24	Enthalpy of Beryllium Oxide . . . . .	62
25	Enthalpy of Cb-10W-1Zr-0.1C Alloy . . . . .	63
26	Enthalpy of Cb-5Mo-5V-1Zr Alloy . . . . .	64
27	Enthalpy of Cb-10W-5Zr Alloy . . . . .	65
28	Enthalpy of Cb-10Ti-5Zr Alloy . . . . .	66
29	Enthalpy of Cb-15W-5Mo-1Zr-0.05C Alloy . . . . .	67
30	Enthalpy of Cb-27Ta-12W-0.5Zr Alloy . . . . .	68
31	Enthalpy of Mo-0.5Ti-0.08Zr Alloy . . . . .	69
32	Enthalpy of Mo-29.83W-0.07Zr-0.012C Alloy . . . . .	70
33	Enthalpy of Ta-10W Alloy . . . . .	71
34	Enthalpy of Ta-8W-2Hf Alloy . . . . .	72
35	Enthalpy of Ta-30Cb-7.5V Alloy . . . . .	73
36	Specific Heat of Four Ceramic Materials . . . . .	78
37	Specific Heat of Six Columbium Alloys . . . . .	79
38	Specific Heat of Two Molybdenum Alloys . . . . .	80
39	Specific Heat of Three Tantalum Alloys . . . . .	81
40	Apparatus for Measuring Thermal Conductivity . . . . .	83
41	Cutaway View of Diffusivity Furnace . . . . .	89
42	View of Heat Sink Mount . . . . .	90
43	View of Optical Mount . . . . .	91
44	View of Instrumentation System . . . . .	92
45	Typical Temperature-Time Trace . . . . .	95

# LIST OF ILLUSTRATIONS (Continued)

Figure		Page
46	Thermal Conductivity of Boron Carbide . . . . .	113
47	Thermal Conductivity of Spinel ( $\text{MgO-Al}_2\text{O}_3$ ) . . . . .	114
48	Thermal Conductivity of Zirconium Nitride . . . . .	115
49	Thermal Conductivity of Beryllium Oxide . . . . .	116
50	Thermal Conductivity of Cb-10W-1Zr-0.1C Alloy . . . . .	117
51	Thermal Conductivity of Cb-5Mo-5V-1Zr Alloy . . . . .	118
52	Thermal Conductivity of Cb-10W-5Zr Alloy . . . . .	119
53	Thermal Conductivity of Cb-10Ti-5Zr Alloy . . . . .	120
54	Thermal Conductivity of Cb-15W-5Mo-1Zr-0.05C Alloy . .	121
55	Thermal Conductivity of Cb-27Ta-12W-0.5Zr Alloy. . . . .	122
56	Thermal Conductivity of Mo-0.5Ti-0.08Zr Alloy . . . . .	123
57	Thermal Conductivity of Mo-29.83W-0.07Zr-0.012C Alloy. . . . .	124
58	Thermal Conductivity of Ta-10W Alloy . . . . .	125
59	Thermal Conductivity of Ta-8W-2Hf Alloy. . . . .	126
60	Thermal Conductivity of Ta-30Cb-7.5V Alloy . . . . .	127

# LIST OF TABLES

Table		Page
1	Chemical Analysis of Refractory Metal Alloys . . . . .	2
2	Chemical Analysis of Ceramic Materials . . . . .	3
3	Linear Thermal Expansion of Boron Carbide . . . . .	9
4	Linear Thermal Expansion of Spinel . . . . .	10
5	Linear Thermal Expansion of Zirconium Nitride . . . . .	11
6	Linear Thermal Expansion of Beryllium Oxide . . . . .	12
7	Linear Thermal Expansion of Cb-10W-1Zr-0.01C Alloy .	13
8	Linear Thermal Expansion of Cb-5Mo-5V-1Zr Alloy . . .	14
9	Linear Thermal Expansion of Cb-10W-5Zr Alloy . . . . .	15
10	Linear Thermal Expansion of Cb-10Ti-5Zr Alloy . . . . .	16
11	Linear Thermal Expansion of Cb-15W-5Mo-1Zr-0.05C Alloy. . . . .	17
12	Linear Thermal Expansion of Cb-27Ta-12W-0.5Zr Alloy.	18
13	Linear Thermal Expansion of Mo-0.5Ti-0.08Zr Alloy . .	19
14	Linear Thermal Expansion of Mo-29.83W-0.07Zr-0.012C Alloy. . . . .	20
15	Linear Thermal Expansion of Ta-10W Alloy. . . . .	21
16	Linear Thermal Expansion of Ta-8W-2Hf Alloy . . . . .	22
17	Linear Thermal Expansion of Ta-30Cb-7.5V Alloy . . . . .	23
18	Enthalpy Values for Boron Carbide. . . . .	44
19	Enthalpy Values for Spinel . . . . .	45
20	Enthalpy Values for Zirconium Nitride. . . . .	46
21	Enthalpy Values for Beryllium Oxide. . . . .	47
22	Enthalpy Values for Cb-10W-1Zr-0.1C Alloy . . . . .	48
23	Enthalpy Values for Cb-5Mo-5V-1Zr Alloy . . . . .	49

# LIST OF TABLES (Continued)

Table		Page
24	Enthalpy Values for Cb-10W-5Zr Alloy . . . . .	50
25	Enthalpy Values for Cb-10Ti-5Zr Alloy. . . . .	51
26	Enthalpy Values for Cb-15W-5Mo-1Zr-0.05C Alloy . . . .	52
27	Enthalpy Values for Cb-27Ta-12W-0.5Zr Alloy . . . . .	53
28	Enthalpy Values for Mo-0.5Ti-0.08Zr Alloy . . . . .	54
29	Enthalpy Values for Mo-29.83W-0.07Zr-0.012C Alloy. . .	55
30	Enthalpy Values for Ta-10W Alloy . . . . .	56
31	Enthalpy Values for Ta-8W-2Hf Alloy. . . . .	57
32	Enthalpy Values for Ta-30Cb-7.5V Alloy . . . . .	58
33	Enthalpy Coefficients. . . . .	75
34	Specific Heat Coefficients . . . . .	76
35	Enthalpy of Synthetic Sapphire. . . . .	77
36	Thermal Conductivity of Boron Carbide. . . . .	98
37	Thermal Conductivity of Spinel ( $\text{MgO-Al}_2\text{O}_3$ ) . . . . .	99
38	Thermal Conductivity of Zirconium Nitride. . . . .	100
39	Thermal Conductivity of Beryllium Oxide. . . . .	101
40	Thermal Conductivity of Cb-10W-1Zr-0.1C Alloy . . . . .	102
41	Thermal Conductivity of Cb-5Mo-5V-1Zr Alloy. . . . .	103
42	Thermal Conductivity of Cb-10W-5Zr Alloy. . . . .	104
43	Thermal Conductivity of Cb-10Ti-5Zr Alloy . . . . .	105
44	Thermal Conductivity of Cb-15W-5Mo-1Zr-0.05C Alloy . .	106
45	Thermal Conductivity of Cb-27Ta-12W-0.5Zr Alloy . . . .	107

# LIST OF TABLES (Continued)

Table		Page
46	Thermal Conductivity of Mo-0.5Ti-0.08Zr Alloy . . . . .	108
47	Thermal Conductivity of Mo-29.83W-0.07Zr-0.012C Alloy. . . . .	109
48	Thermal Conductivity of Ta-10W Alloy. . . . .	110
49	Thermal Conductivity of Ta-8W-2Hf Alloy. . . . .	111
50	Thermal Conductivity of Ta-30Cb-7.5V Alloy . . . . .	112

## I. INTRODUCTION

This report describes the experimental determination of the thermal conductivity, specific heat, and linear thermal expansion of fifteen materials from room temperature to their melting point, or a maximum temperature of 5000°F. The program was initiated by the AF Materials Laboratory, Aeronautical Systems Division, Wright-Patterson Air Force Base, Ohio, beginning May 1, 1962.

The fifteen materials, together with the name of the supplier are:

- |  |   |
|--|---|
| 1. Boron Carbide                                   | - Carborundum Co.   |
| 2. Spinel ( $\text{MgO} : \text{Al}_2\text{O}_3$ ) | - Laboratory Equipment Corp.  |
| 3. Zirconium Nitride                               | - Norton Co.  |
| 4. Beryllium Oxide                                 | - Brush Beryllium Co.   |
| 5. Cb-10W-1Zr-0.1C Alloy                           | - Du Pont   |
| 6. Cb-5Mo-5V-1Zr Alloy                             | - Westinghouse Electric Corp.   |
| 7. Cb-10W-5Zr Alloy                                | - Haynes Stellite Co.   |
| 8. Cb-10Ti-5Zr Alloy                               | - Du Pont   |
| 9. Cb-15W-5Mo-1Zr-0.05C Alloy                      | - General Electric Co., Du Pont<br>(thermal conductivity sample only) |
| 10. Cb-27Ta-12W-0.5Zr Alloy                        | - Fansteel Metallurgical Corp.  |
| 11. Mo-0.5Ti-0.08Zr Alloy                          | - Climax Molybdenum   |
| 12. Mo-29.83W-0.07Zr-0.012C Alloy                  | - Climax Molybdenum   |
| 13. Ta-10W Alloy                                   | - Fansteel Metallurgical Corp.  |
| 14. Ta-8W-2Hf Alloy                                | - Westinghouse Electric Corp.   |
| 15. Ta-30Cb-7.5V Alloy                             | - Wah Chang Corp.   |

The chemical analysis of the materials is given in Table 1 and Table 2. The analysis of the as-received materials was determined by the supplier except for spinel, which was analyzed in the Analytical Laboratory of the IIT Research Institute.

Table 1  
CHEMICAL ANALYSIS OF REFRACTORY METAL ALLOYS

Material	Density lb/ft <sup>3</sup>	Cb %	W %	Mo %	Ta %	Zr %	V %	Hf %	Ti %	Fe %	Ni %	Si %	C %	O <sub>2</sub> ppm	H <sub>2</sub> ppm	N <sub>2</sub> ppm
1. Cb-10W-12r-0.1C A** B**	564		9.6 9.7			0.95 0.88							0.0510 0.0810	53 52	3 4	33 33
2. Cb-5Mo-5V-12r A B	538			5.03 5.03		1.13 1.13	5.02 5.02						0.0280 0.0280	93 93		136 136
3. Cb-10W-5Zr A B	572		9.88 9.93			2.80 2.58							0.002 0.002	80 120	11 9	40 60
4. Cb-10Ti-5Zr A B	485					5.5 4.9			10.5 10.0				0.0071 0.0014	249 244	9 14	27 24
5. Cb-15W-5Mo-12r-0.05C A B	599		15.6 15.3	4.7 5.26	.01	0.84 1.08							0.0489 0.0340	163 167	5 61	20 11
6. Cb-27Ta-12W-0.5Zr A B	669		10.40 10.40		27.84 27.84	0.92 0.92			0.005 0.005	0.007 0.007	0.009 0.009	0.01 0.01	0.0040 0.0040	50 50		20 20
7. Mo-0.5Ti-0.08Zr A B	622					0.07 0.07			0.49 0.50	<0.001 <0.002	<0.001 <0.001	<0.005 <0.005	0.0260 0.0290	7 5	1 1	1 3
8. Mo-29.83W-0.072r-0.012C A B	620		29.83 29.83			.07 .07							0.0120 0.0120			
9. Ta-10W A B	1035	0.10 0.087	9.40 9.50	0.01 0.015					0.02 0.02	0.005 0.005	0.01 0.01	0.02 0.02	0.0040 0.0010	90 50		30 30
10. Ta-8W-2Hf A B	1058		9.0 9.0					2.2 2.2					0.0041 0.0041	40 40		13 13
11. Ta-30Cb-7.5V A B	721	30.3 30.3				7.47 7.47							0.090 0.090	150 150		65 65

\*Thermal conductivity sample

\*\*Specific heat and thermal expansion sample

Table 2  
CHEMICAL ANALYSIS OF CERAMIC MATERIALS

Material	Boron Carbide	Zirconium Nitride	Spinel	Beryllium Oxide
Density lb/ft <sup>3</sup>	156	406	164	179
Forming Method	Hot pressed	Hot pressed	Cold pressed	Cold pressed
Firing Temperature °F	3940	3812	3300	2880
Composition	75.97% B 21.18% C 0.07% B <sub>2</sub> O <sub>7</sub> 0.27% Fe 0.40% Si 0.015% Al <sub>2</sub> O <sub>3</sub>	84.6% Zr 13.5% N 0.2% Fe 0.8% H 0.4% Si 0.5% Alkali Metal Oxides	68.26% Al <sub>2</sub> O <sub>3</sub> 26.74% MgO 3.17% Na <sub>2</sub> O 0.33% SiO <sub>2</sub> 0.26% Fe <sub>2</sub> O <sub>3</sub> 1.20% B	99.5% BeO 50 ppm Al 10 ppm Fe 20 ppm Mo - 10 ppm Ni 3 ppm Mn - 10 ppm Cr 10 ppm Ca 90 ppm Si 10 ppm Na 1 or less B, Cd, Li 1 or less Co, Cu

## II. LINEAR THERMAL EXPANSION

### A. Description of Equipment

The linear thermal expansion was determined by measuring the change in length of a rod of the sample material with a telemicroscope as the specimen was heated.

The linear thermal expansion was determined in two steps: first, over the temperature range from room temperature to 3000°F, and second, from 3000°F to the melting point.

A schematic view of the experimental apparatus used in the temperature range from room temperature to 3000°F is shown in Figure 1. The furnace was electrically heated by a molybdenum wire-wound resistor mounted on an alumina tube. The heater is housed inside a water-cooled steel shell and the space between the heater and outside shell is filled with bubbled alumina insulation. Two sight ports are located on each side of the furnace directly opposite each other. Ceramic tubes extend from the sight port to the interior of the furnace, thus providing a means to directly view the test sample from outside the furnace. The test specimen is placed in the center of the furnace in a molybdenum container which supports the sample and helps to protect it from any oxygen which might remain in the furnace. The molybdenum container has sight holes in it which line up with the ceramic tubes. Provision is made so that the molybdenum container and furnace can be continuously flushed with inert gas through independent lines.

The telemicroscope is positioned outside the furnace so that both ends of the test specimen can be seen. The test specimen temperature is measured by a platinum/platinum-10% rhodium thermocouple which is inserted in a hole drilled in one end of the specimen. A photograph of the equipment is shown in Figure 2.

At temperatures above 3000°F, the thermal expansion was measured in a furnace having a graphite heater. The furnace shell was water-cooled and graphite powder insulation filled the space between the protection tube surrounding the heater and the furnace shell. The test specimen was mounted inside a tantalum tube which was continuously flushed with argon to protect the specimen from oxidation and from graphite vapor. Holes were drilled in the tantalum tube to allow the ends of the test specimen to be viewed through water-cooled sight glasses on opposite sides of the furnace. The change in specimen length was measured by telemicroscopes mounted outside the furnace. The specimen temperature was measured with an optical pyrometer. A photograph of the apparatus is shown in Figure 3.

### B. Experimental Procedure

The following procedures were used in measuring the linear thermal expansion of the test specimens:

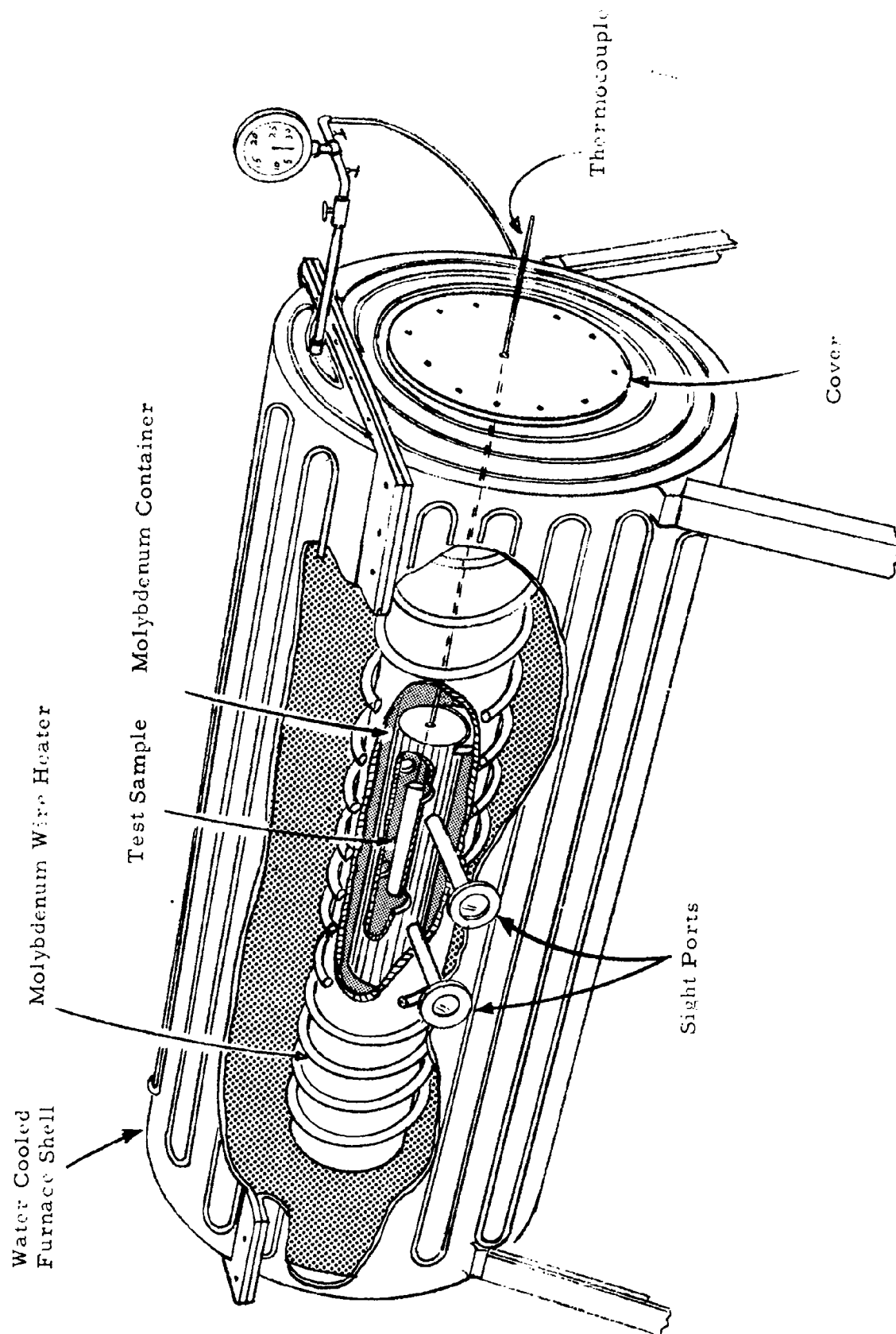
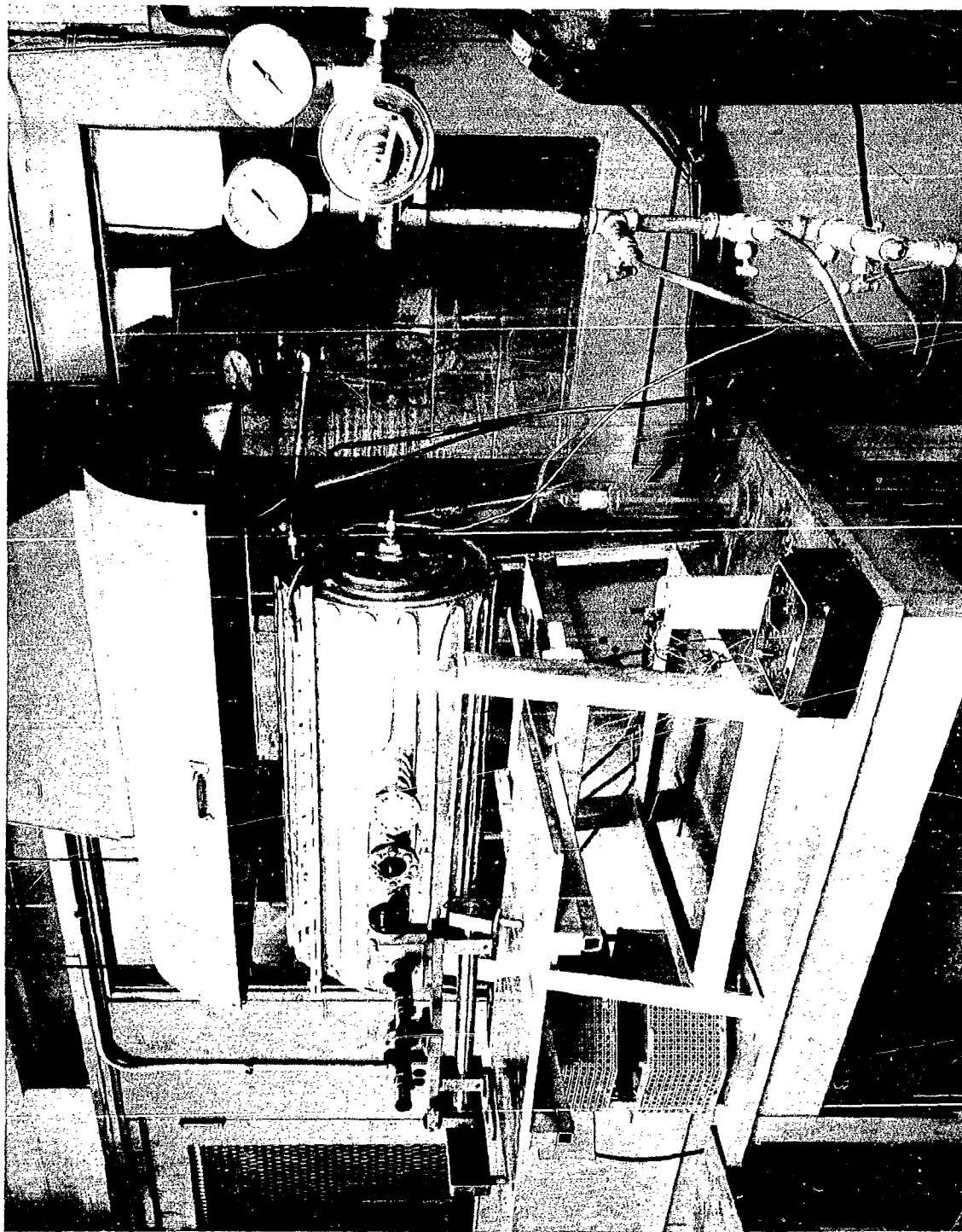


Fig. 1 APPARATUS FOR MEASURING LINEAR THERMAL EXPANSION TO 3000°F



**Fig. 2 LINEAR THERMAL EXPANSION APPARATUS FOR USE TO 3000°F**

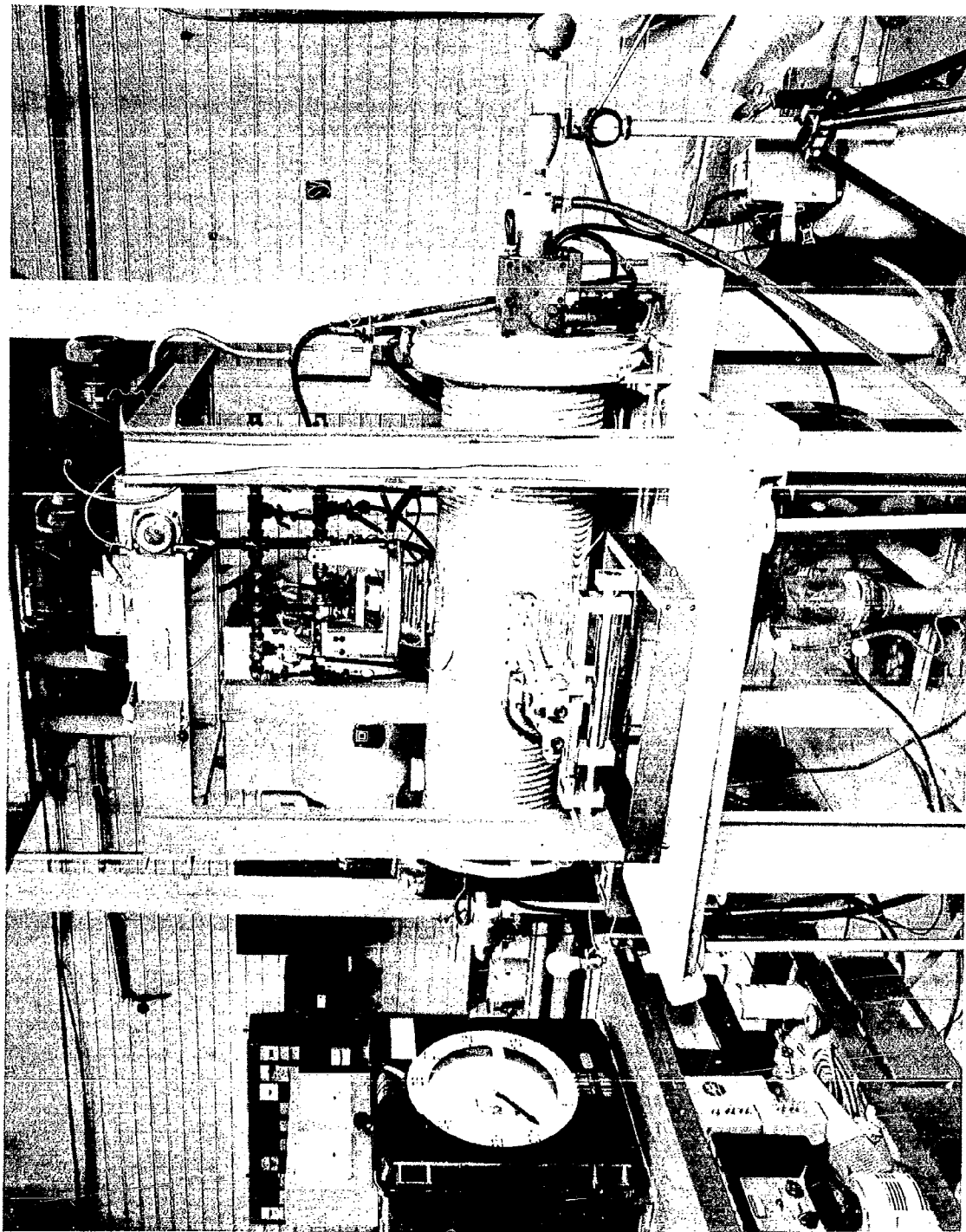


Fig. 3 LINEAR THERMAL EXPANSION APPARATUS FOR USE FROM 3000 TO 5000°F

Table 3

LINEAR THERMAL EXPANSION  
OF BORON CARBIDE

Temperature °F	Thermal Expansion $\Delta L/L$ , %
80	0.000
191	0.021
413	0.067
612	0.123
828	0.177
985	0.245
1112	0.304
1259	0.348
1451	0.412
1585	0.471
1763	0.547
2018	0.641
2182	0.688
2424	0.800
2540	0.849
2815	0.956
3227	1.124
3380	1.181
3614	1.292
3776	1.367
4082	1.499
4228	1.570

pg. 8

This Document Contains Missing  
Page/s That Are Unavailable In  
The Original Document

Table 4

LINEAR THERMAL EXPANSION  
OF SPINEL

Temperature °F	Thermal Expansion $\Delta L/L$ , %
80	0.000
222	0.040
606	0.213
729	0.277
916	0.374
1155	0.497
1365	0.618
1511	0.700
1648	0.772
1803	0.858
1949	0.972
2060	1.045
2181	1.135
2274	1.180
2606	1.400
2849	1.550
3011	1.662
3252	1.831

Table 5

LINEAR THERMAL EXPANSION  
OF ZIRCONIUM NITRIDE

Temperature °F	Thermal Expansion $\Delta L/L$ , %
80	0.000
287	0.044
502	0.156
604	0.222
674	0.262
890	0.373
1133	0.465
1614	0.700
1915	0.862
1983	0.891
2224	1.024
2512	1.192
3007	1.438
3344	1.623
3578	1.758
3938	1.945

Table 6

LINEAR THERMAL EXPANSION  
OF BERYLLIUM OXIDE

Temperature °F	Thermal Expansion $\Delta L/L$ , %
80	0.000
265	0.077
515	0.178
685	0.251
856	0.321
1114	0.458
1384	0.613
1674	0.791
1794	0.872
2026	1.043
2142	1.134
2275	1.234
2456	1.340
2620	1.458
2804	1.611
3091	1.763
3400	1.992
3560	2.088

Table 7

LINEAR THERMAL EXPANSION  
OF Cb-10W-1Zr-0.1C ALLOY

Temperature °F	Thermal Expansion $\Delta L/L$ , %
80	0.000
168	0.024
319	0.090
517	0.168
683	0.269
900	0.345
1084	0.407
1247	0.505
1362	0.557
1554	0.648
1762	0.738
1914	0.840
2079	0.925
2236	0.987
2302	1.020
2382	1.062
2505	1.120
2622	1.201
2804	1.329
3119	1.492
3389	1.640
3596	1.767
3812	1.903
4028	2.075
4145	2.191

Table 8

LINEAR THERMAL EXPANSION  
OF Cb-5Mo-5V-1Zr ALLOY

Temperature °F	Thermal Expansion $\Delta L/L$ , %
80	0.000
316	0.097
618	0.215
800	0.315
1063	0.421
1236	0.525
1484	0.633
1711	0.739
2004	0.897
2195	1.010
2384	1.125
2560	1.218
2695	1.280
2957	1.470
3155	1.550
3434	1.721
3668	1.891
3848	2.000
4037	2.132
4195	2.241

Table 9

LINEAR THERMAL EXPANSION  
OF Cb-10W-5Zr ALLOY

Temperature °F	Thermal Expansion $\Delta L/L$ , %
80	0.000
294	0.092
499	0.167
650	0.216
809	0.301
1007	0.363
1265	0.483
1528	0.570
1695	0.682
1868	0.752
1999	0.801
2252	0.960
2444	1.039
2679	1.171
2831	1.294
3128	1.453
3407	1.611
3614	1.733
3794	1.815
3992	1.973
4160	2.080

Table 10

LINEAR THERMAL EXPANSION  
OF Cb-10Ti-5Zr ALLOY

Temperature °F	Thermal Expansion $\Delta L/L$ , %
80	0.000
289	0.088
460	0.151
628	0.209
784	0.279
1056	0.379
1265	0.474
1400	0.545
1650	0.660
1833	0.759
1998	0.862
2161	0.953
2357	1.060
2569	1.200
2681	1.278
2750	1.322
3047	1.480
3380	1.732
3605	1.856
3870	1.988
4180	2.175

Table 11

LINEAR THERMAL EXPANSION  
OF Cb-15W-5Mo-1Zr-0.05C ALLOY

Temperature °F	Thermal Expansion $\Delta L/L$ , %
80	0.000
328	0.112
581	0.215
802	0.297
1087	0.415
1174	0.448
1376	0.537
1568	0.625
1715	0.704
1980	0.850
2210	0.985
2386	1.063
2510	1.125
2703	1.241
2858	1.325
3092	1.470
3371	1.641
3587	1.765
3758	1.907
3983	2.057
4118	2.149

Table 12

LINEAR THERMAL EXPANSION  
OF Cb-27Ta-12W-0.5Zr ALLOY

Temperature °F	Thermal Expansion $\Delta L/L$ , %
80	0.000
206	0.042
413	0.122
606	0.187
802	0.284
1134	0.418
1400	0.558
1612	0.637
1820	0.753
2048	0.870
2194	0.935
2413	1.075
2552	1.137
2741	1.224
2812	1.305
3213	1.464
3524	1.669
3866	1.862
4078	1.931
4260	2.045
4485	2.200

Table 13

LINEAR THERMAL EXPANSION  
OF Mo-0.5Ti-0.08Zr ALLOY

Temperature °F	Thermal Expansion $\Delta L/L$ , %
80	0.000
222	0.043
326	0.074
538	0.129
736	0.189
903	0.240
1008	0.282
1093	0.304
1241	0.371
1459	0.451
1633	0.521
1773	0.580
1967	0.662
2137	0.727
2400	0.841
2589	0.928
2713	0.963
2801	1.032
2974	1.131
3312	1.272
3652	1.455
4024	1.690
4305	1.892
4489	2.041

Table 14

LINEAR THERMAL EXPANSION  
OF Mo-29.83W-0.07Zr-0.012C ALLOY

Temperature °F	Thermal Expansion $\Delta L/L$ , %
80	0.000
272	0.041
510	0.112
735	0.180
968	0.245
1210	0.320
1475	0.408
1742	0.492
2070	0.618
2322	0.723
2764	0.905
2975	1.001
3389	1.204
3740	1.400
3992	1.534
4320	1.728
4663	1.952
4892	2.120

Table 15

LINEAR THERMAL EXPANSION  
OF Ta-10W ALLOY

Temperature °F	Thermal Expansion $\Delta L/L$ , %
80	0.000
349	0.085
586	0.162
882	0.258
1155	0.354
1420	0.478
1685	0.585
1966	0.723
2190	0.832
2354	0.895
2664	
2903	1.168
3173	1.303
3497	1.472
3794	1.600
4091	1.754
4253	1.862
4510	2.017
4788	2.158
4905	2.240

Table 16

LINEAR THERMAL EXPANSION  
OF Ta-8W-2Hf ALLOY

Temperature °F	Thermal Expansion $\Delta L/L$ , %
80	0.000
160	0.028
365	0.103
656	0.208
959	0.320
1216	0.437
1463	0.503
1670	0.612
1955	0.760
2054	0.808
2107	0.818
2282	0.908
2394	0.970
2484	0.988
2584	1.002
2855	1.147
3175	1.305
3472	1.455
3710	1.600
4003	1.800
4291	1.983
4580	2.134
4892	2.365

Table 17

LINEAR THERMAL EXPANSION  
OF Ta-30Cb-7.5V ALLOY

Temperature °F	Thermal Expansion $\Delta L/L$ , %
80	0.000
240	0.047
583	0.195
725	0.244
1067	0.402
1244	0.492
1449	0.564
1760	0.720
1922	0.798
2212	0.962
2580	1.163
2876	1.320
3028	1.408
3204	1.521
3458	1.665
3710	1.820
3938	2.011

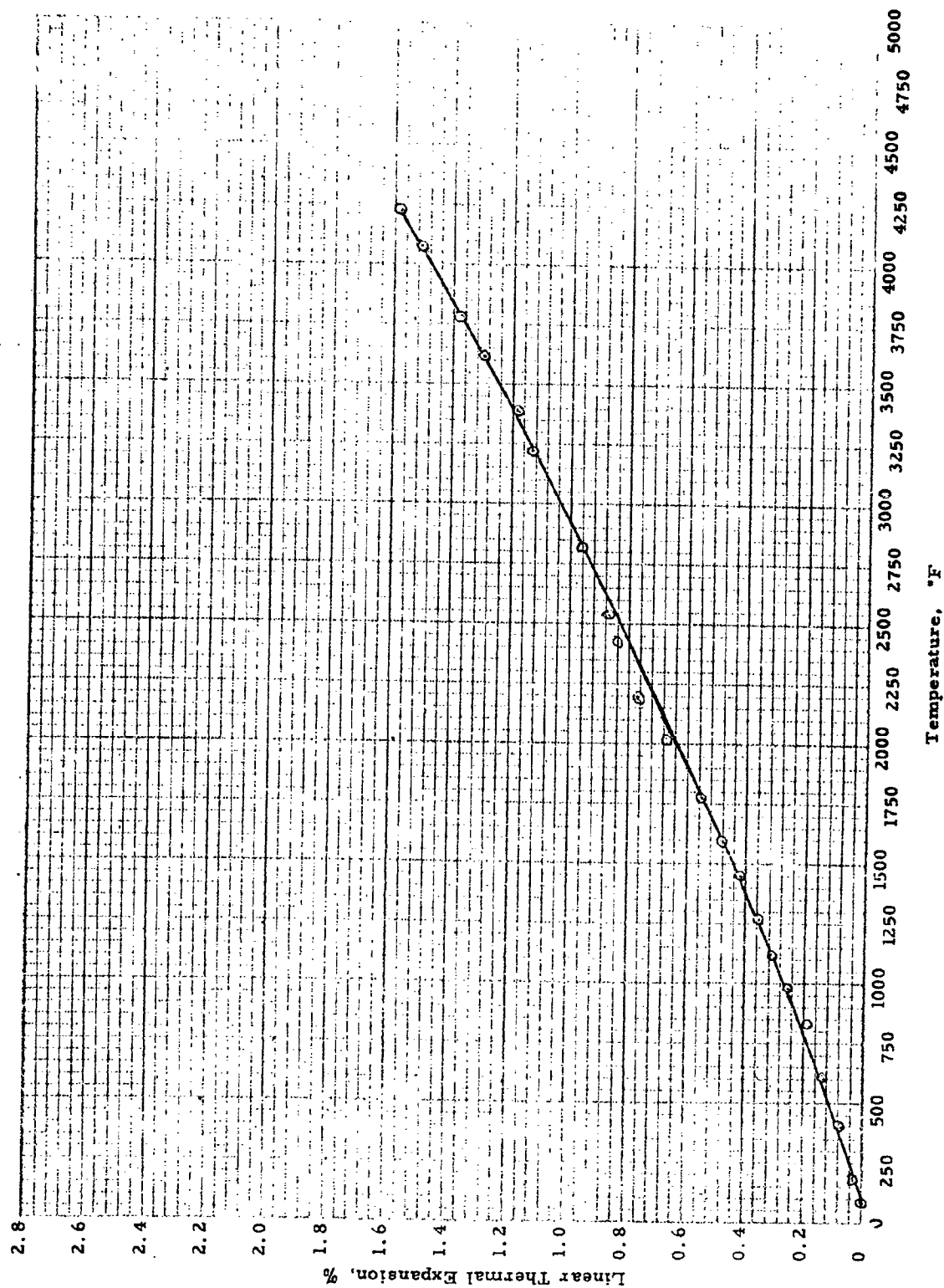


Fig. 4 LINEAR THERMAL EXPANSION OF BORON CARBIDE

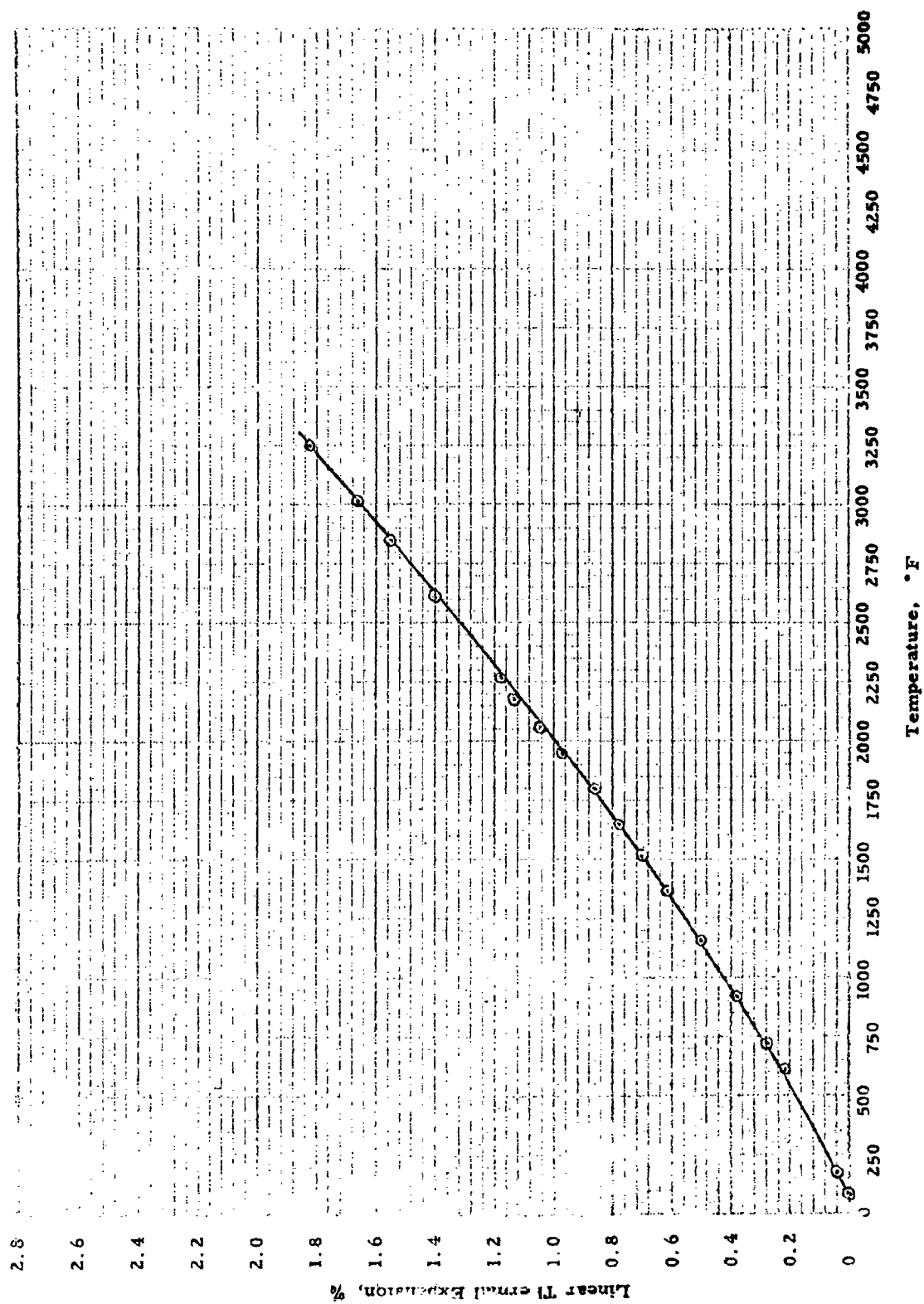


Fig. 5 LINEAR THERMAL EXPANSION OF SPINEL

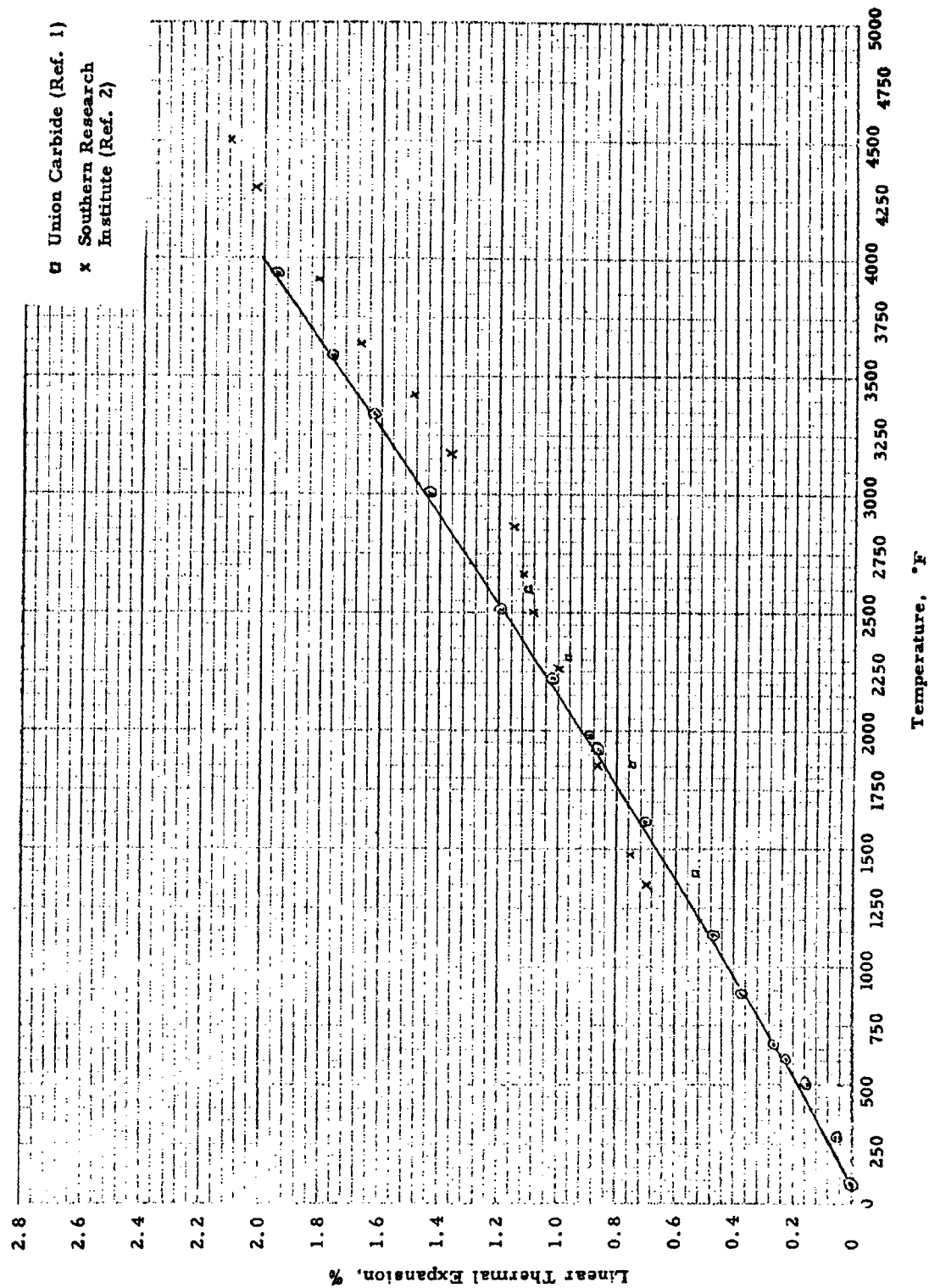


Fig. 6 LINEAR THERMAL EXPANSION OF ZIRCONIUM NITRIDE

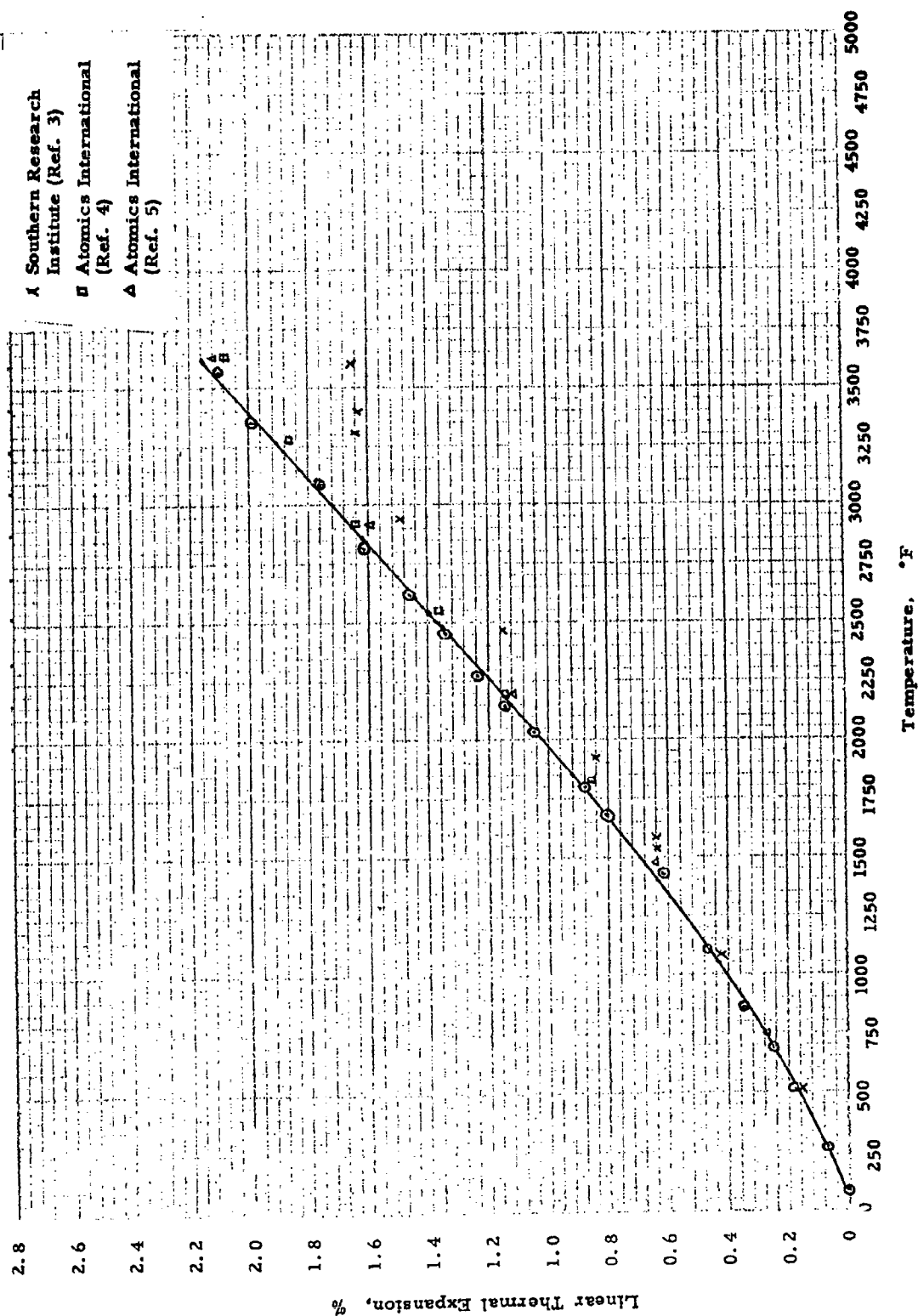


Fig. 7 LINEAR THERMAL EXPANSION OF BERYLLIUM OXIDE

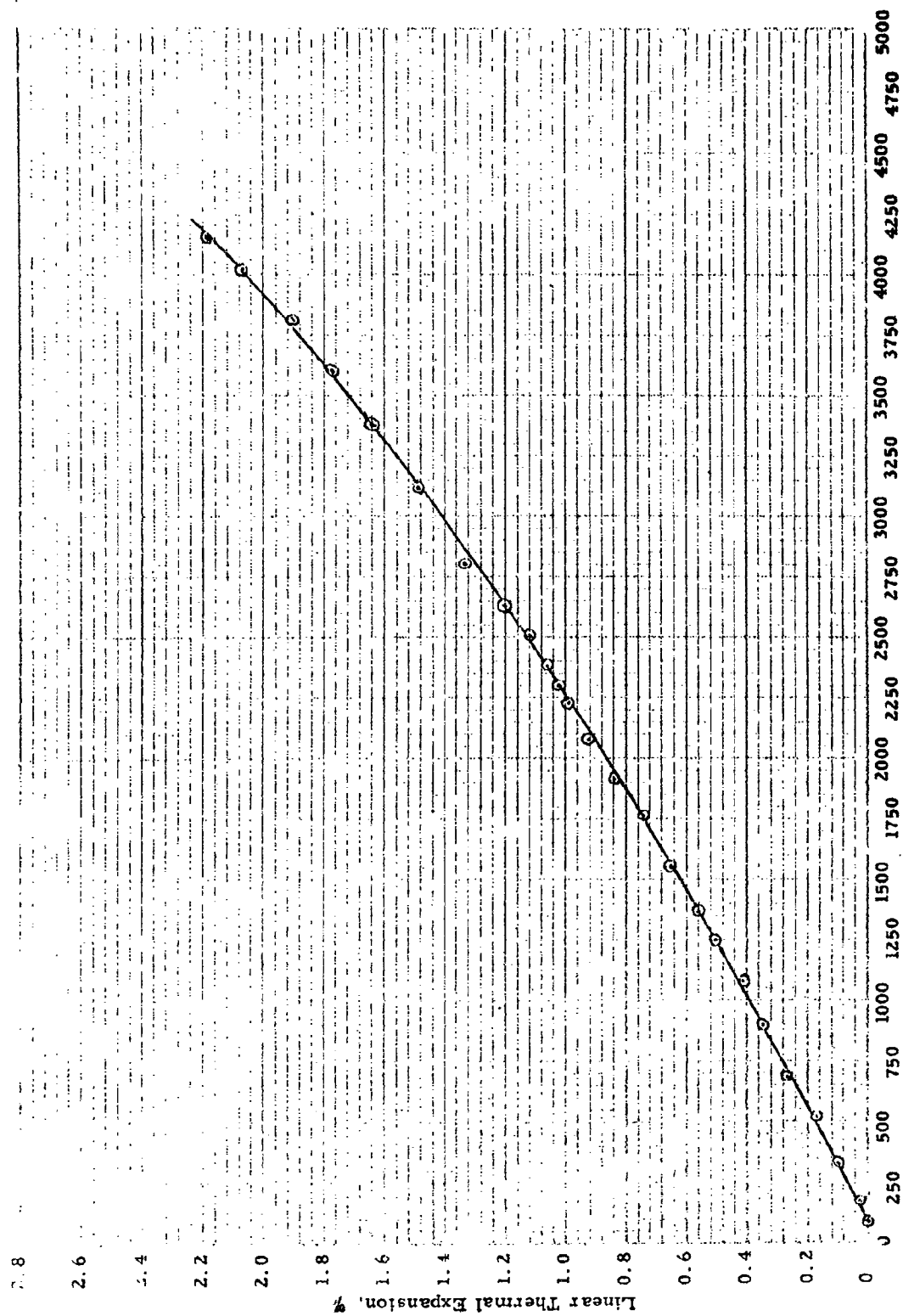


Fig. 8 LINEAR THERMAL EXPANSION OF Cb-10W-1Zr-0.1C ALLOY

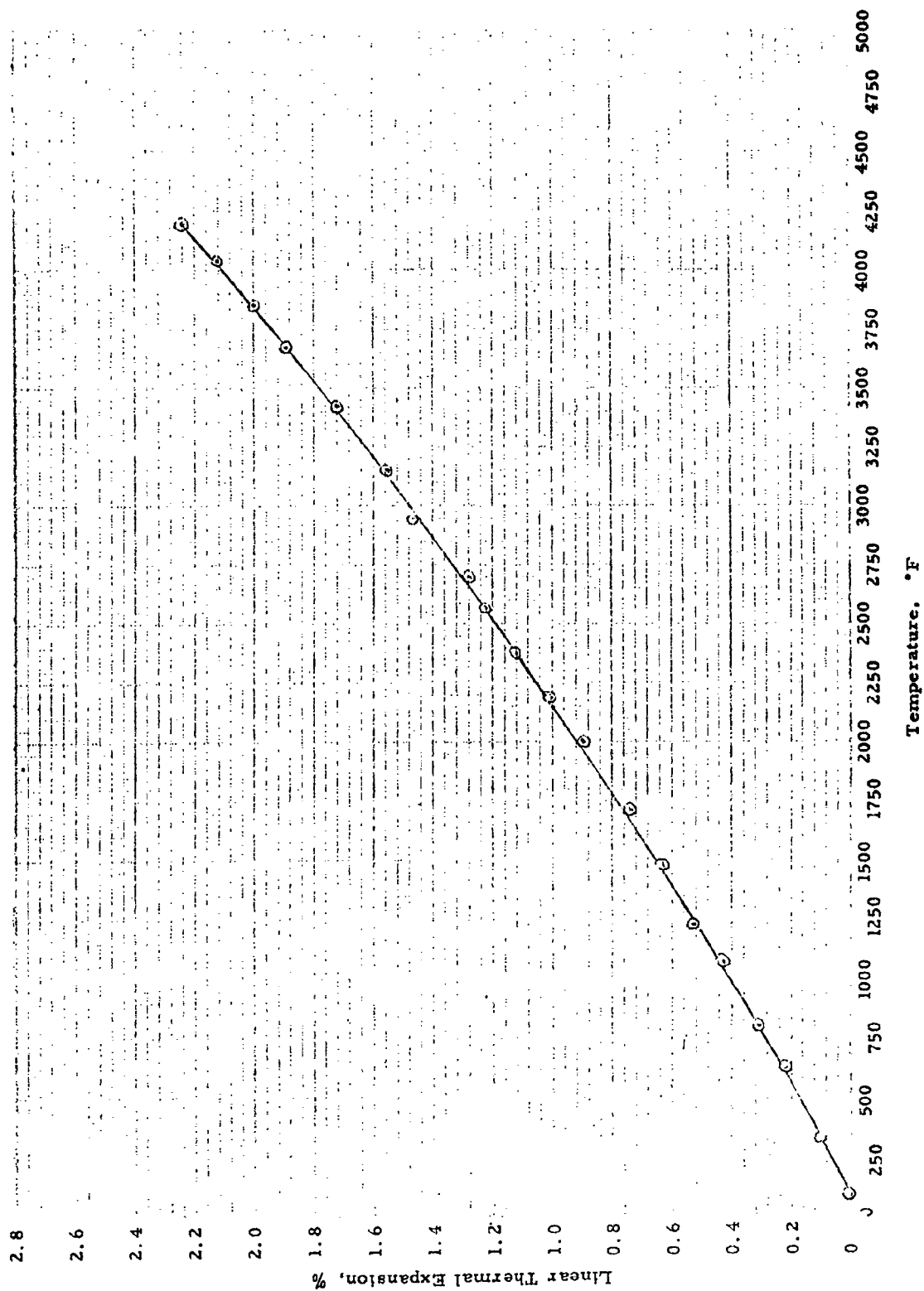


Fig. 9 LINEAR THERMAL EXPANSION OF Cb-5Mo-5V-1Zr ALLOY

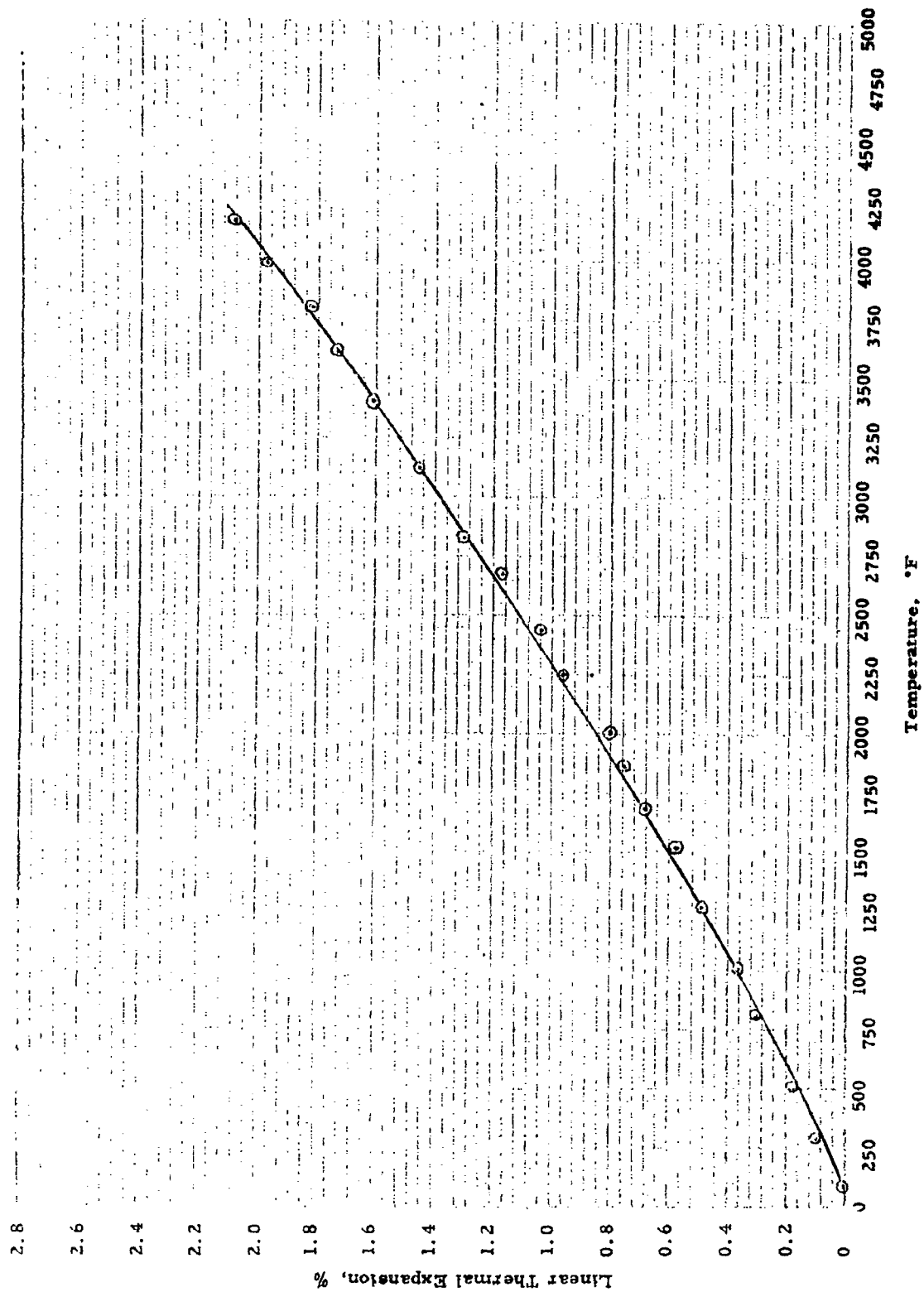


Fig. 10 LINEAR THERMAL EXPANSION OF Cb-10W-5Zr ALLOY

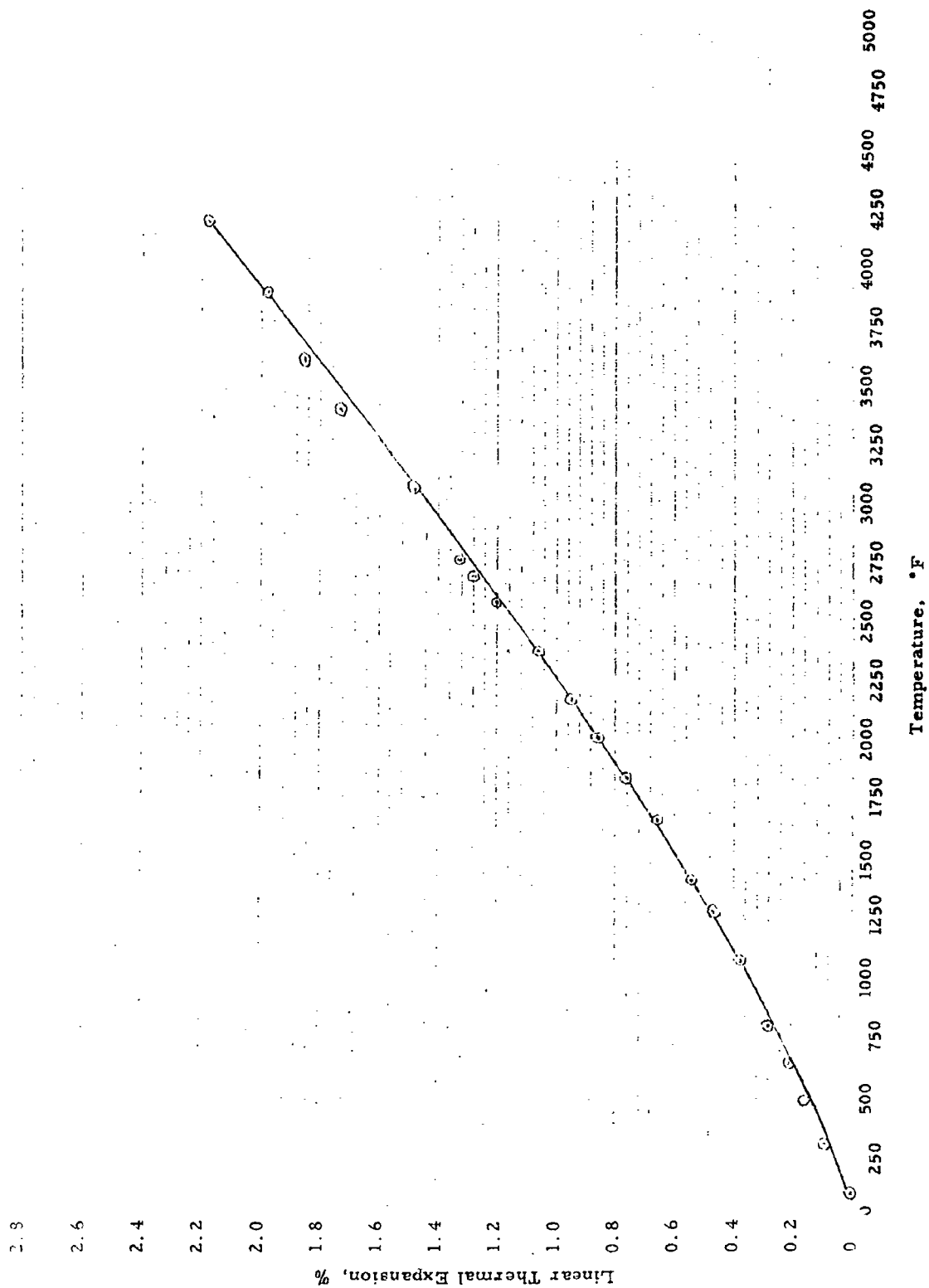


Fig. 11 LINEAR THERMAL EXPANSION OF Cb-10Ti-5Zr ALLOY

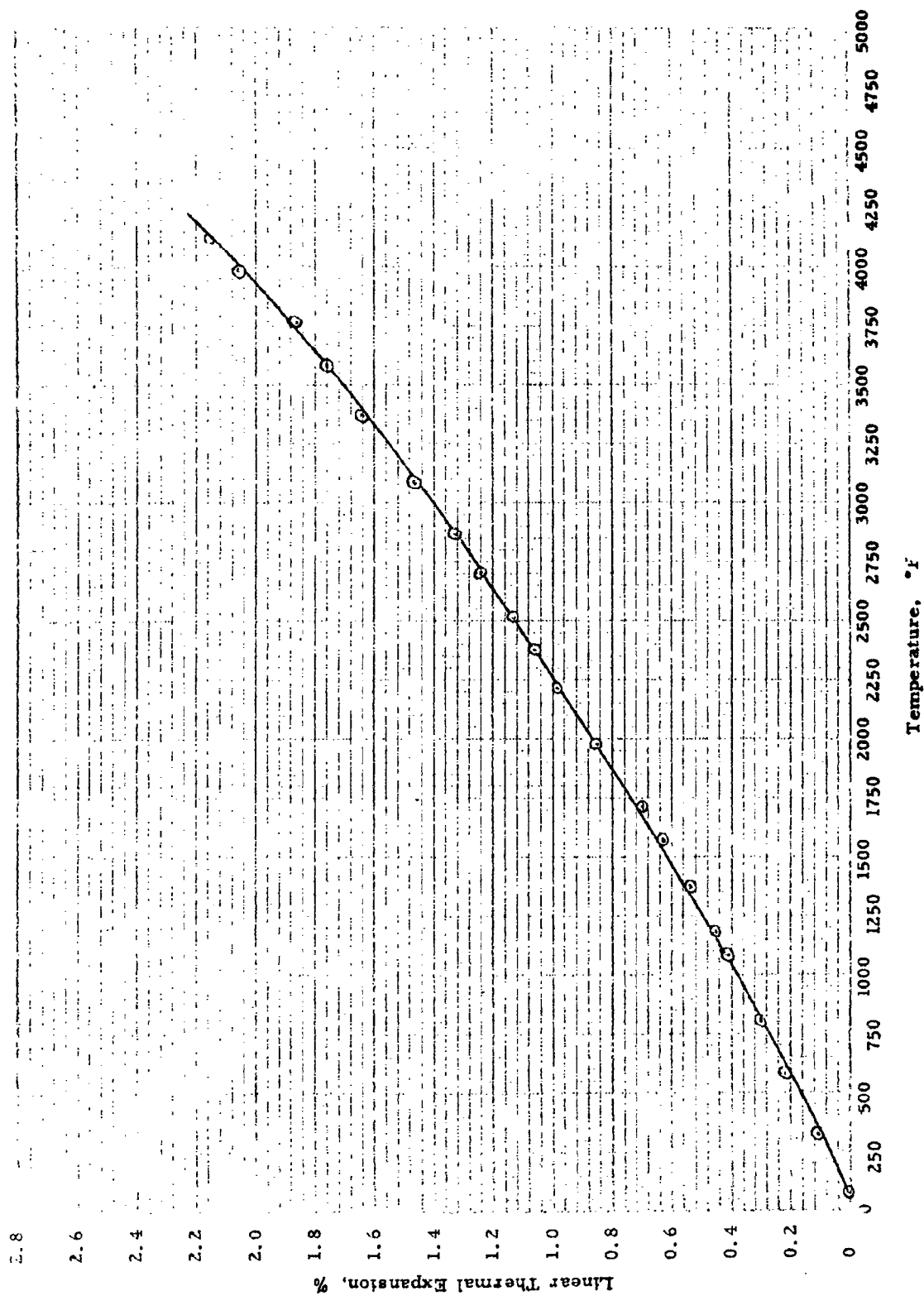


Fig. 12 LINEAR THERMAL EXPANSION OF Cb-15W-5Mo-1Zr-0.05C ALLOY

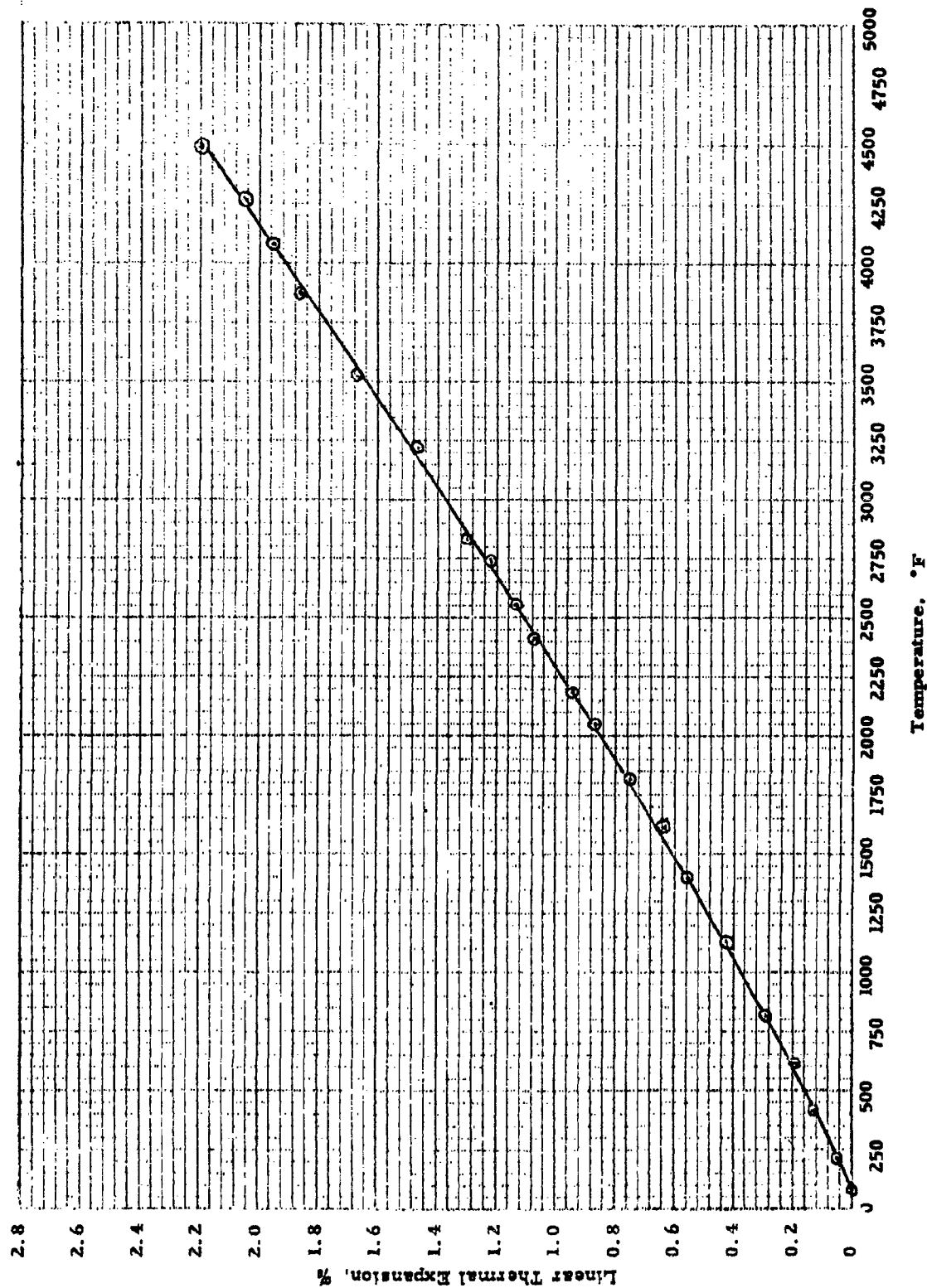


Fig. 13 LINEAR THERMAL EXPANSION OF Cb-27Ta-12W-0.5Zr ALLOY

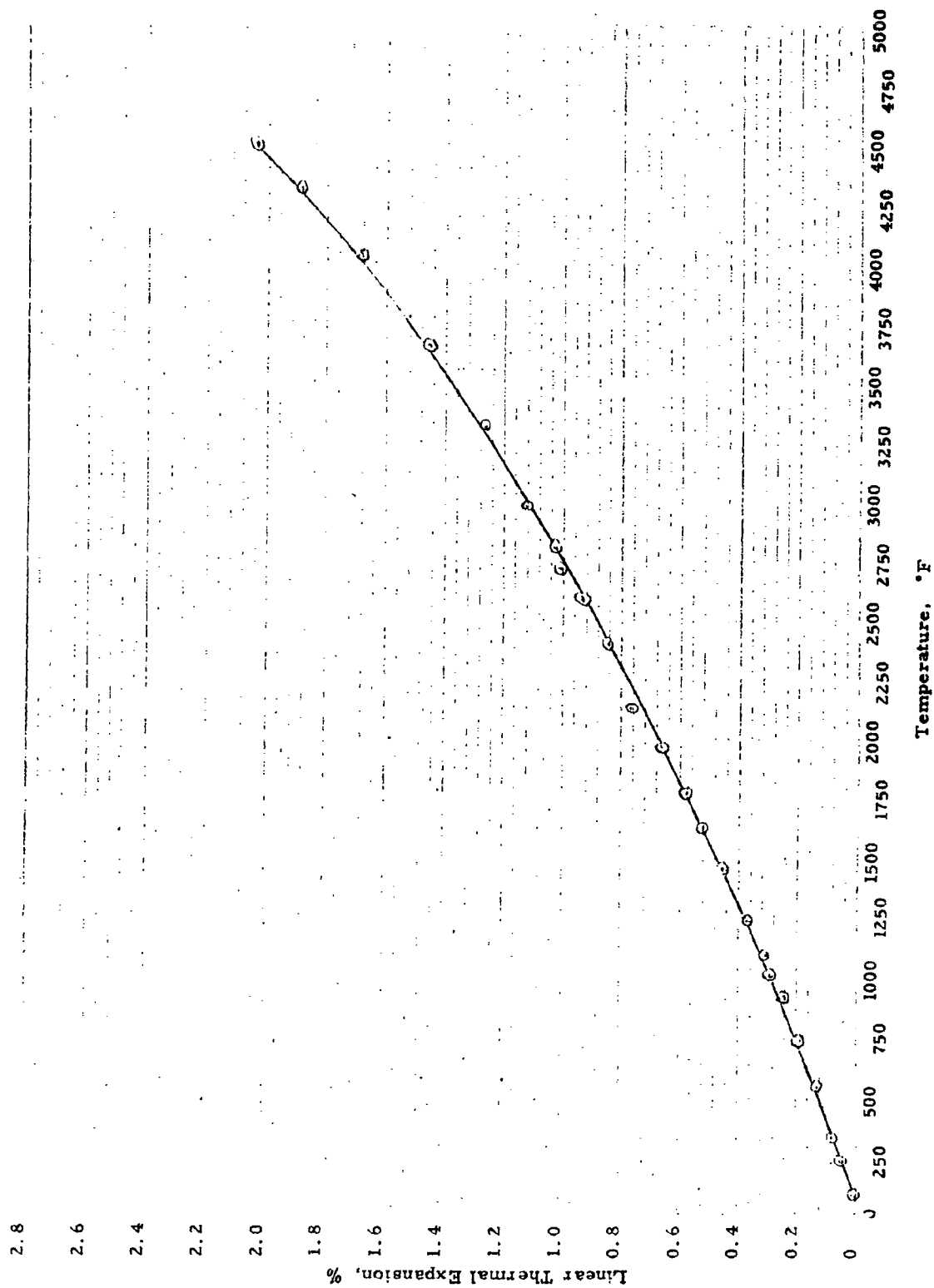


Fig. 14 LINEAR THERMAL EXPANSION OF Mo-0.5Ti-0.08Zr ALLOY

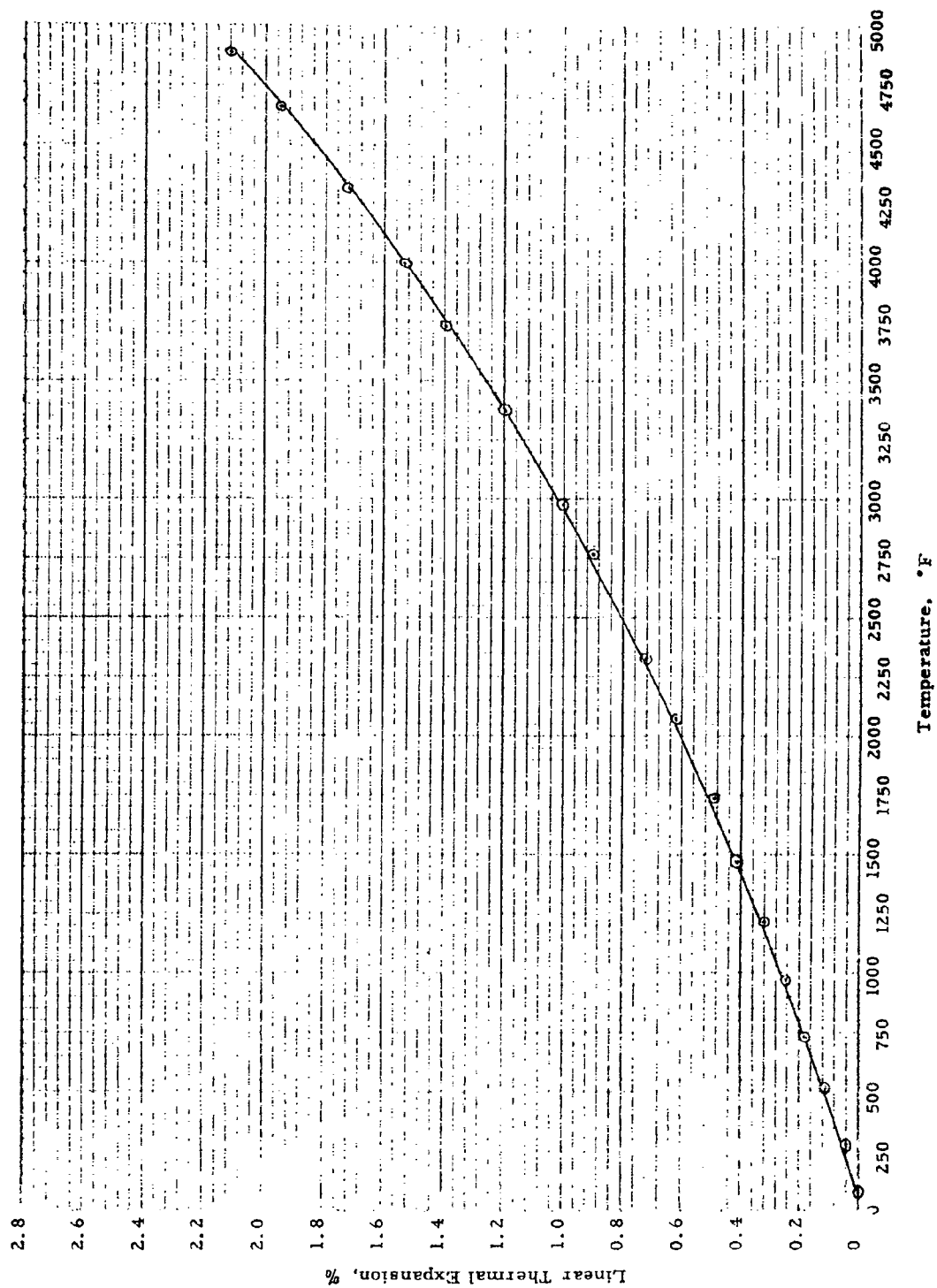


Fig. 15 LINEAR THERMAL EXPANSION OF Mo-29.83W-0.07Zr-0.012C ALLOY

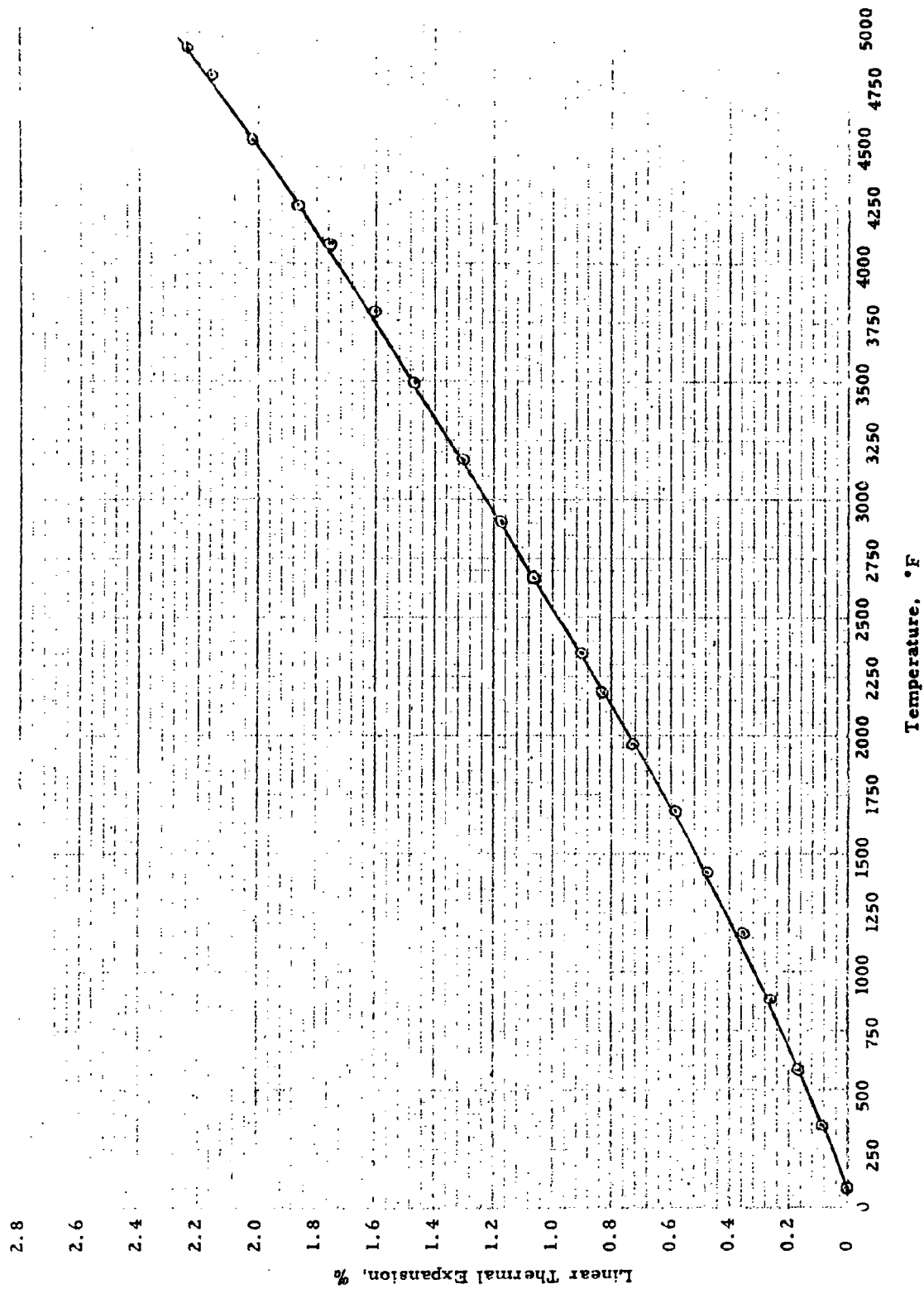


Fig. 16 LINEAR THERMAL EXPANSION OF Ta-10W ALLOY

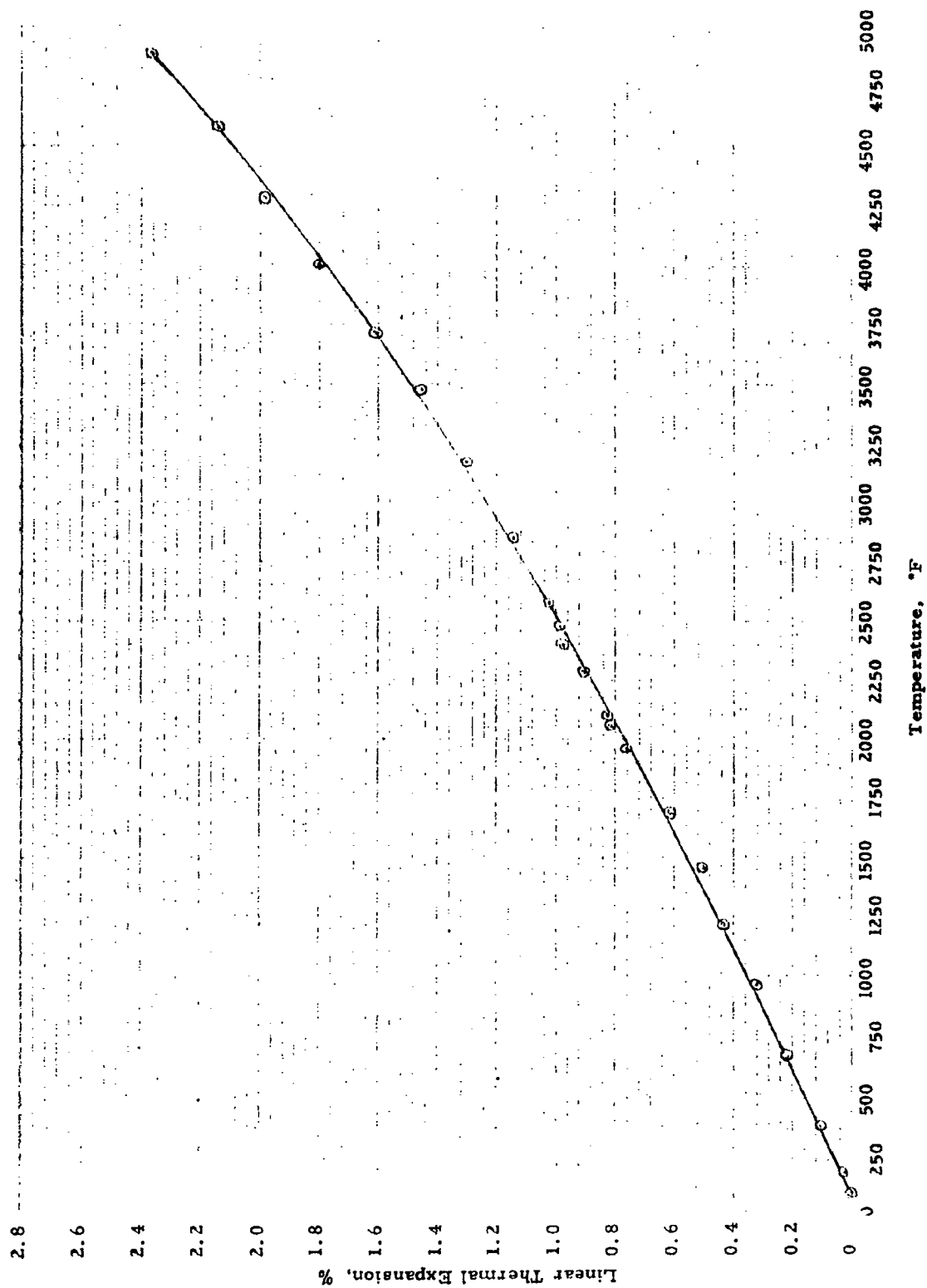


Fig. 17 LINEAR THERMAL EXPANSION OF Ta-8W-2Hf ALLOY

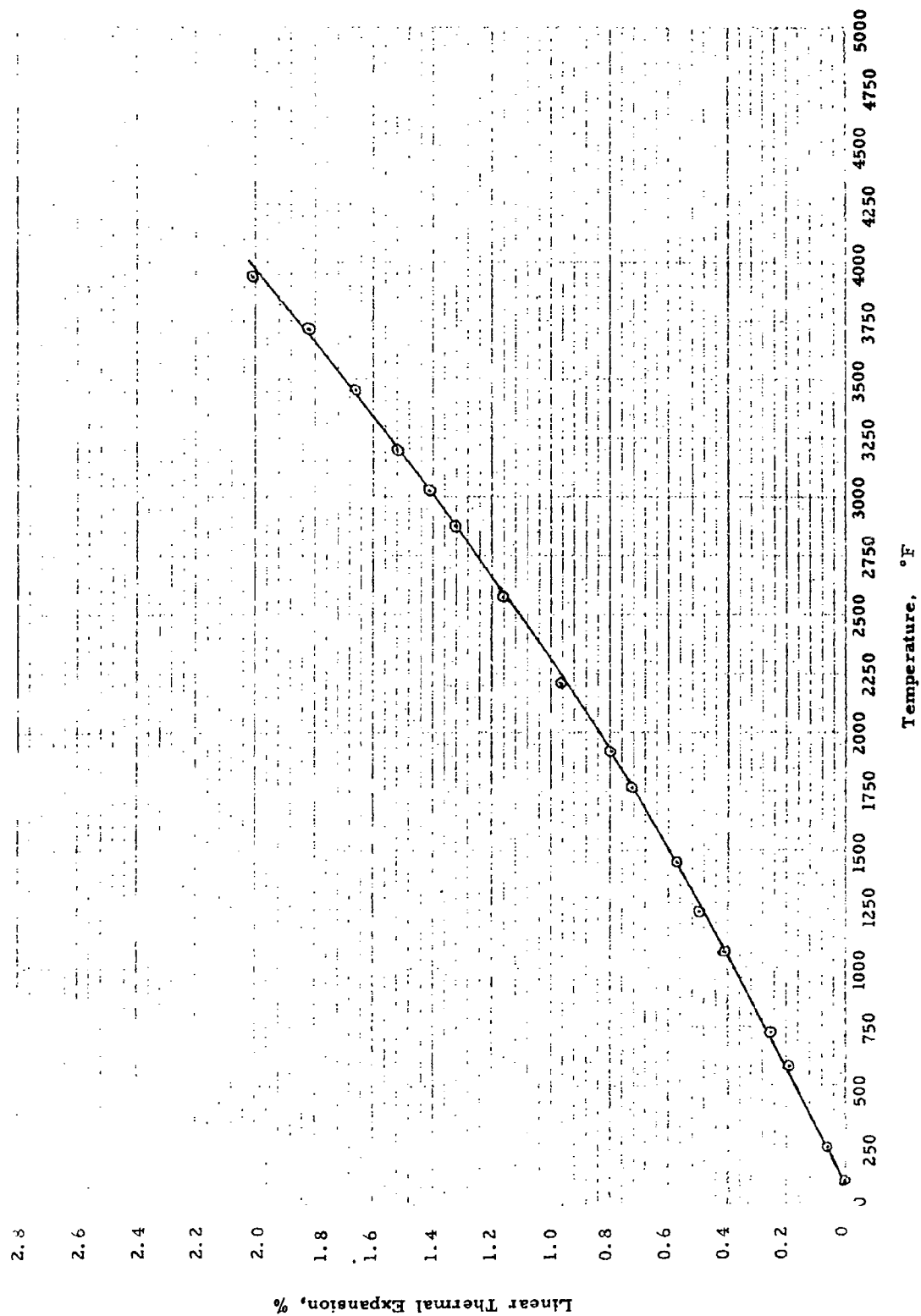


Fig. 18 LINEAR THERMAL EXPANSION OF Ta-30Cb-7.5V ALLOY

### III. SPECIFIC HEAT

#### A. Description of Equipment

The specific heat of fifteen materials was determined in the temperature range of 500°F to 4600°F by the drop calorimeter method. The apparatus used in these measurements consisted of a low temperature furnace, a high temperature furnace, and two calorimeters. The low temperature furnace was used for measurements to 3000°F, and is described first.

A diagram of the apparatus used is shown in Figure 19. The furnace is a vertical tube type purchased from the Harper Electric Company. The interior of the furnace contains an alundum tube, 1-1/2 inches inside diameter, 44 inches in length. The tube length and diameter were specified to assure a uniform temperature region surrounding the sample.

The furnace was heated electrically by a globar tube, exterior and concentric with the alundum tube. Power input to the globar element was controlled by a 3-step, 6-position transformer. An inert atmosphere for the furnace interior was assured by constant purging with helium. Sealing at the top of the tube was attained by a pipe flange; bottom sealing was provided by a gate valve.

The temperature of the furnace at the point where the sample was suspended was measured by two platinum/platinum-10% rhodium thermocouples contained in protection tubes and suspended from the furnace top. The thermocouple signals were circuited to a Leeds and Northrup portable precision potentiometer. An axial temperature survey at the in-furnace sample position indicated a temperature gradient of less than 1°F/inch, at a mean furnace temperature of 2500°F.

The calorimeter used was a Parr Adiabatic Calorimeter, modified for the specific heat measurements. The calorimeter assembly is shown in Figure 20. The left view of Figure 20 shows the conventional calorimeter consisting of a water jacket containing water in circulation, and an interior bucket containing a measured quantity of water. A receiver is shown in the left view of Figure 20, mounted vertically in the bucket. The calorimeter cover was modified to allow passage of a vertical tube attached to the top of the receiver. This tube, extending out of the top of the calorimeter, was connected to the pipe connected to the bottom of the furnace.

The center view of Figure 20 shows an enlarged view of the receiver. A cutaway in this view indicates the details of the receiver gate. After passage of the test sample into the receiver, the gate was closed to prevent loss of heat by convection from the calorimeter. A second cutaway in the center view shows a pad of copper wool, or graphite cloth, which was used to reduce the shock of the sample impact on the calorimeter bottom. The right angle tube shown mounted to the receiver provided purging of the receiver system with an inert gas.

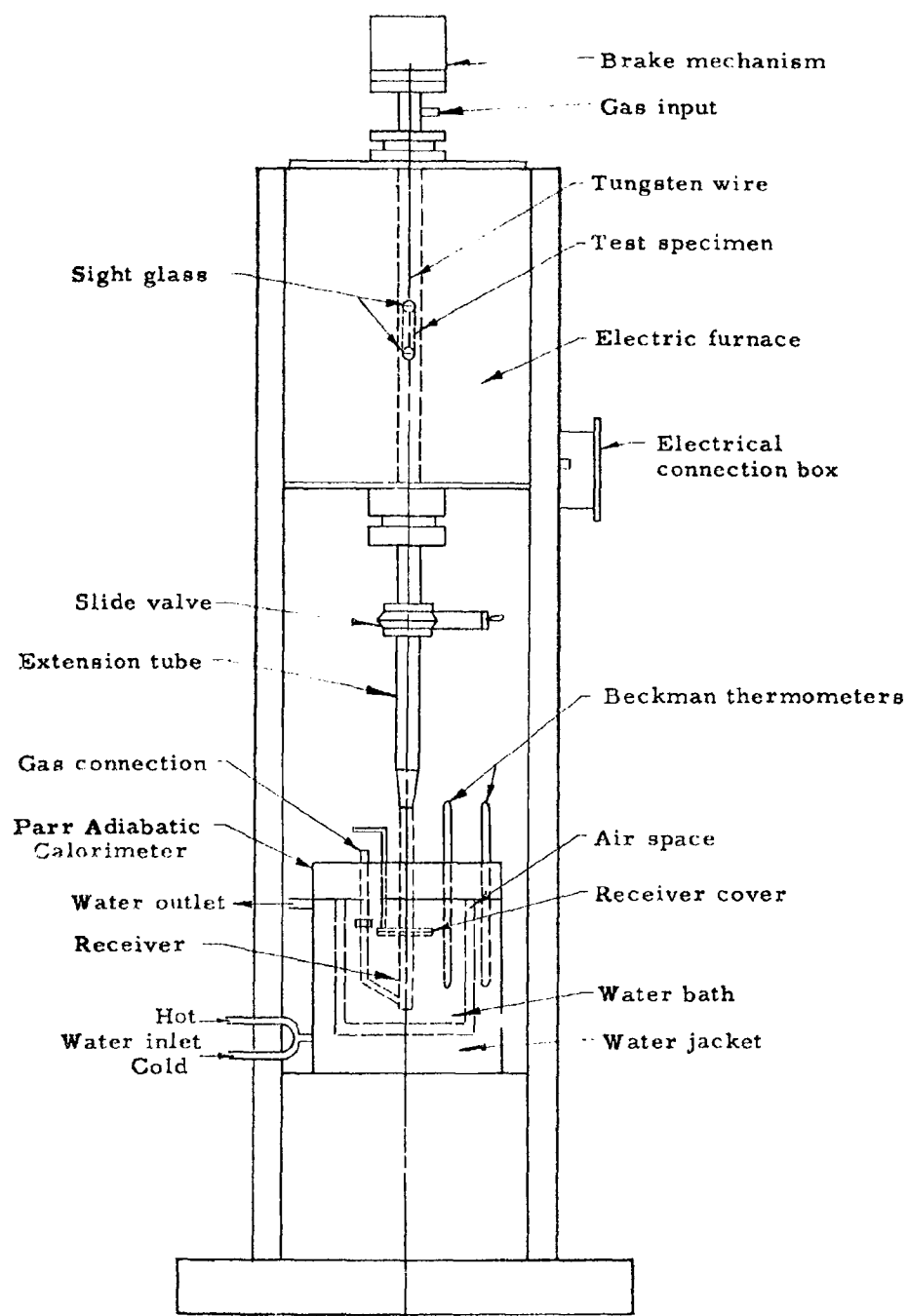


Fig.19 SCHEMATIC DIAGRAM OF APPARATUS  
FOR MEASURING SPECIFIC HEAT

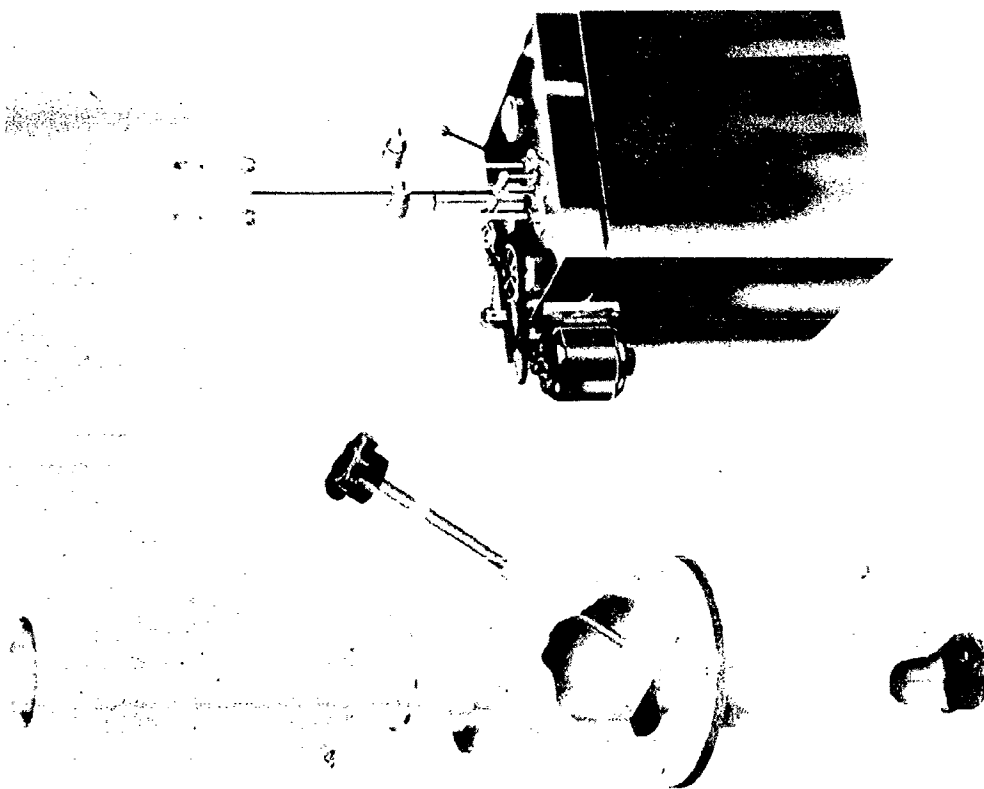
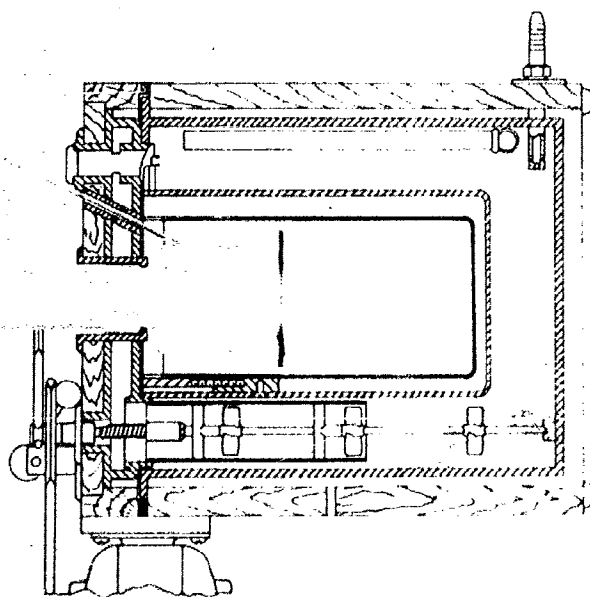


Fig. 20 PARR CALORIMETER FOR HEAT CAPACITY MEASUREMENTS

The temperatures in the calorimeter and in the calorimeter jacket were measured with calibrated thermometers supplied by the Parr Instrument Company. Water to the calorimeter jacket was heated by means of a 500-watt heater.

A 20-kw vertical tube graphite furnace was used for heating the sample to temperatures in excess of 3000°F. The graphite heater tube was 1-1/2" in diameter by 45" long. In-furnace sample temperatures were measured by an optical pyrometer sighting on the sample through a small horizontal tube located at the axial furnace center.

#### B. Experimental Procedure

The procedure for operation of the system is outlined below. The outline is presented in chronological order:

1. The sample weight was measured using an analytical balance precise to 0.1 milligram. The sample weight was determined prior to each test.

2. The sample was then suspended in the furnace by means of a wire. The length of the wire was carefully measured before attaching the sample to assure that the sample was correctly positioned in the furnace, respective to the monitor thermocouples.

3. The sample was maintained in the furnace for 25 minutes. This time period was considered sufficient for the sample to attain thermal equilibrium. The period of time required for the sample to attain 0.95 of the difference between room temperature and furnace temperature was calculated. For a sample emissivity of 0.7, and assuming infinite sample thermal diffusivity, the period of time for 0.95 temperature rise was 3 minutes.

4. The weight of water contained in the bucket was measured using a pan balance precise to 0.1 gram. The bucket was then placed in the calorimeter jacket, the calorimeter cover set in position, and the calorimeter elevated to the connecting tube. The calorimeter was then brought to thermal equilibrium by equalizing the temperature level in the jacket and bucket. The receiver and connecting tube were then purged with helium.

5. The system was then in readiness for the sample drop. During the preparatory stages of this operation, the furnace thermocouple signals were recorded on a Leeds and Northrup Speedomax, which provided visual observation of in-furnace temperature behavior. Injection of the sample into the furnace caused the furnace temperature to decrease; this behavior and the subsequent rise in temperature to a non-varying level was also noted. At this point in the operation the furnace thermocouple signals were circuited to a Leeds and Northrup portable precision potentiometer; emf output of each thermocouple was determined to a precision of approximately 1°F.

6. The helium purging of receiver and connecting tube was stopped immediately before sample drop. Then the gate valve at the furnace bottom was opened, the sample dropped, and the receiver gate closed. The operation from this point consisted simply in regulating the hot water input to the calorimeter jacket to maintain equal temperature level with the rising temperature level of the water in the bucket. The calorimeter attained thermal equilibrium after a period of fifteen to twenty minutes, then the final temperatures were recorded.

The procedure listed above was used for all samples through the complete temperature range of operation. Over-all procedure was to obtain heat content of all samples at one specified temperature level, then the power input to the furnace was increased, and the above procedure was repeated at the new temperature level.

At temperatures in excess of 2000°F the samples were encapsulated to prevent excessive heat loss during sample drop. The calorimetric heat attributable to the capsule was determined by measurements with empty capsules. Encapsulating was done with thick-walled tantalum and molybdenum capsules.

### C. Test Results

The results of the measurements are presented in both tabular and graphical form. The test data are presented in Tables 18 through 32, and enthalpy change of each material, and measured sample temperatures, are presented in Figures 21 through 35. The specific heat values obtained from Figures 21 through 35 are presented in analytical form, and are also tabulated.

The enthalpy was calculated from the experimental measurements using the following equation:

$$\Delta H = \frac{W_e (t_f - t_i) - m_c h_c}{m_s} \quad (1)$$

$W_e$  = water equivalent of bucket, receiver, and weighed water contained in bucket, in units of Btu/°F

$t_f, t_i$  = final and initial calorimeter temperatures, respectively, as measured by the calorimeter thermometer, in °F

$m_c$  = capsule mass, pounds

$h_c$  = enthalpy of capsule, Btu/lb

$m_s$  = mass of samples, pounds

Table 18

ENTHALPY VALUES FOR BORON CARBIDE

Datum Temperature: 80°F

Temperature, °F	$\Delta H$ , Btu/lb
407	109
665	194
981	300
1054	326
1189	380
1429	492
1506	493
1702	618
1711	605
1785	679
1805	705
1910	748
2058	810
2207	905
2362	978
2482	1030
2787	1240
3020	1340
3380	1600
3630	1740
3830	1810
4060	1950

Table 19

ENTHALPY VALUES FOR SPINEL

Datum Temperature: 80°F

Temperature, °F	$\Delta H$ , Btu/lb
571	72.8
803	133
995	183
1161	242
1333	287
1483	336
1508	342
1662	389
1799	443
1881	459
2044	508
2205	573
2343	617
2485	665
2793	753
3010	835
3335	955
3495	1040

Table 20

ENTHALPY VALUES FOR ZIRCONIUM NITRIDE

Datum Temperature: 80°F

Temperature, °F	$\Delta H$ , Btu/lb
481	41.5
824	68.1
1109	109
1380	138
1579	158
1848	194
2001	207
2163	233
2332	257
2597	291
2840	317
3155	355
3335	393
3580	423
3835	448
4075	495
4340	502
4530	546

Table 21

ENTHALPY VALUES FOR BERYLLIUM OXIDE

Datum Temperature: 80°F

Temperature °F	$\Delta H$ $\frac{\text{Btu}}{\text{lb}}$
489	133
602	179
789	246
1013	336
1357	506
1542	582
1705	678
1986	803
2133	887
2341	1018
2517	1063
2681	1182
2802	1247
2960	1303
3150	1435
3390	1565
3585	1670
3640	1740

Table 22

ENTHALPY VALUES FOR Cb-10W-1Zr-0.1C ALLOY

Datum Temperature: 80°F

Temperature, °F	$\Delta H$ , Btu/lb
324	16.5
538	28.4
758	42.8
948	56.5
1058	60.4
1245	73.5
1390	83.1
1600	98.0
1697	110
1864	119
2065	138
2209	145
2456	161
2613	180
2830	189
3044	216
3280	238
3465	243
3675	266
3890	295
4065	301

Table 23

ENTHALPY VALUES FOR Cb-5Mo-5V-1Zr ALLOY

Datum Temperature: 80°F

Temperature, °F	ΔH, Btu/lb
450	19.0
676	31.5
806	38.7
965	51.2
1066	56.2
1245	72.1
1360	81.2
1503	92.0
1687	106.0
1703	108.0
1798	115.0
1855	120.0
1908	123.0
2055	137.0
2143	142.0
2210	150.0
2345	165.0
2517	183.0
2760	199.0
2905	226
3045	222
3345	258
3530	267
3810	307
3985	317

Table 24

ENTHALPY VALUES FOR Cb-10W-5Zr ALLOY

Datum Temperature: 80°F

Temperature, °F	$\Delta H$ , Btu/lb
529	28.4
693	38.3
802	45.4
897	52.8
1060	63.6
1107	64.8
1291	79.4
1341	81.9
1613	106.0
1667	108.0
1819	117.0
1840	118.0
1981	130.0
2049	135.0
2100	138.0
2210	146.0
2376	156.0
2400	157.0
2557	177
2788	194
3020	218
3340	252
3575	264
3835	283
4170	329

Table 25

ENTHALPY VALUES FOR Cb-10Ti-5Zr ALLOY

Datum Temperature: 80°F

Temperature, °F	ΔH, Btu/lb
516	31.0
694	43.7
809	52.9
838	55.4
1076	74.2
1082	75.3
1279	89.9
1288	90.0
1555	112
1666	120
1816	136
1853	139
1996	150
2045	159
2085	161
2256	176
2359	183
2402	189
2644	211
2775	224
2930	237
3330	283
3565	300
3855	333
4150	381

Table 26

ENTHALPY VALUES FOR Cb-15W-5Mo-1Zr-0.05C ALLOY

Datum Temperature: 80°F

Temperature, °F	ΔH, Btu/lb
417	19.4
513	26.8
694	38.9
773	43.1
897	52.1
1071	63.2
1088	64.5
1279	76.7
1296	79.0
1570	99.0
1650	106
1798	116
1814	118
1852	121
1983	129
2059	132
2093	138
2214	148
2352	154
2408	163
2695	184
2801	190
2945	206
3105	218
3360	244
3480	251
3890	279
4140	316
4480	333

Table 27

ENTHALPY VALUES FOR Cb-27Ta-12W-0.5Zr ALLOY

Datum Temperature: 80°F

Temperature, °F	$\Delta H$ , Btu/lb
390	16.6
658	30.6
821	38.1
944	47.9
1059	51.1
1075	56.0
1188	60.0
1196	62.2
1403	72.1
1507	79.4
1704	93.4
1704	93.1
1800	96.5
1894	104.0
2053	112.0
2110	116.0
2207	123.0
2345	134.0
2510	144.0
2778	163.0
2895	177
3130	199
3345	209
3615	223
3900	240
4065	277
4410	302

Table 28

ENTHALPY VALUES FOR Mo-0.5Ti-0.08Zr ALLOY

Datum Temperature: 80°F

Temperature, °F	ΔH, Btu/lb
396	21.3
407	23.1
507	27.2
601	33.6
710	43.1
820	50.3
873	54.5
1012	61.9
1078	68.3
1212	75.4
1241	78.4
1335	84.0
1582	102
1620	107
1689	111
1828	120
1854	124
1977	131
1998	132
2050	136
2071	137
2223	148
2365	161
2445	166
2580	181
2764	199
2925	209
3305	247
3590	265
3845	282
4080	328
4395	348

Table 29

ENTHALPY VALUES FOR Mo-29.83W-0.07Zr-0.012C ALLOY

Datum Temperature: 80°F

Temperature, °F	ΔH, Btu/lb
535	24.1
834	35.4
1099	52.7
1342	67.2
1538	82.1
1696	93.5
1870	107
1971	118
2079	124
2230	132
2433	141
2605	158
2815	173
3005	187
3118	202
3470	226
3690	257
3925	275
4205	312
4430	324
4680	366

Table 30

ENTHALPY VALUES FOR Ta-10W ALLOY

Datum Temperature: 80°F

Temperature, °F	$\Delta H$ , Btu/lb
508	14.9
708	22.3
817	25.7
874	27.3
1046	34.6
1073	35.8
1202	40.6
1235	40.9
1310	43.7
1320	45.1
1502	51.3
1593	54.5
1672	59.5
1821	65.8
1983	71.5
2060	74.4
2098	77.1
2269	85.6
2358	89.0
2415	91.5
2592	100
2786	111
2935	116
3310	134
3650	156
4005	169
4468	203
4740	218

Table 31

ENTHALPY VALUES FOR Ta-8W-2Hf ALLOY

Datum Temperature: 80°F

Temperature, °F	$\Delta H$ , Btu/lb
550	14.5
809	23.3
987	27.8
1162	33.1
1322	39.0
1483	44.8
1678	51.9
1811	56.2
1906	61.3
2055	66.3
2209	71.5
2325	76.6
2341	76.9
2503	83.3
2653	88.7
2776	92.9
2975	103
3270	115
3595	123
3615	139
4115	151
4460	175

Table 32

ENTHALPY VALUES FOR Ta-30Cb-7.5V ALLOY

Datum Temperature 80°F

Temperature, °F	$\Delta H$ , Btu/lb
300	10.0
608	22.3
899	40.6
1265	63.7
1277	64.3
1640	39.7
1830	97.5
1960	109
2205	129
2340	141
2580	160
2715	171
2962	191
3088	205
3395	235
3530	237
3695	255
3860	277
4055	294

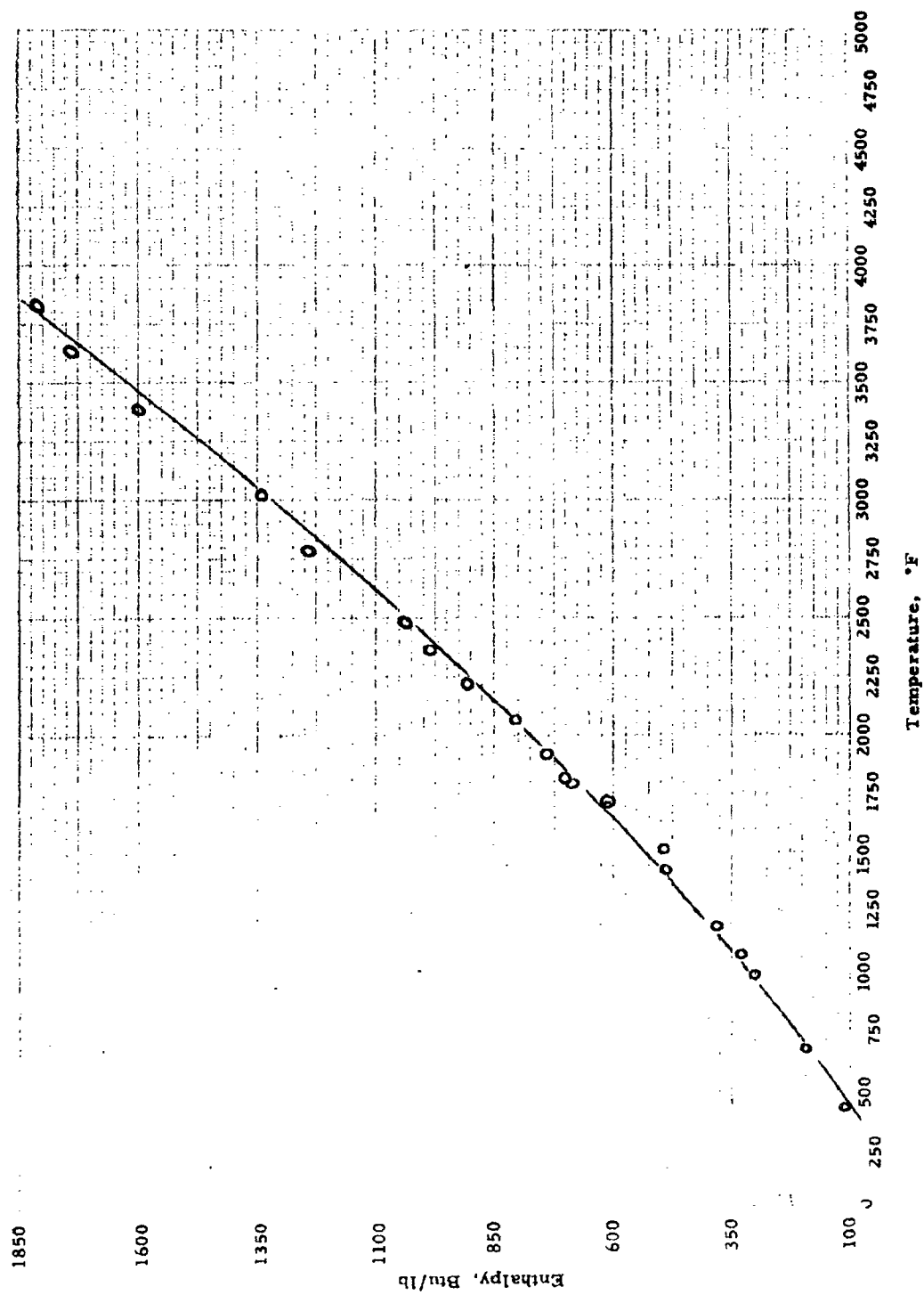


Fig. 21 ENTHALPY OF BORON CARBIDE

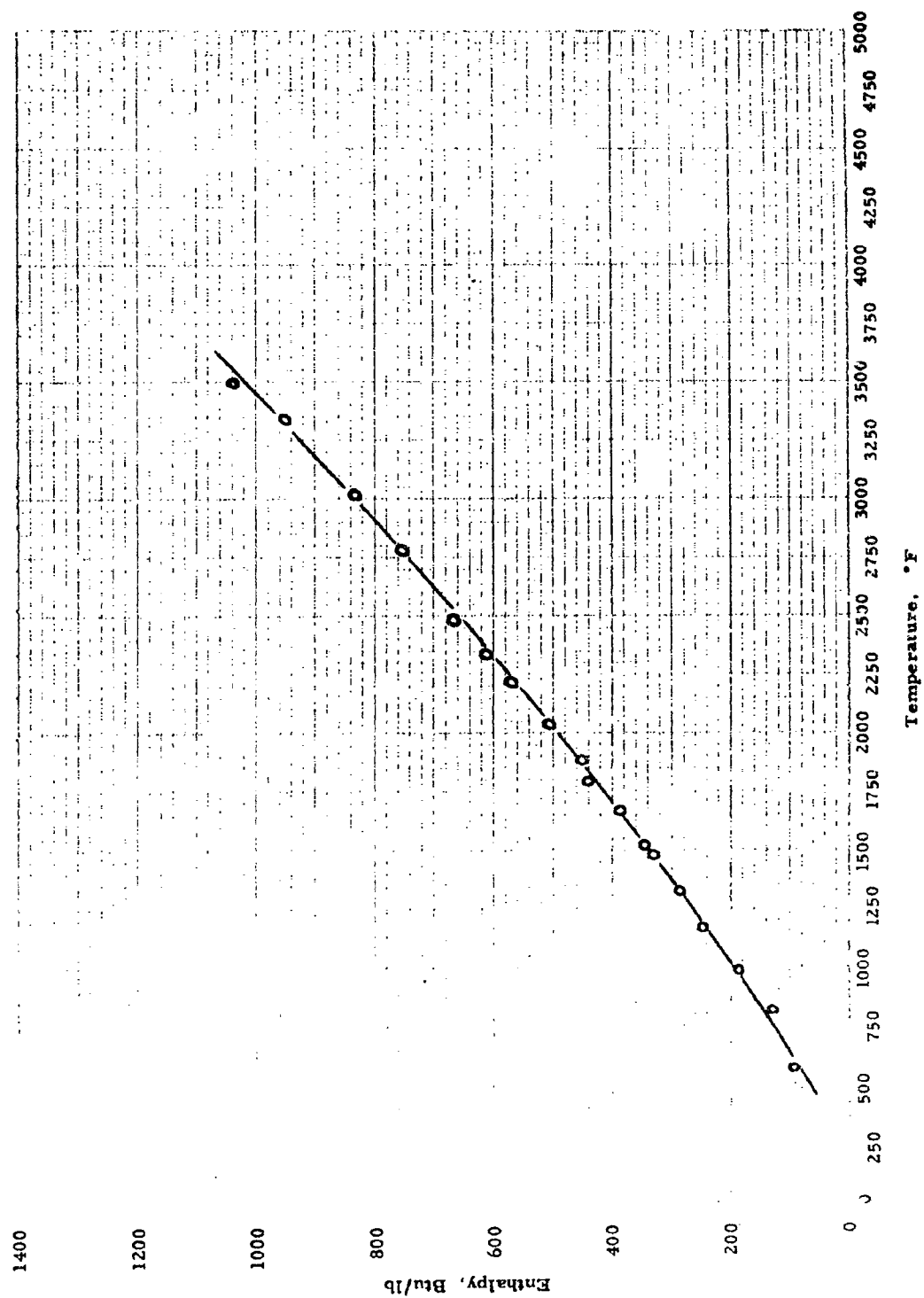


Fig. 22 ENTHALPY OF SPINEL

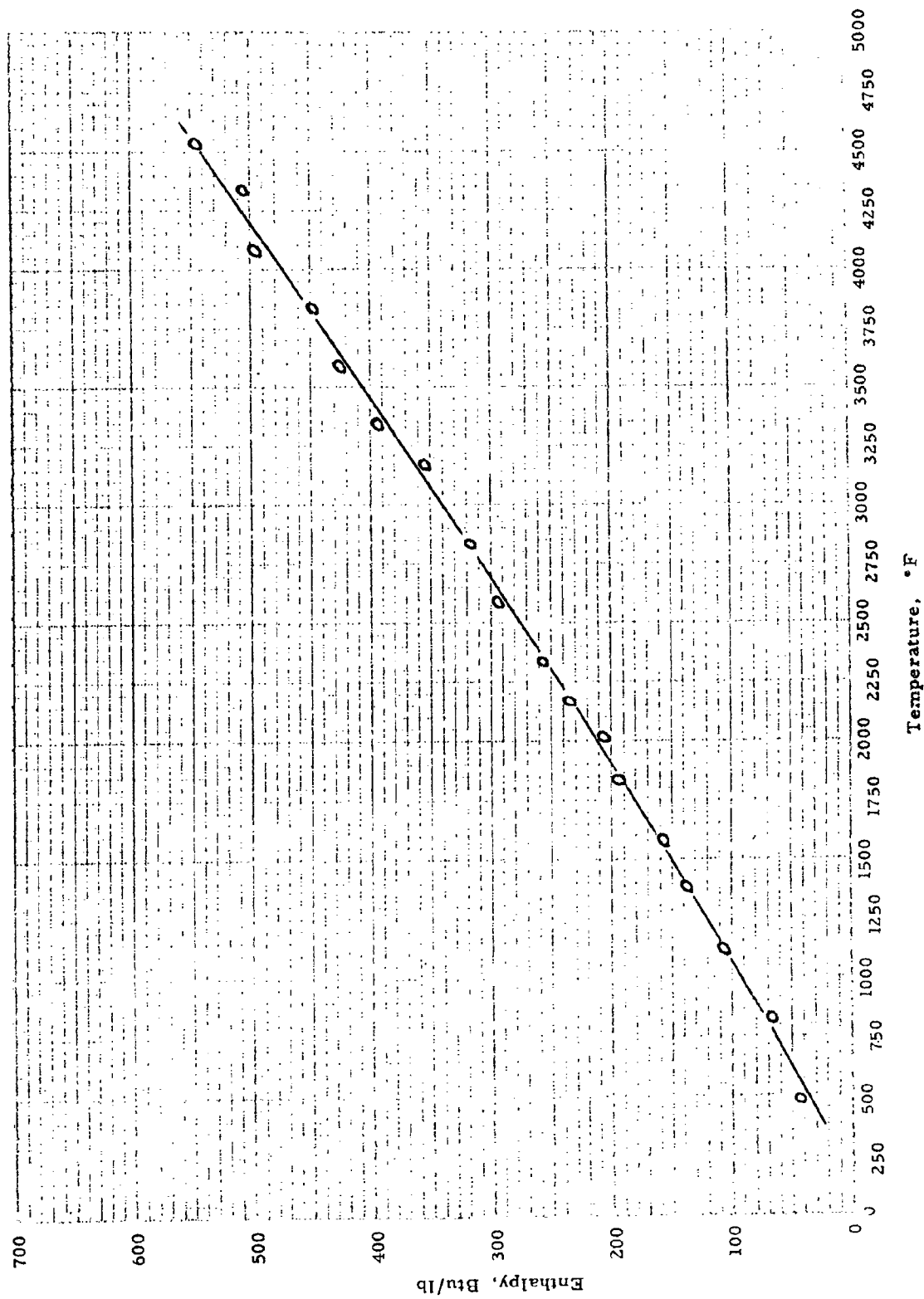


Fig. 23 ENTHALPY OF ZIRCONIUM NITRIDE

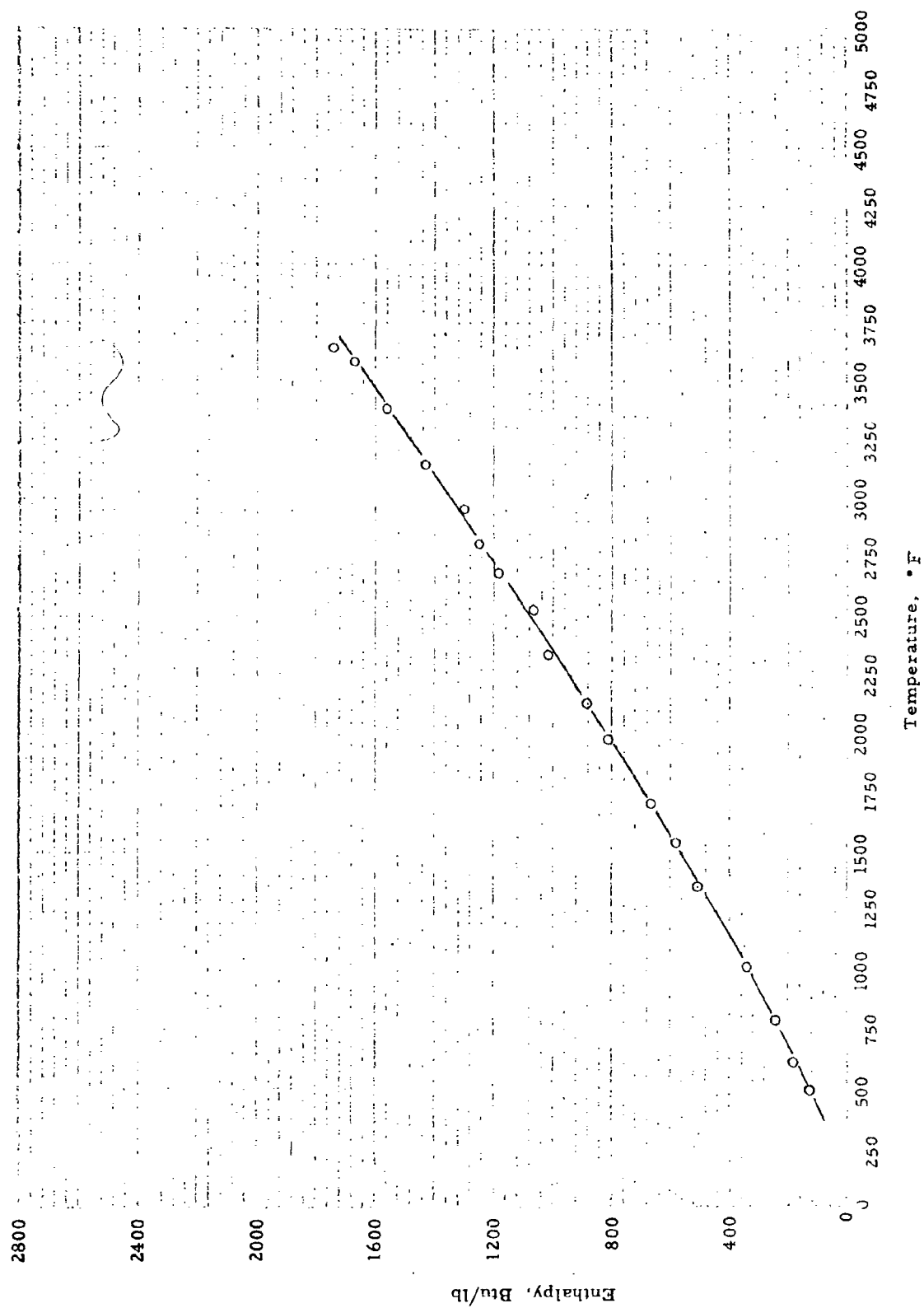


Fig. 24 ENTHALPY OF BERYLLIUM OXIDE

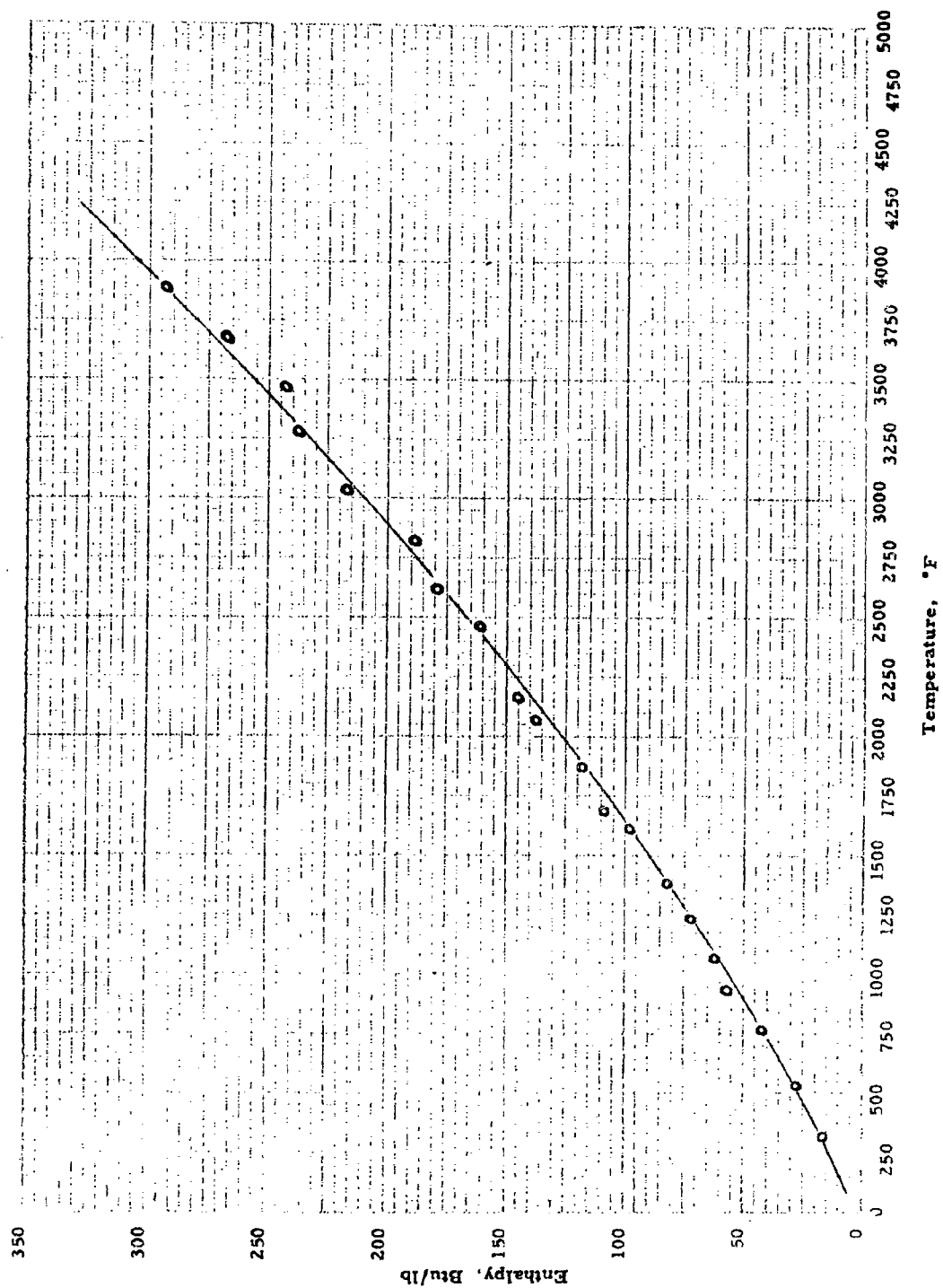


Fig. 25 ENTHALPY OF Cb-10W-1Zr-0.1C ALLOY

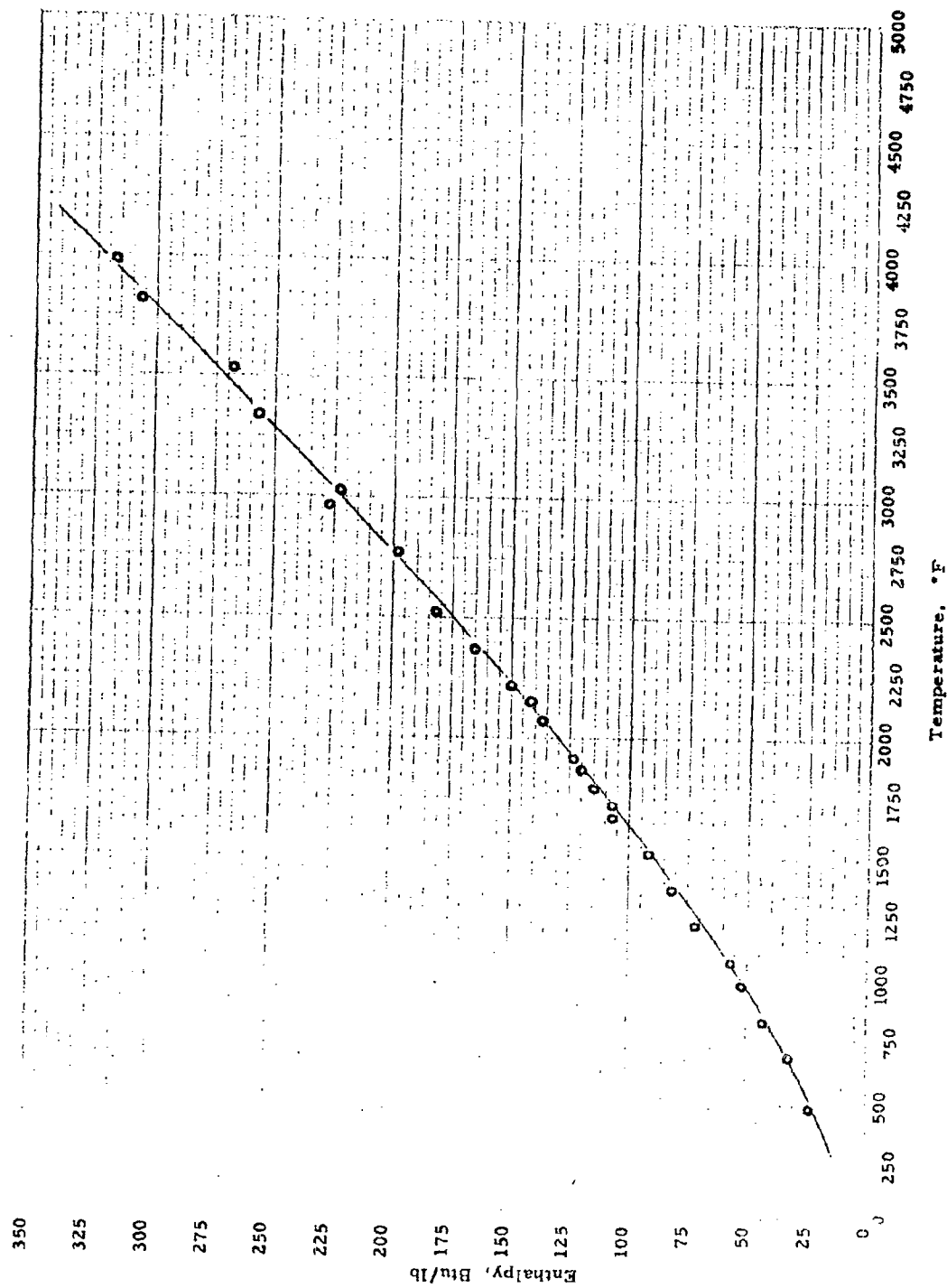


Fig. 26 ENTHALPY OF Cb-5Mo-5V-1Zr ALLOY

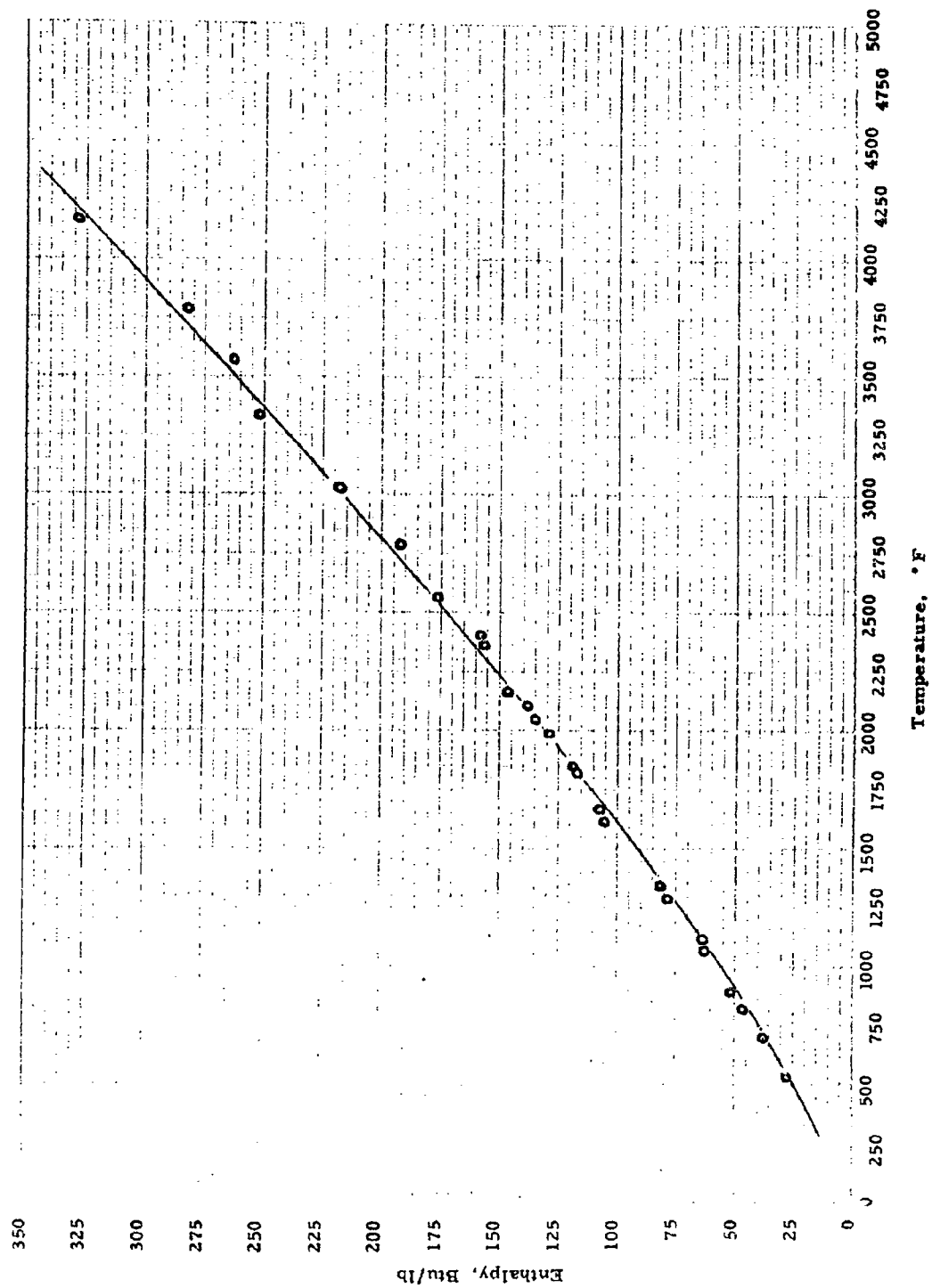


Fig. 27 ENTHALPY OF Cb-10W-5Zr ALLOY

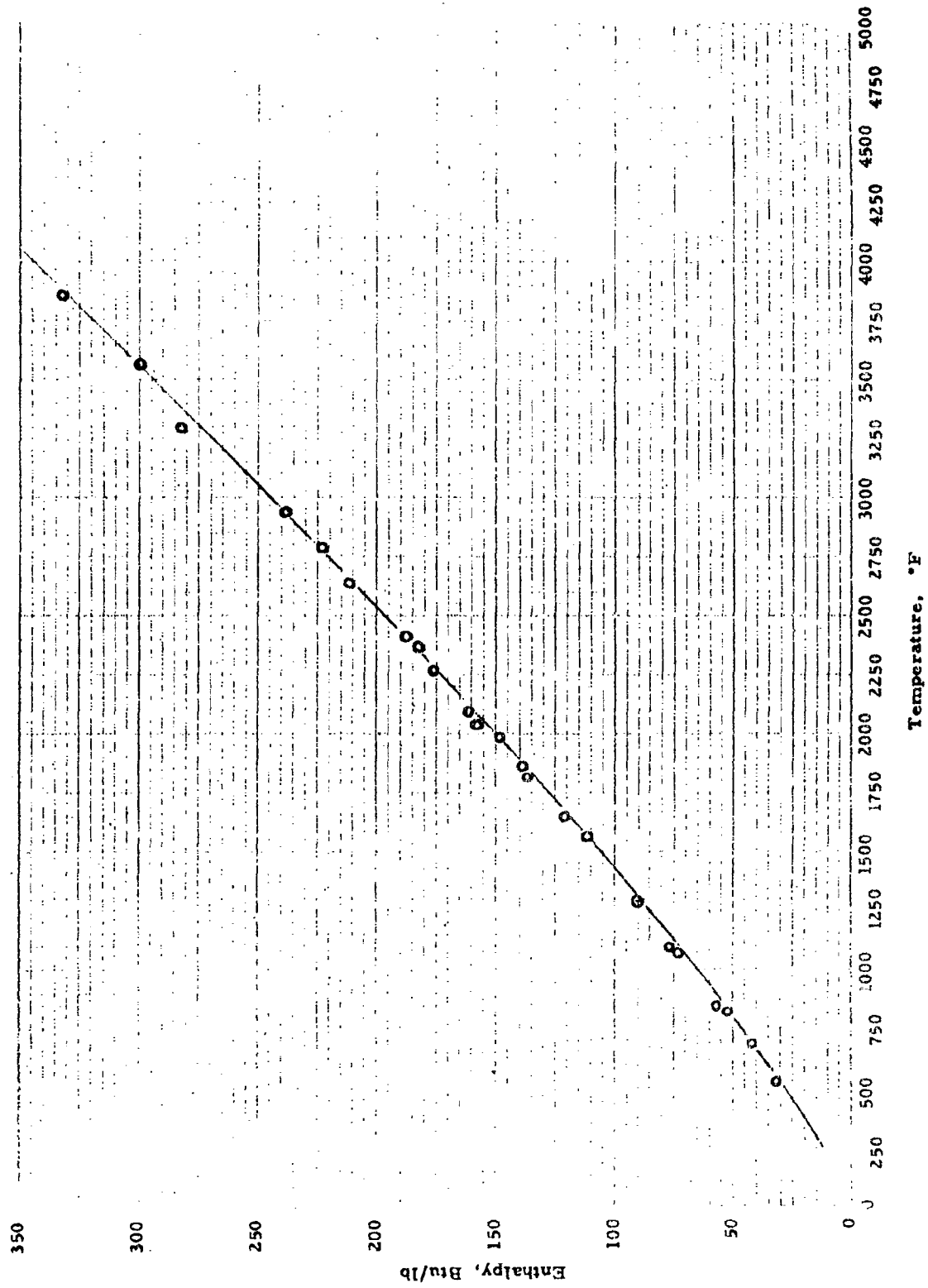


Fig. 28 ENTHALPY OF Cb-10Ti-5Zr ALLOY

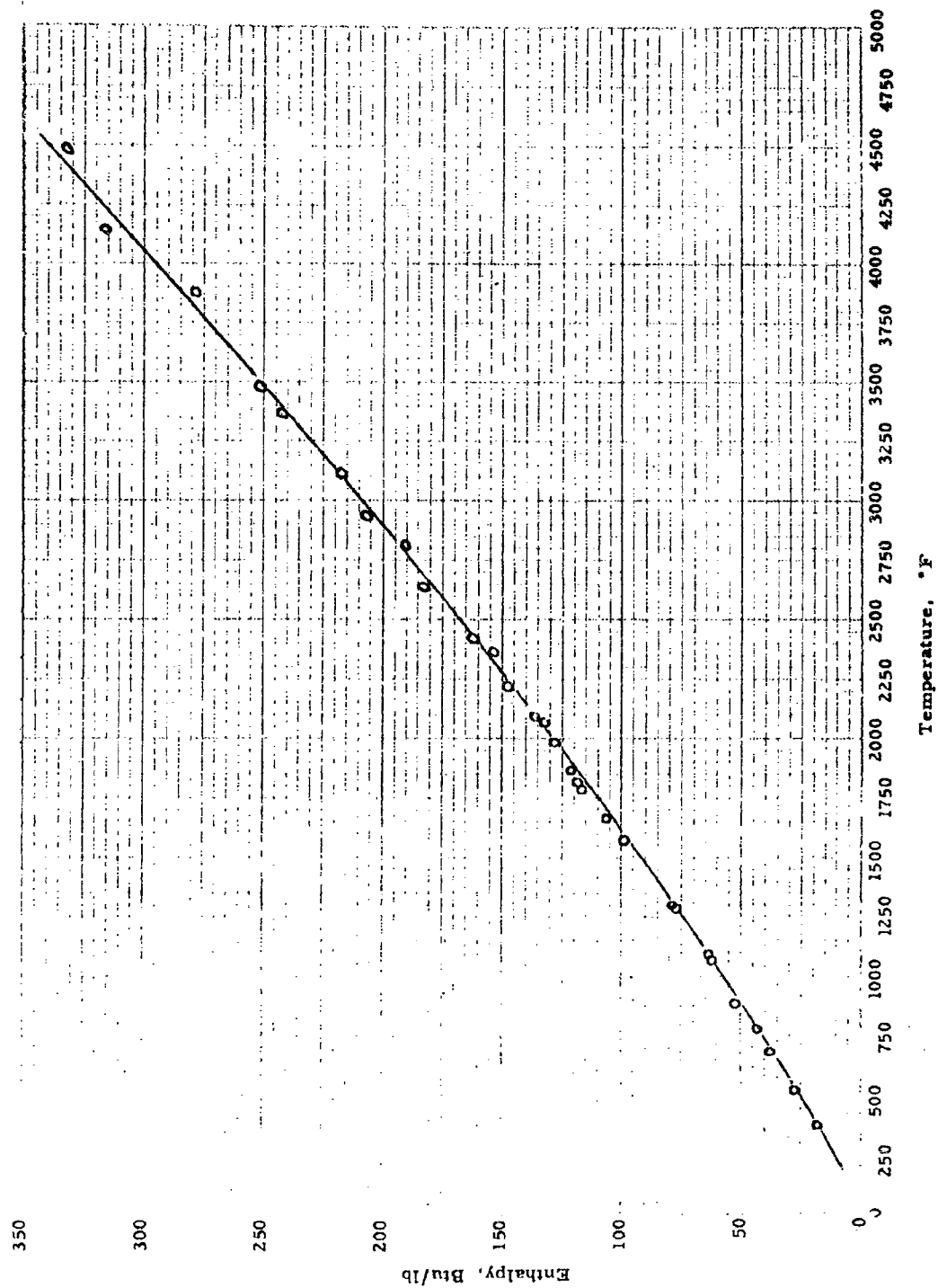


Fig. 29 ENTHALPY OF Cb-15W-5Mo-1Zr-0.05C ALLOY

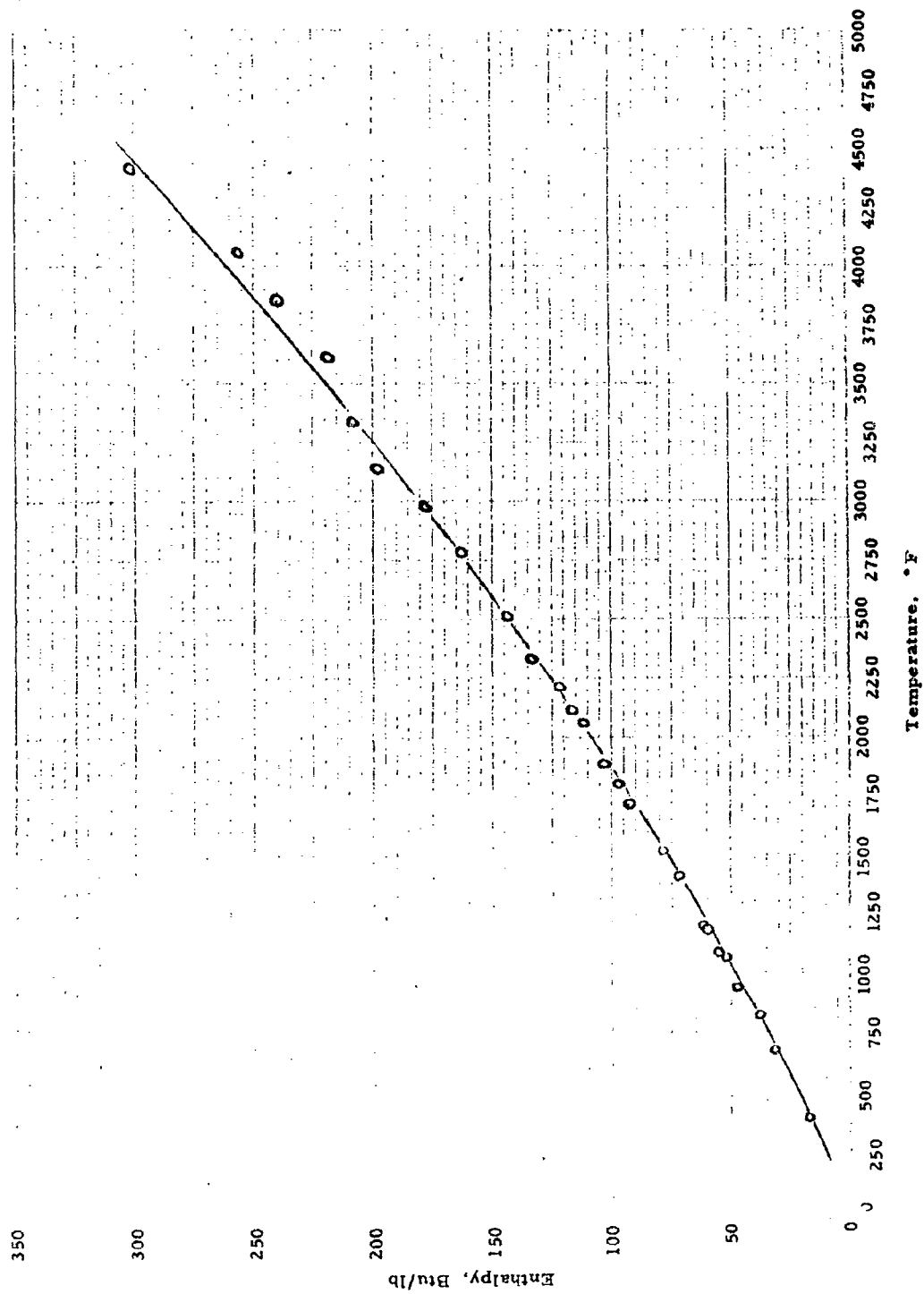


Fig. 30 ENTHALPY OF Cb-27Ta-12W-0.5Zr ALLOY

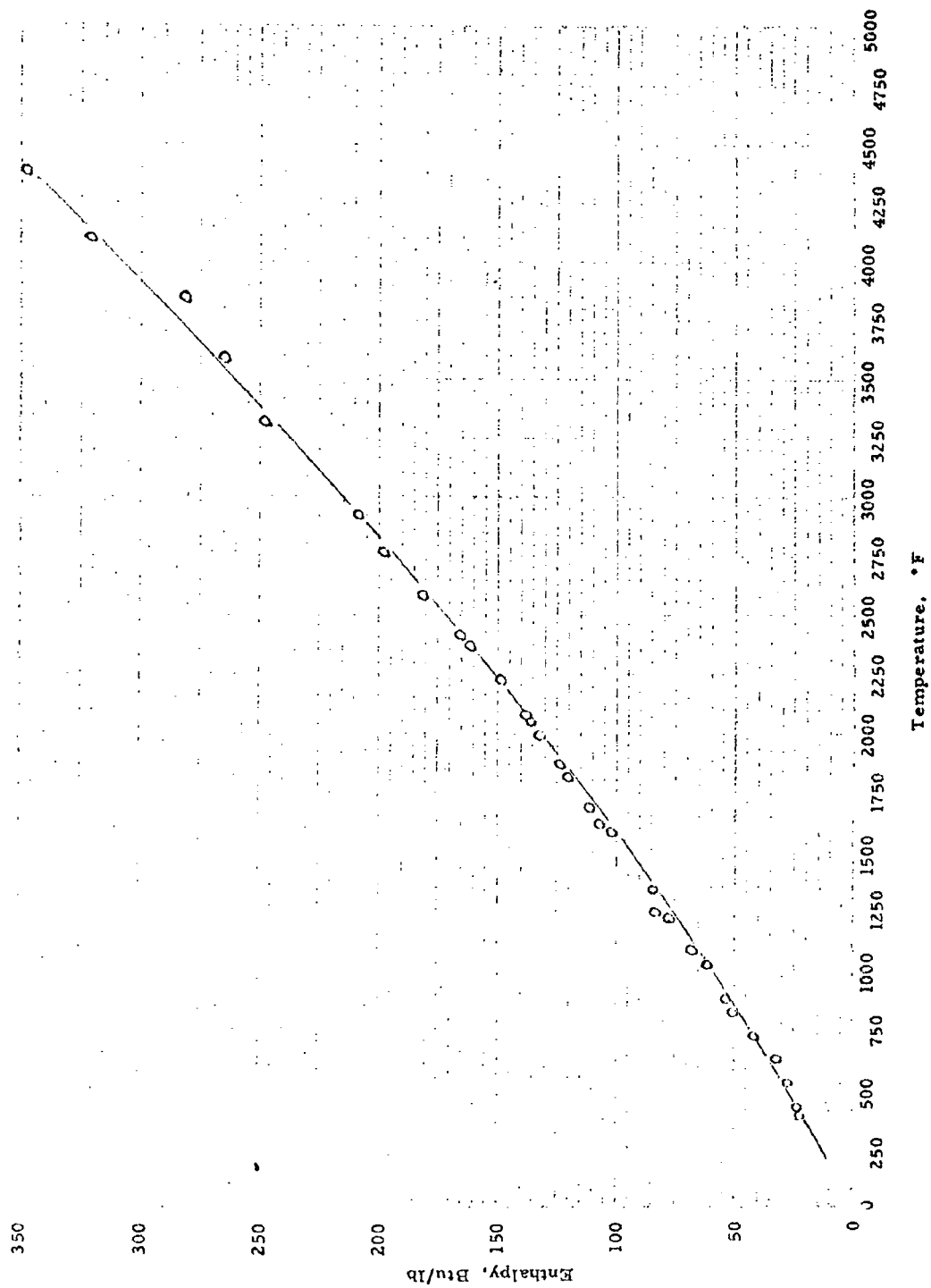


Fig. 31 ENTHALPY OF Mo-0.5Ti-0.08Zr ALLOY

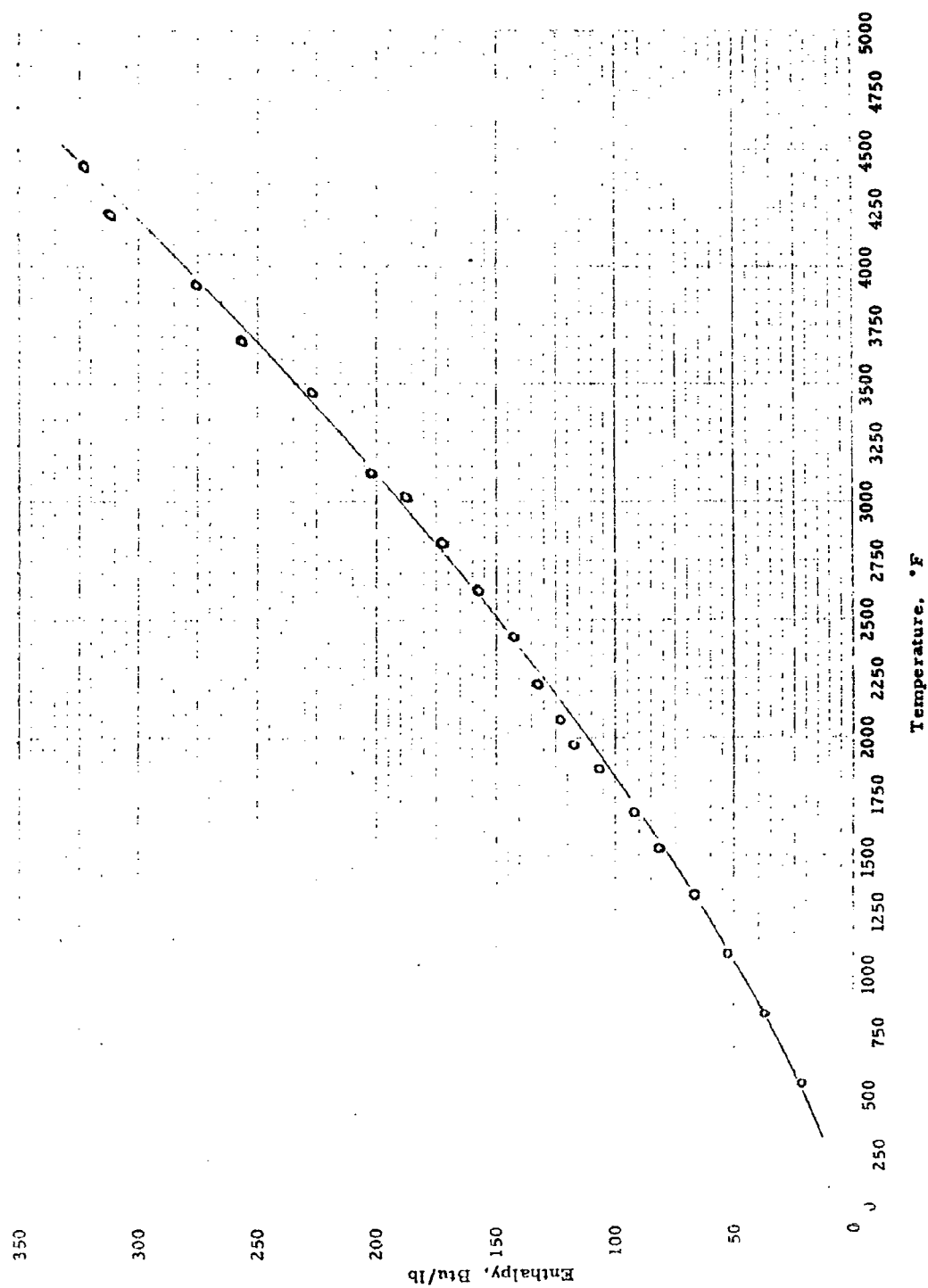


Fig. 32 ENTHALPY OF Mo-29.83W-0.07Zr-0.012C ALLOY

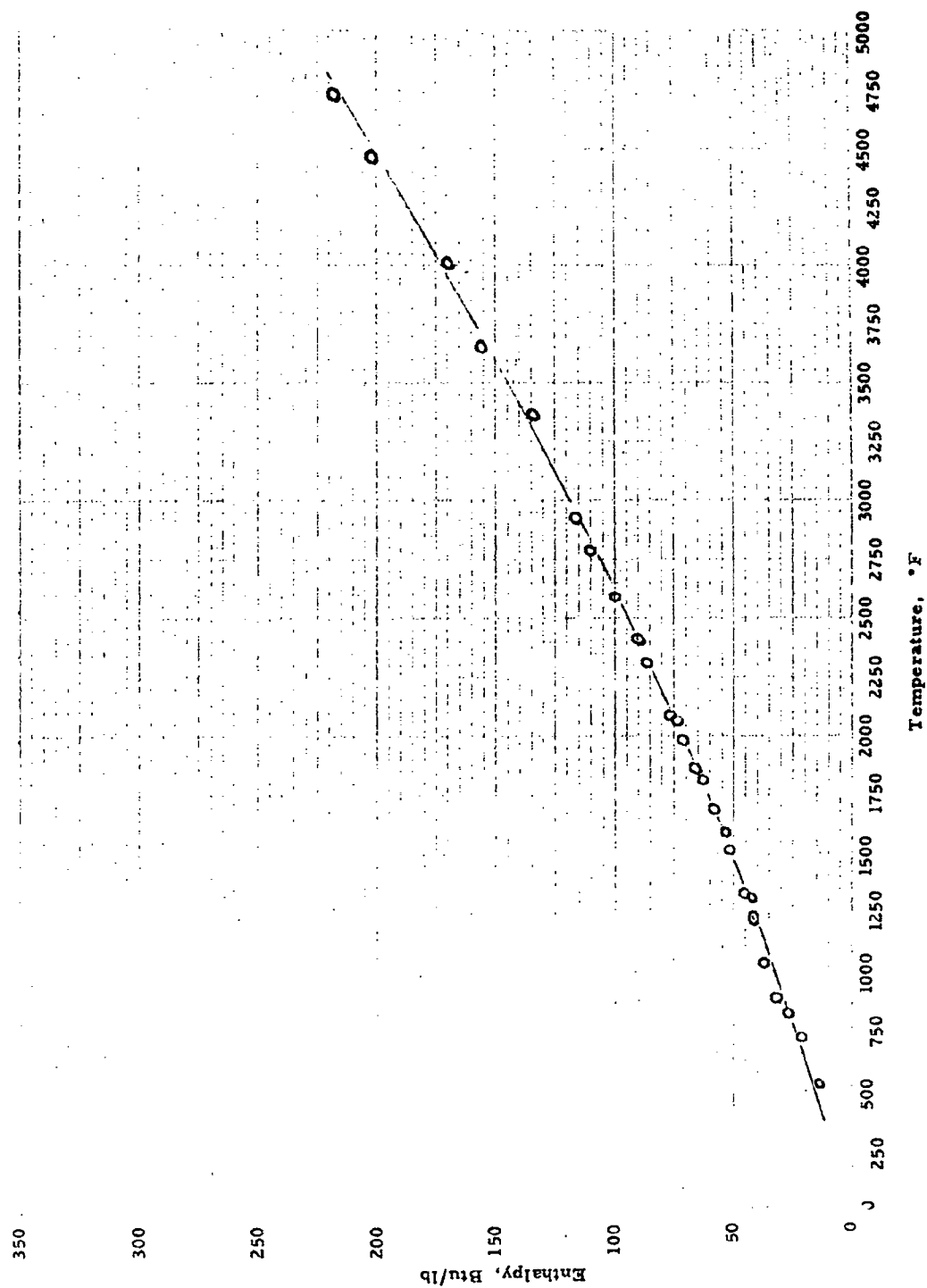


Fig. 33 ENTHALPY OF Ta-10W ALLOY

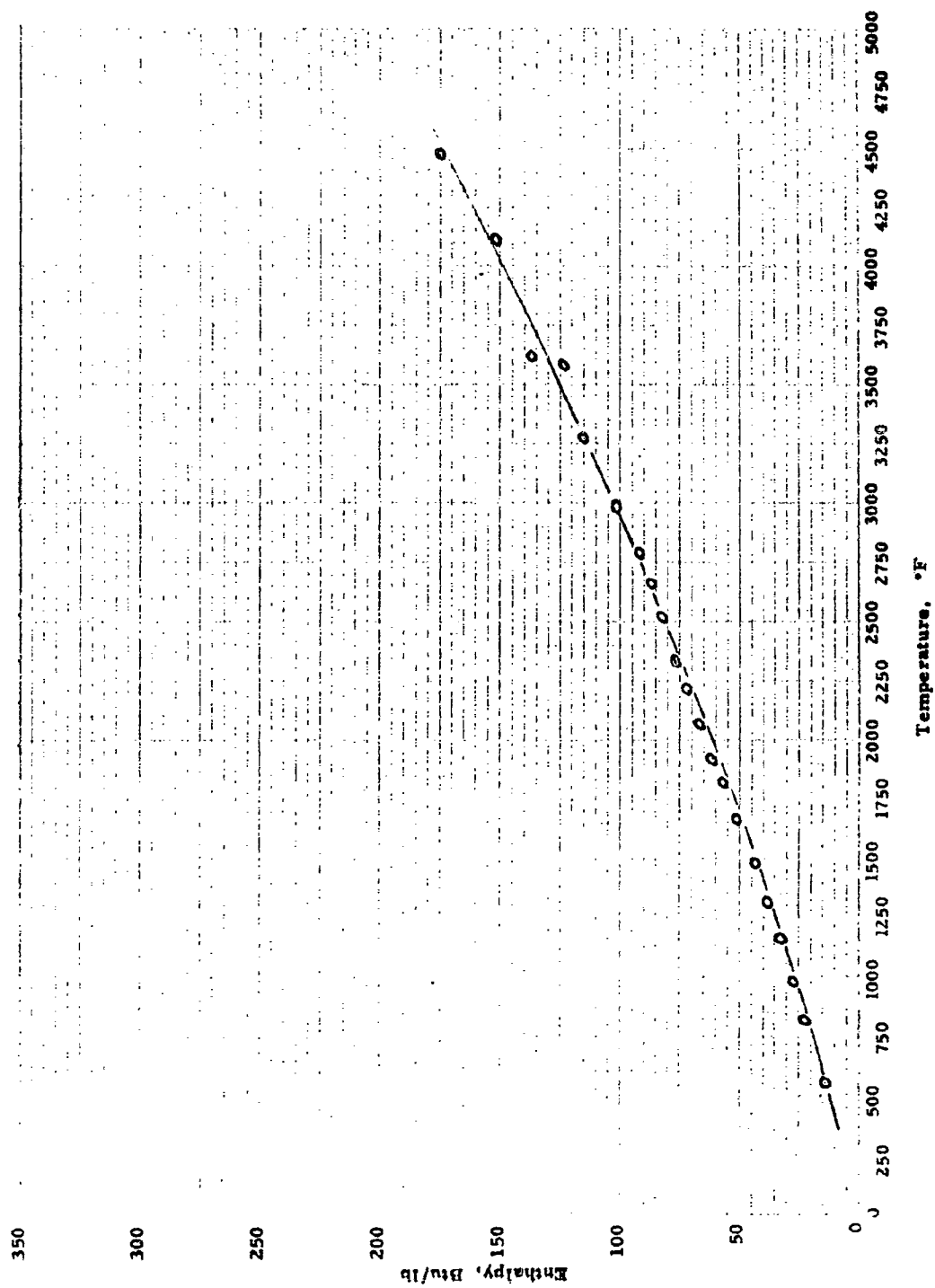


Fig. 34 ENTHALPY OF Ta-8W-2Hf ALLOY

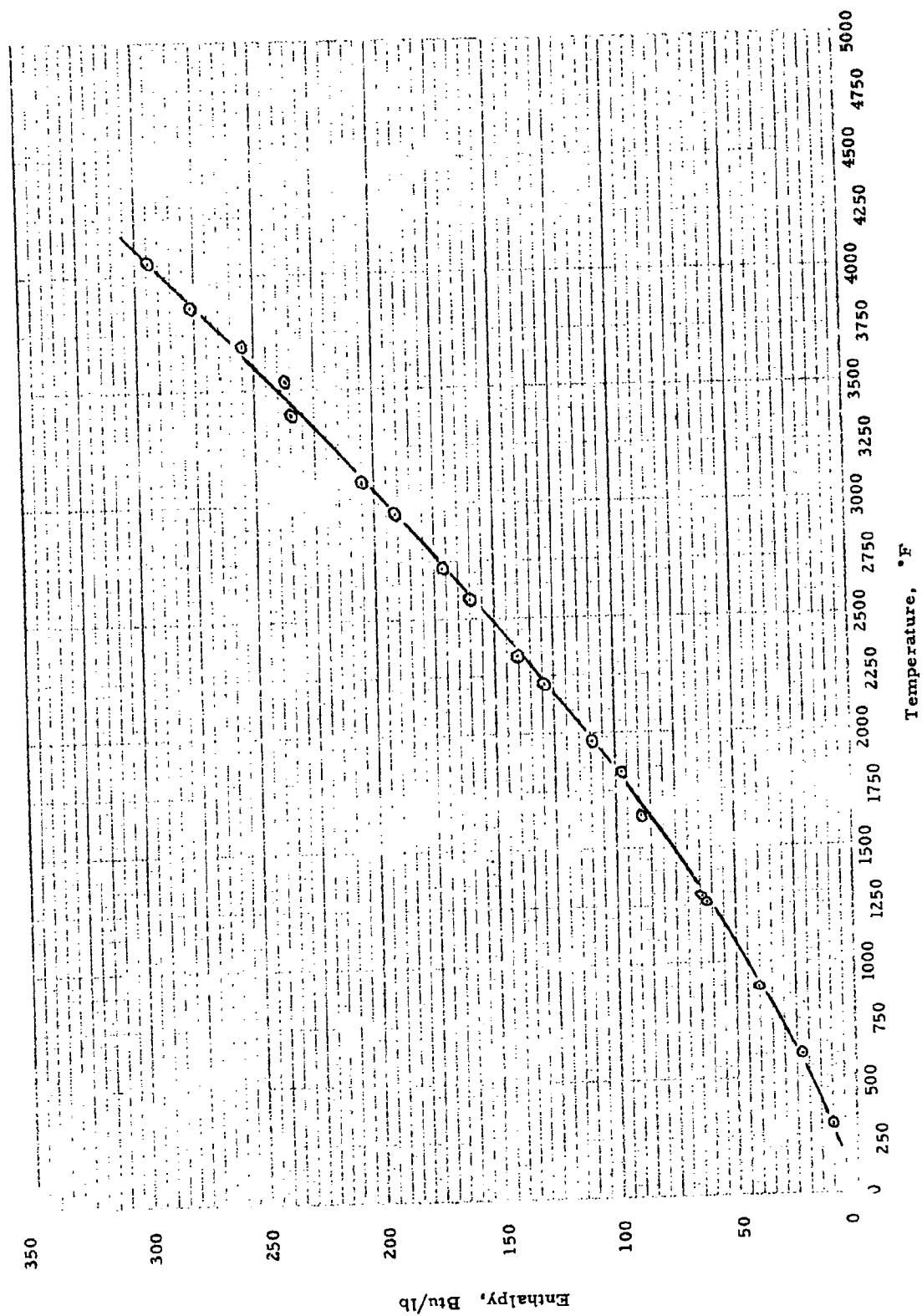


Fig. 35 ENTHALPY OF Ta-30Cb-7.5V ALLOY

The water equivalent of the system was determined by calibration with synthetic sapphire using the data of D. C. Ginnings.<sup>6</sup>

The enthalpy data were fitted by a least squares analysis to the cubic expression

$$\Delta H = a + b \cdot 10^{-3}T + c \cdot 10^{-6}T^2 + d \cdot 10^{-9}T^3 \quad (2)$$

Specific heat was then determined by differentiation of the above.

$$c_p = b \cdot 10^{-3} + 2c \cdot 10^{-6}T + 3d \cdot 10^{-9}T^2 \quad (3)$$

The enthalpy coefficients resulting from the analysis are presented in Table 33. The coefficients for the specific heat equation are given in Table 34. Specific heat for the materials tested are given in Figures 36, 37, 38, 39.

Specific heat data for Beryllia and Zirconium Nitride are shown in Figure 36 from References 2 and 3.

#### D. Experimental Accuracy

The accuracy of the specific heat data is determined by the accuracy of measurements of sample temperature and sample energy content. The sample temperature was determined by the use of two platinum/platinum-10% rhodium thermocouples in the temperature range 400° F to 3000° F. These thermocouples were suspended from the top of the furnace, and had junctions at the axial furnace position at which the sample is suspended. A thermocouple was inserted in a dummy sample to provide a comparison between the temperatures measured by the suspended thermocouples with the true sample temperature, as indicated by the thermocouple inserted in the sample. The temperature average measured by the suspended thermocouple agreed with that of the sample thermocouple to  $\pm 2^\circ$  F.

Sample temperatures in excess of 3000° F were measured with an optical pyrometer. This device has a precision of about  $\pm 5^\circ$  F.

The accuracy of measurement of sample energy content was determined by calibration of the system with synthetic sapphire using the enthalpy data of Ginnings.<sup>6</sup> There was excellent agreement between the two sets of data, as shown in Table 35.

The accuracy of the specific heat measurements is about  $\pm 5\%$  as based upon the indicated precision of sample temperature and sample energy content.

Table 33

ENTHALPY COEFFICIENTS

$$\Delta H = a + b \cdot 10^{-3}T + c \cdot 10^{-6}T^2 + d \cdot 10^{-9}T^3$$

with  $\Delta H \sim \text{Btu/lb}$

$T \sim ^\circ\text{F}$

Material	a	b	c	d
Boron Carbide	20	203	102	-8.1
Spinel	-71.4	249	22.9	-1.28
Zirconium Nitride	- 5.9	89.2	11.7	-0.91
Beryllium Oxide	- 9.00	317	53.0	-2.81
Cb-10W-1Zr-0.1C Alloy	0	57.7	2.43	0.460
Cb-5Mo-5V-1Zr Alloy	- 6.3	52.7	8.90	-0.463
Cb-10W-5Zr Alloy	1.2	60.1	- 1.28	1.34
Cb-10Ti-5Zr Alloy	1.90	59.8	6.10	0.260
Cb-15W-5Mo-1Zr-0.05C Alloy	1.70	58.6	0.222	1.03
Cb-27Ta-12W-0.5Zr Alloy	- 2.0	47.6	4.30	0.020
Mo-0.5Ti-0.08Zr Alloy	- 2.0	65.0	- 0.780	0.977
Mo-29.83W-0.07Zr-0.012C Alloy	0	44.7	3.74	0.630
Ta-10W Alloy	- 1.4	27.9	4.52	-0.206
Ta-8W-2Hf Alloy	5.8	22	2.61	0.163
Ta-30Cb- 7.5V Alloy	4.2	27.2	15.8	-1.26

Table 34

SPECIFIC HEAT COEFFICIENTS

$$c_p = b + 2c \cdot 10^{-3}T + 3d \cdot 10^{-6}T^2$$

with  $c_p \sim \text{Btu/lb-}^\circ\text{F}$   
 $T \sim ^\circ\text{F}$

Material	b	2c	3d
Boron Carbide	0.203	0.204	-0.0243
Spinel	0.249	0.0458	-0.00384
Zirconium Nitride	0.0892	0.0234	-0.00273
Beryllium Oxide	0.317	0.106	-0.00843
Cb-10W-1Zr-0.1C Alloy	0.0577	0.00486	0.00138
Cb-5Mo-5V-1Zr Alloy	0.0527	0.0178	-0.00139
Cb-10W-5Zr Alloy	0.0601	-0.00256	0.00402
Cb-10Ti-5Zr Alloy	0.0598	0.0122	0.000781
Cb-15W-5Mo-1Zr-0.05C Alloy	0.0586	0.000444	0.00309
Cb-27Ta-12W-0.5Zr Alloy	0.0476	0.00860	0.00006
Mo-0.5Ti-0.08Zr Alloy	0.0650	-0.00156	0.00293
Mo-29.83W-0.07Zr-0.012C Alloy	0.0447	0.00748	0.00189
Ta-10W Alloy	0.0279	0.00904	-0.000617
Ta-8W-2Hf Alloy	0.022	0.00532	0.000489
Ta-30Cb- 7.5V Alloy	0.0272	0.0316	-0.00378

Table 35  
ENTHALPY OF SYNTHETIC SAPPHIRE

Temperature, °F	Enthalpy Content, Btu/lb		
	NBS	ARF	Difference, %
423	78.4	77.9	-0.64
713	154.5	155.5	+0.65
971	225.6	223.7	-0.84
1169	281.2	282.0	+0.28

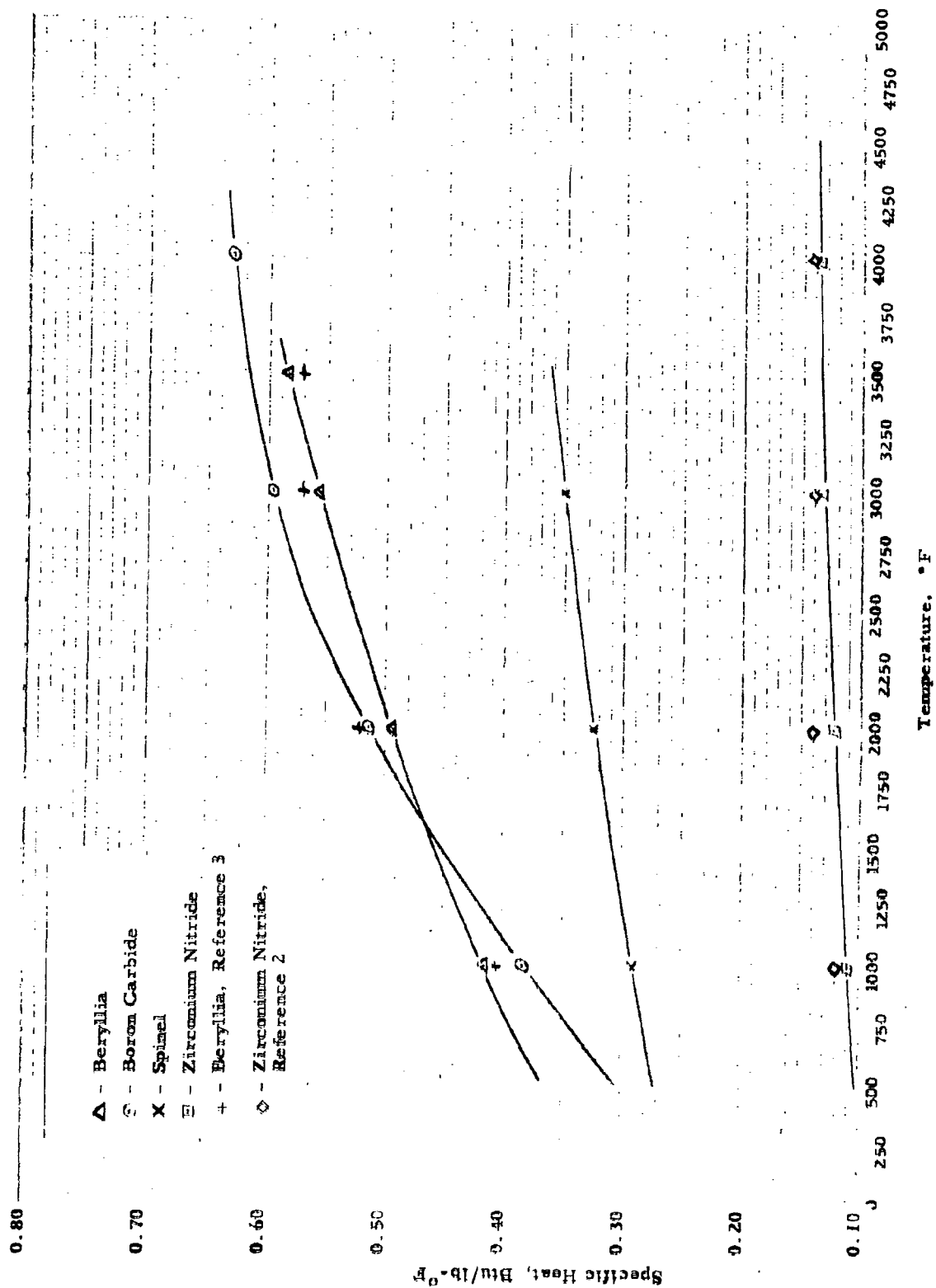


Fig. 36 SPECIFIC HEAT OF FOUR CERAMIC MATERIALS

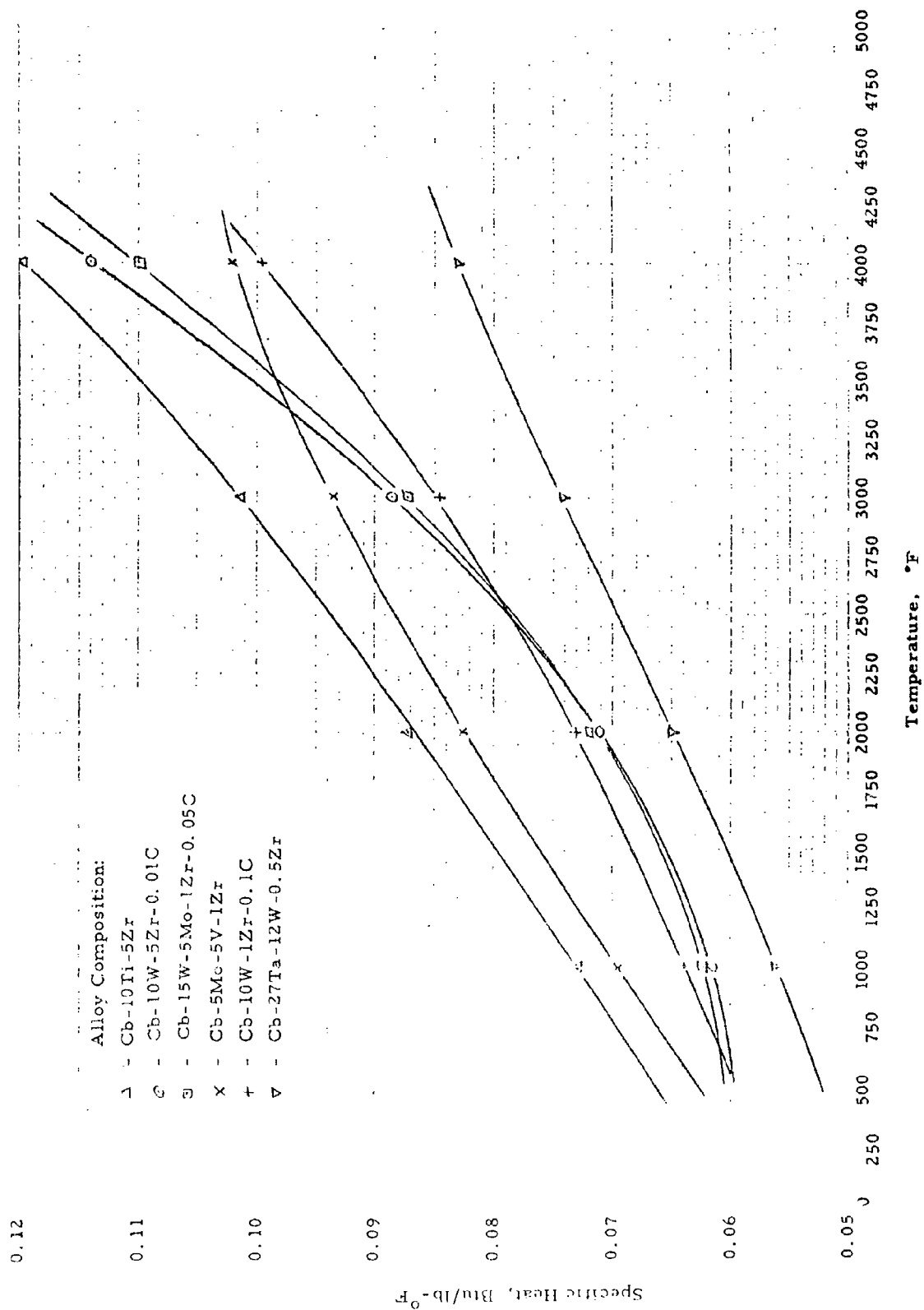


Fig. 37 SPECIFIC HEAT OF SIX COLUMBIUM ALLOYS

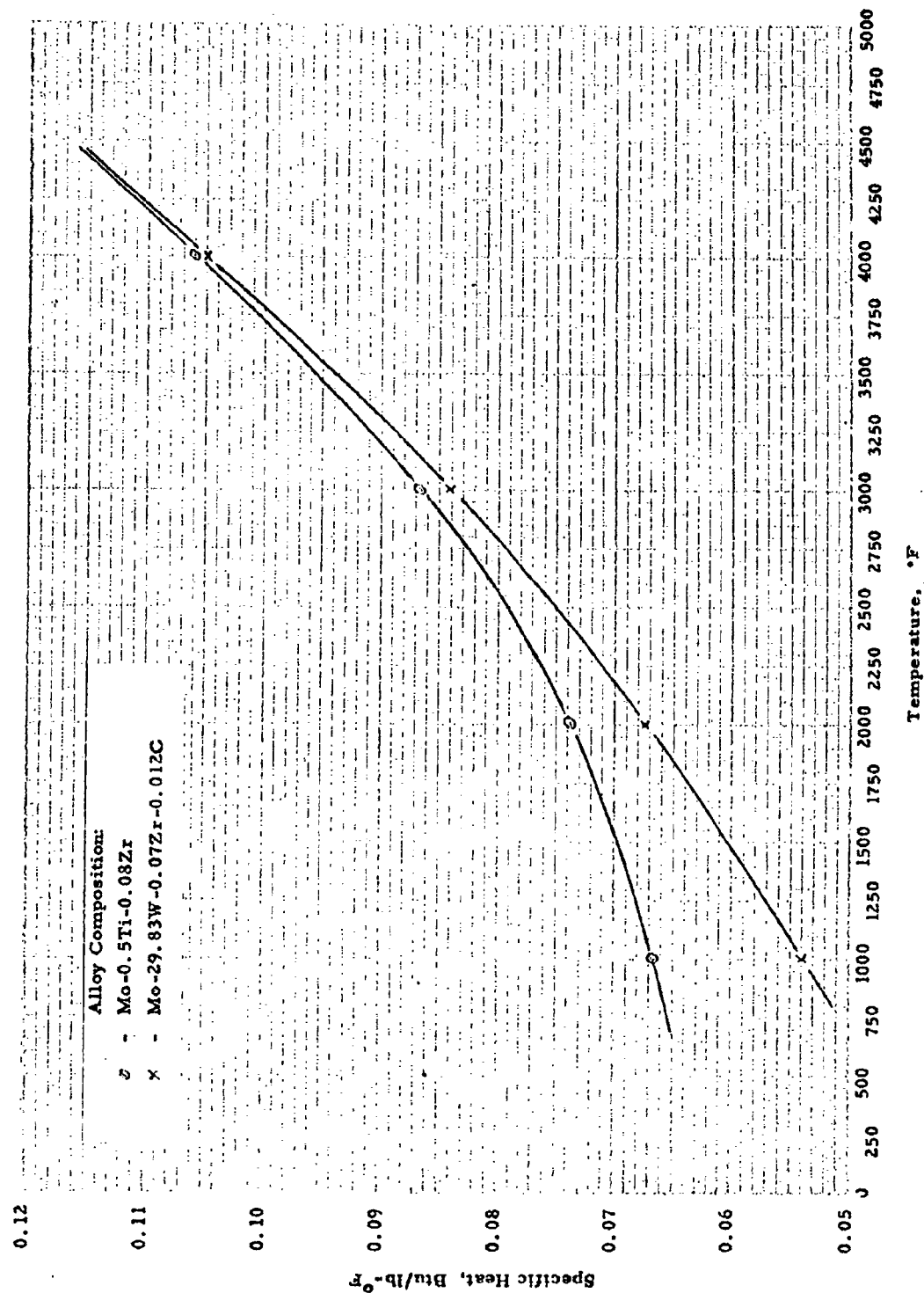


Fig. 38 SPECIFIC HEAT OF TWO MOLYBDENUM ALLOYS

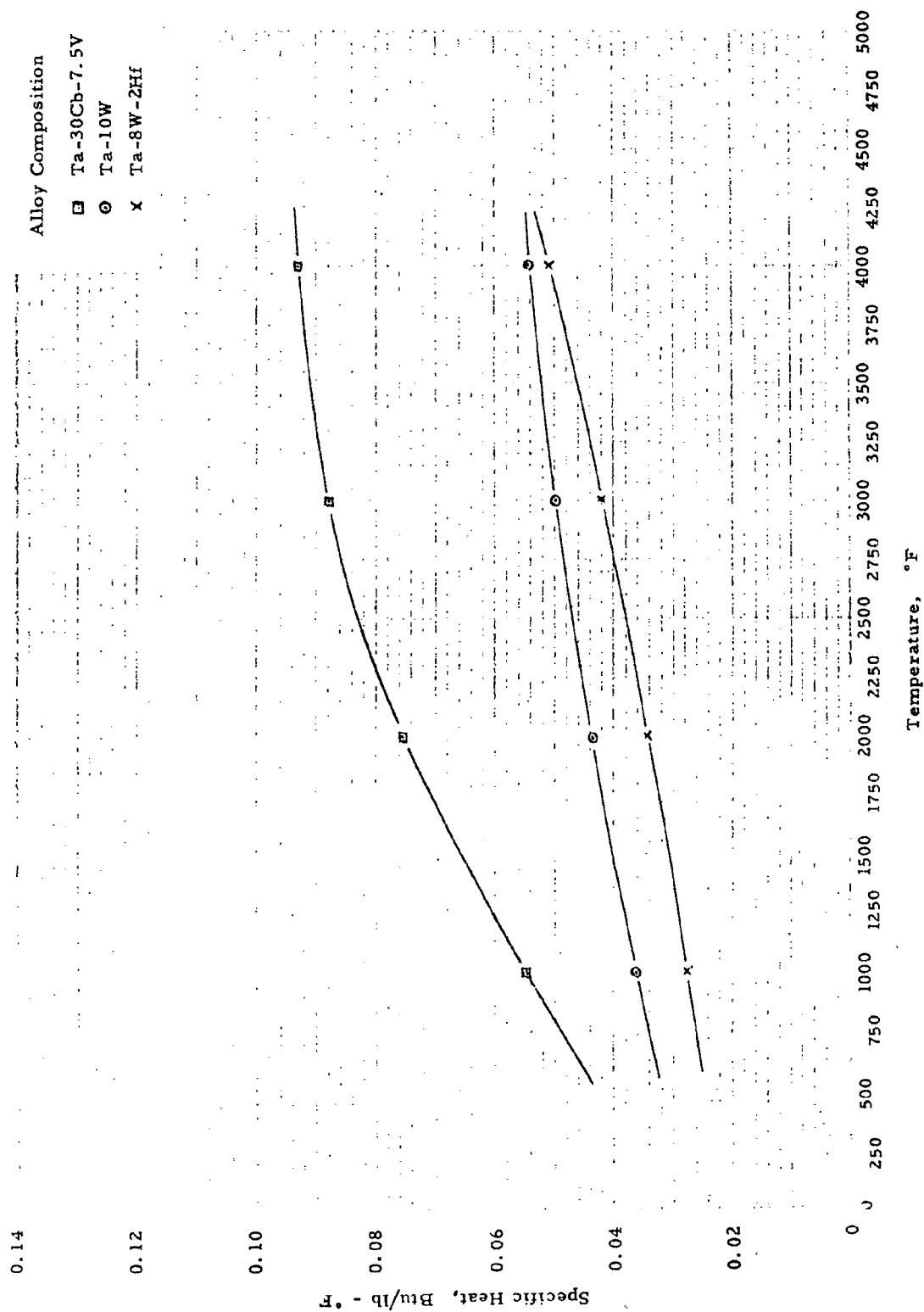


Fig. 39 SPECIFIC HEAT OF THREE TANTALUM ALLOYS

#### IV. THERMAL CONDUCTIVITY

The thermal conductivity of the selected materials was determined from room temperature to 1500°F by the split block method and from 1500 to approximately 4600°F by determining the thermal diffusivity and then calculating thermal conductivity from the measured values of thermal diffusivity, specific heat, and density.

##### A. Thermal Conductivity - Room Temperature to 1500°F

###### 1. Description of Equipment

The split block method was used to determine the thermal conductivity of the selected materials from room temperature to 1500°F. This method has the advantage of requiring a small quantity of test sample material; namely, a disk 2 inch diameter by 1 inch thick, which can also be used in the thermal diffusivity determinations. In this comparative method, the temperature drop through a material having a well-known thermal conductivity is compared to that through the unknown material. A vertical stack of three cylinders, two of which are Armco iron and the other being the test sample, are used. Heat flows axially through the cylinders from the top of the stack to the bottom. The temperature gradient in both Armco iron standards and the test specimen are measured by thermocouples located in holes along the length of the stack. The stack of cylinders was placed inside an electrically heated furnace in which an helium atmosphere was maintained. A section through the apparatus is shown in Figure 40.

As can be seen in Figure 40, heaters located at the top and bottom of the cylinders are used to adjust the axial heat flow along the length of the assembly. A guard heater surrounds the cylinders to prevent radial heat losses.

###### 2. Experimental Procedure

One disk of each material was machined to the following size, 2 inch diameter by 1 inch thick. Both faces of the disk were ground flat and parallel to reduce contact resistance to a minimum. Two 0.065 inch holes were drilled in the specimen as shown in Figure 40. Chromel-alumel thermocouple wires in alumina insulators were inserted in each hole. Three thermocouples were similarly installed in each of the Armco iron standards.

The furnace was continuously purged with helium during the experiments. Power was supplied to the top, bottom, and guard heaters to maintain the desired temperature gradient in the test sample at the temperature level desired. The temperature gradient in the test samples was maintained at approximately 10 to 20°F per inch during the tests.

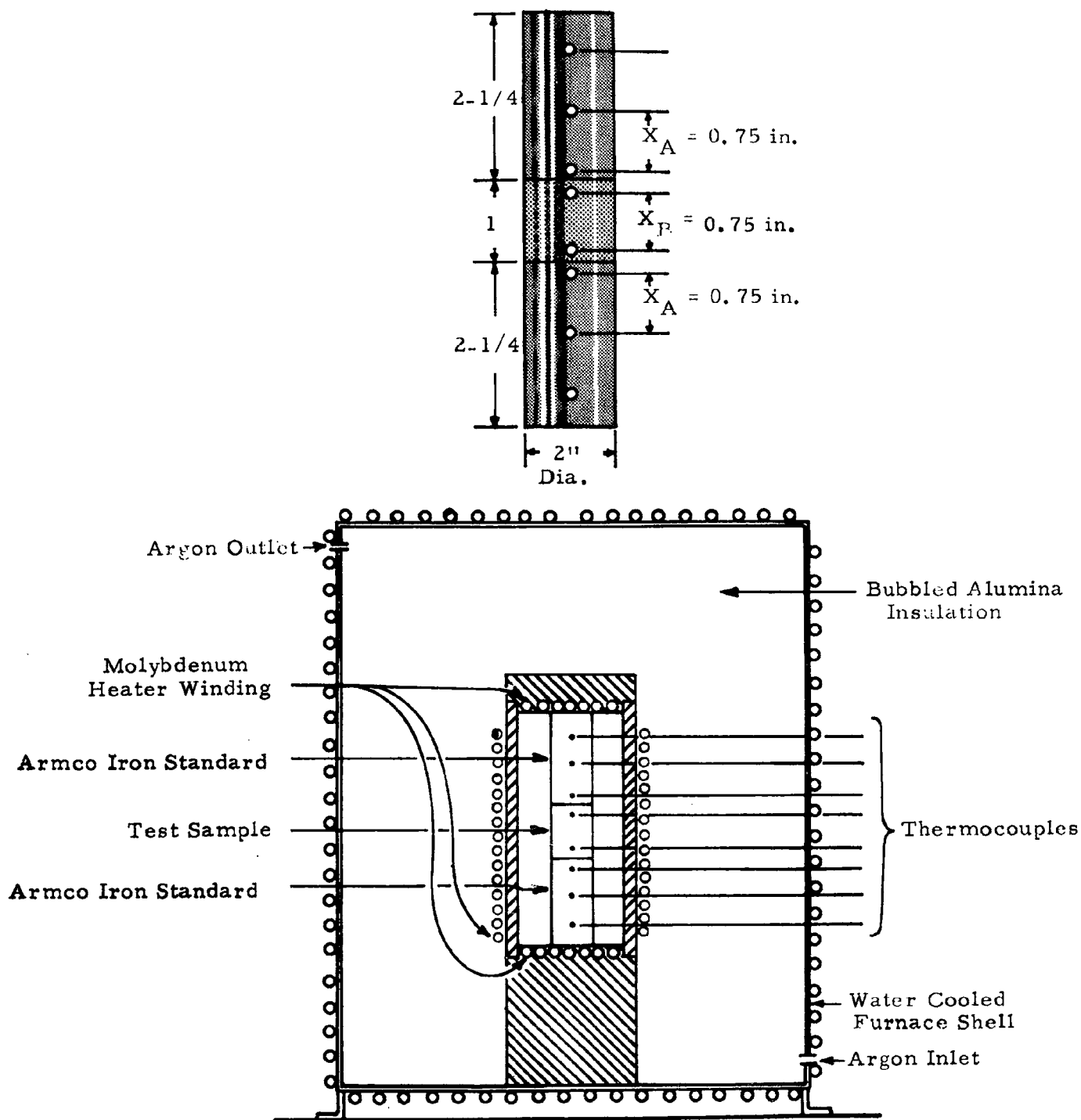


Fig. 40 APPARATUS FOR MEASURING THERMAL CONDUCTIVITY

After steady state conditions were reached at each desired temperature level, the thermocouple readings were recorded and the thermal conductivity was calculated as follows:

$$q = \frac{k A \Delta t}{\Delta x} \quad (4)$$

where:

$q$  = heat flow, Btu/hr

$A$  = cross sectional area,  $\text{ft}^2$

$\Delta t$  = temperature drop along the cylinder length,  $^{\circ}\text{F}$

$k$  = thermal conductivity, Btu/hr ft  $^{\circ}\text{F}$

$\Delta x$  = distance between thermocouples, ft

By proper guarding, the heat flow through the Armco iron standard will be equal to that through the test sample. Therefore, we can write:

$$q = \frac{k_a A_a \Delta t_a}{\Delta x_a} = \frac{k_b A_b \Delta t_b}{\Delta x_b} \quad (5)$$

where the subscripts  $a$  and  $b$  refer to the standards and test sample, respectively.

Solving for the thermal conductivity of the test sample, we have:

$$k_b = k_a \cdot \frac{A_a}{A_b} \cdot \frac{\Delta x_b}{\Delta x_a} \cdot \frac{\Delta t_a}{\Delta t_b} \quad (6)$$

### 3. Test Results

The thermal conductivity of fifteen materials is given in Tables 36 through 50 and in Figures 46 through 60.

### 4. Experimental Accuracy

Results of determinations of thermal conductivity of materials by the split block method and by the Powell stacked disk method, an absolute method, compare very well. Errors in measurement may result from improper guarding which allows heat loss from the periphery of the cylinders, poor contact between cylinder faces which distorts the heat flow pattern, etc. It is felt that the accuracy of results using this apparatus is within  $\pm 4\%$ .

### B. Thermal Diffusivity

#### 1. Introduction

This section describes a technique for the measurement of thermal diffusivity at elevated temperatures. Thermal diffusivity is defined as the ratio

$$\alpha = \frac{k}{\rho c_p} \quad (7)$$

where:

k is thermal conductivity

$\rho$  is density

$c_p$  is specific heat

It is evident that if thermal diffusivity, specific heat, and density are known, then thermal conductivity can be calculated by equation (7). Density and specific heat are more easily measured at high temperature than is thermal conductivity. The units of thermal diffusivity are  $(\text{length})^2 (\text{time})^{-1}$ ; the simplicity of these units suggest that this property may be more easily measured than the property thermal conductivity. The thermal diffusivity measurements achieved by the technique to be described were used for calculation of thermal conductivity by equation (7). Values of density and specific heat were obtained by independent measurements.

This section of the report is presented in the following order:

1. Discussion of the mathematical formulation
  2. Description of apparatus
  3. Discussion of measurement method.
2. Discussion of the Mathematical Formulation

The discussion will be concerned with isotropic media.

a. Statement of Problem

The problem to be considered is stated as follows: A laboratory model was specified for the thermal diffusivity measurement. It was then desired to find a solution to the analogous heat conduction problem, for boundary conditions which closely approximate the laboratory model. The problem solution then gives rise to an expression for calculation of thermal diffusivity. The laboratory model consists of a slab of material mounted in a furnace, and heated to a constant and uniform temperature. A heat sink which consists of a thin section of material is mounted exterior to the furnace, and is provided with a mechanical drive capable of rapidly thrusting the heat sink into the furnace. The heat sink remains in the furnace, then the drive mechanism rapidly removes it from the furnace. The sink does not physically contact the slab. Since the sink is at room temperature, radiation heat interchange occurs between the slab face and the heat sink, causing the slab to drop in temperature. The temperature behavior at a point in the slab is observed, and it would be expected that the temperature would decrease, the decrease resulting from exposure of the slab face to the heat sink.

b. Mathematical Formulation

The laboratory model presented above was formulated mathematically as follows:

1. Assume a semi-infinite slab, having a semi-infinite extent in the direction of heat flow, and infinite in extent in a direction normal to heat flow. The heat flow is assumed unidirectional, and the slab face is taken as the zero of the coordinate system. The diffusion equation then takes the form:

$$\frac{\partial^2 \theta}{\partial x^2} = \frac{1}{\alpha} \frac{\partial \theta}{\partial t} \quad (8)$$

where:

$\theta$  is temperature

$x$  is a spatial coordinate, measured in a direction normal to the slab face

$t$  is time.

2. The boundary conditions are:

(a) At  $t = 0$ ,  $\theta = 0$  everywhere

(b) At  $t > 0$ ,  $x = 0$ ,  $-k \frac{\partial \theta}{\partial x} = \epsilon \sigma \theta_s^4$ , that is, the heat flux at the slab surface is given by a radiation boundary condition.

It is assumed that the absolute temperature of the heat sink is small. For boundary condition b,

$\epsilon$  is emissivity

$\sigma$  is the Stefan-Boltzmann constant

$\theta_s$  is the absolute temperature at the slab surface.

3. The solution of equation (8) for  $t > 0$ , and the listed boundary conditions is given below.

$$\theta = \theta_0 (1 - 2Y \operatorname{ierfc} X + 16Y^2 i^2 \operatorname{erfc} X - 189.1Y^3 i^3 \operatorname{erfc} X + 2787Y^4 i^4 \operatorname{erfc} X - \dots) \quad (9)$$

where:

$$X = \frac{x}{2\sqrt{\alpha t}} \quad (10)$$

$$Y = \frac{\epsilon \sigma \theta_0^3 t^{1/2}}{\alpha^{1/2} \rho c_p}$$

### 3. Description of Apparatus

The apparatus is to be described in the following order: 1. ) furnace and associated systems, and 2. ) instrumentation.

#### a. Description of Furnace

The furnace and auxiliary furnace systems are described with the aid of Fig. 41, 42, 43 and 44.

##### 1. Furnace Details

Figure 41 is a cutaway view of the furnace. The foreground of this view is occupied by an optical system which is used to detect the temperature change of the sample. The furnace proper is a box fabricated from  $1/8$ " steel, having interior dimensions of 42" in length, 15" high by 15" deep. The box is provided with a bolt on cover, and external cooling coils, as shown in Fig. 41. Two aligned openings were cut in the box sides, at the center of the furnace. One opening was provided with a gate, and was used for entrance of the heat sink into the furnace. The second opposite opening was provided with a gate and window, and was used for sighting the sensor on the sample.

The heat source used in the furnace was a horizontal graphite tube, 52" in length by 3" inside diameter. The central 20" of the tube was machined to a wall thickness of  $1/16$ ", the wall thickness was increased to  $1/8$ " at a distance of 10" from the center, for a length of 13".

Two slots were machined at the heater center. The slots were cut diametrically opposed,  $7/16$ " wide by  $2-1/4$ " long. The slot shown in the tube front of Fig. 41 was used for sample sighting, and had two  $1/4$ " radius cuts as shown. The slot in the back of the tube, was to accommodate the heat sink.

The graphite tube was inserted in copper electrodes mounted exterior to the furnace. The electrodes were water cooled, provided with a water cooled, gasketed window. The electrode was mounted on a bed, and was free to move under the influence of the high temperature heater elongation. A high temperature tape seal was used between the copper electrode, and the furnace ends.

The bulk of the furnace interior was filled with Thermax insulation. A graphite ring having slotted arms was mounted in the furnace center, as shown in Fig. 41. The slotted arms extended to the furnace wall, providing for sample sighting and entrance of the heat sink. A view of the sample configuration is shown encircled in Fig. 41. The sample was mounted on a graphite boat such that the top surface of the sample was exposed to the heat sink. The heat sink was in the form of a flat plate,  $1/8$ " thick,  $2-1/4$ " wide, 16" in length. The heat sink is shown above the sample in

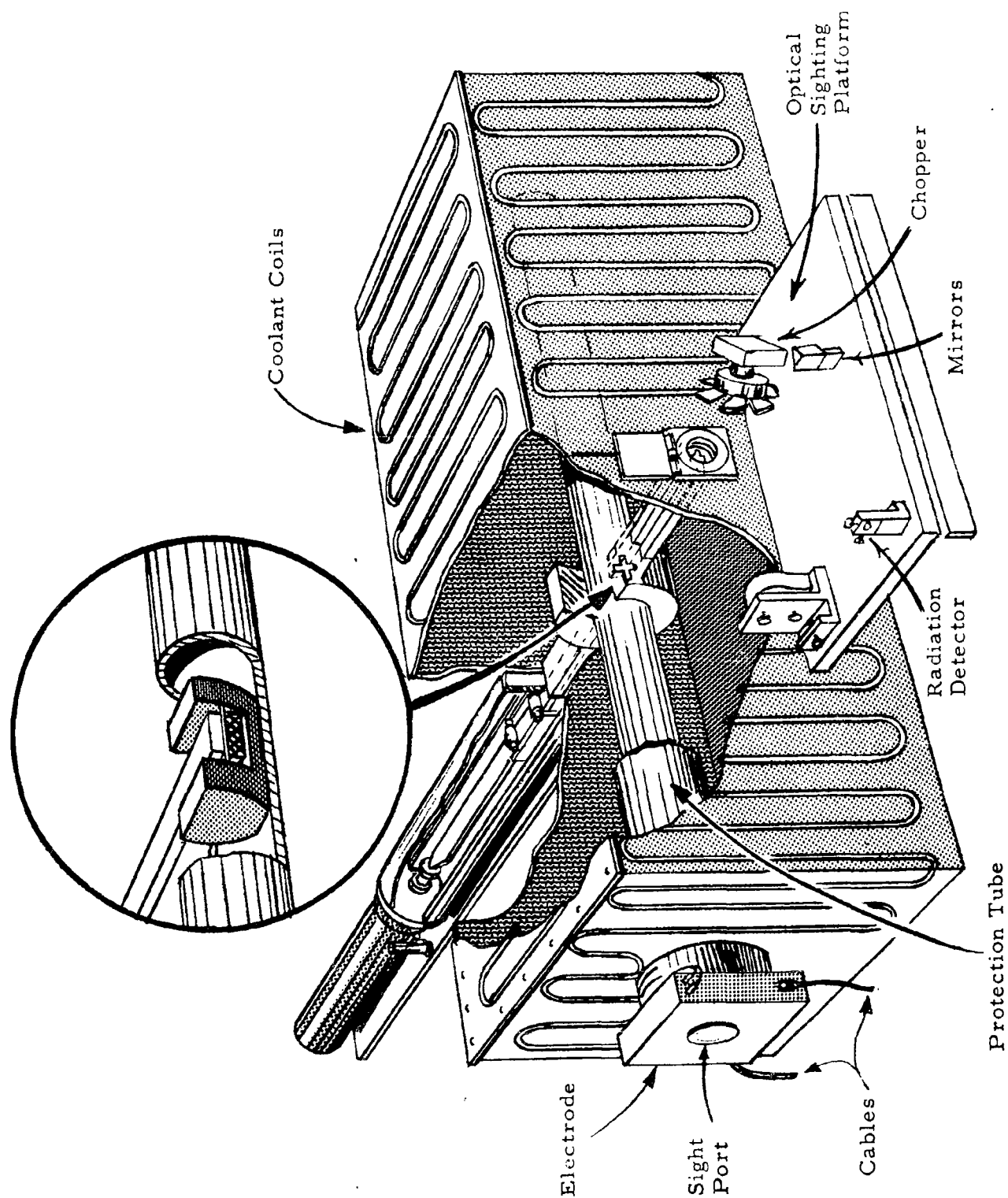
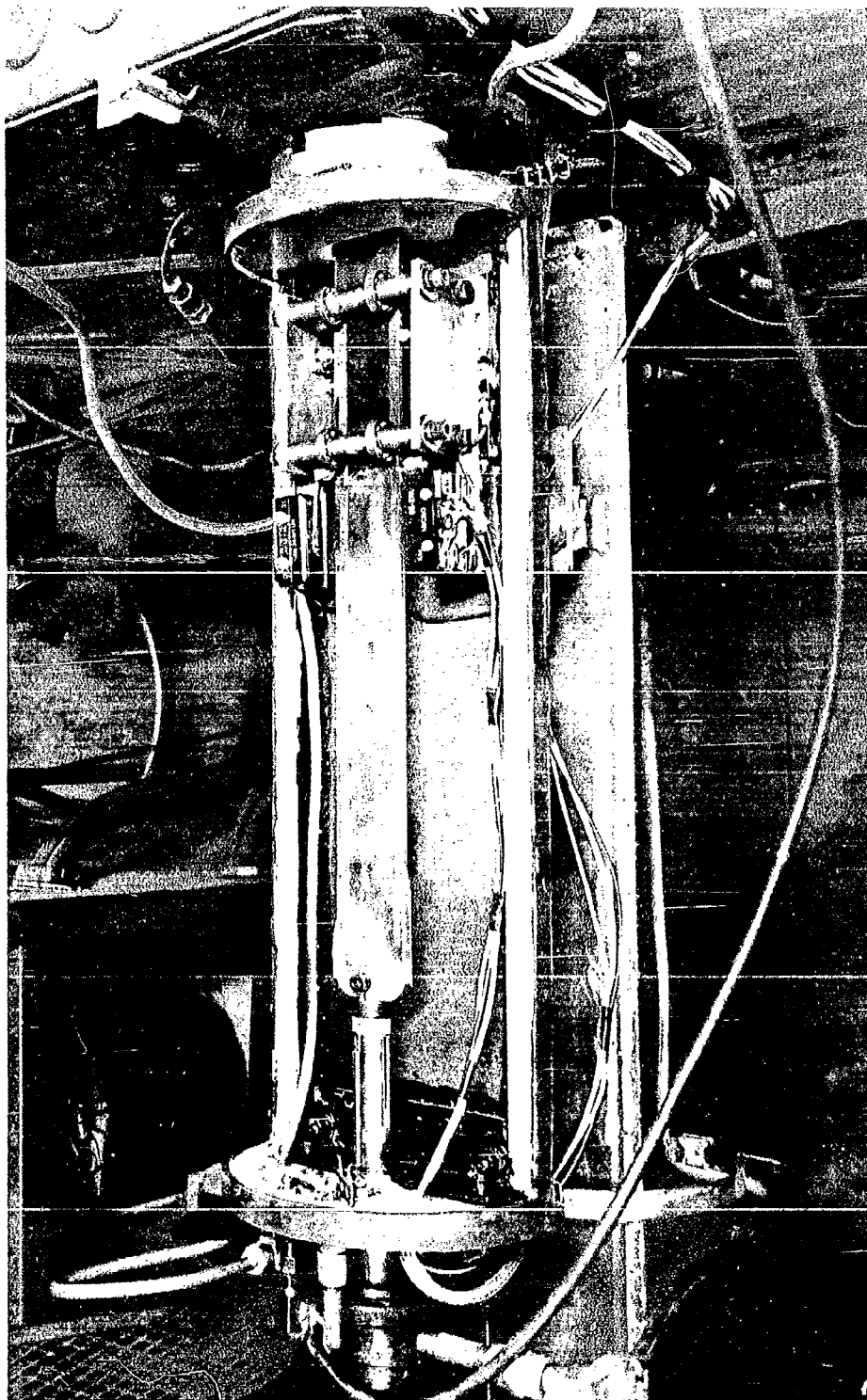
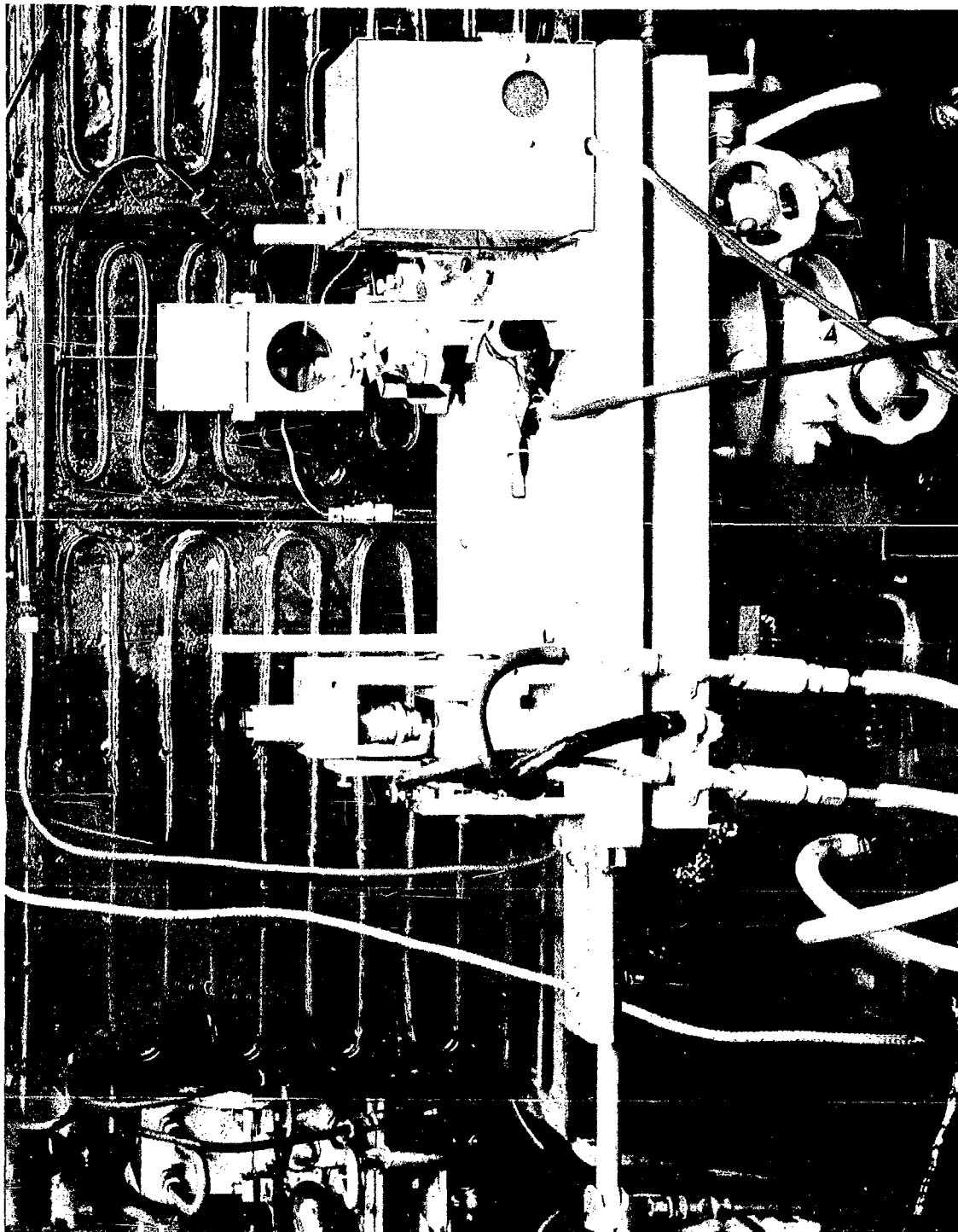


Fig. 41 CUTAWAY VIEW OF DIFFUSIVITY FURNACE.



**Fig. 42** VIEW OF HEAT SINK MOUNT



**Fig. 43** VIEW OF OPTICAL MOUNT

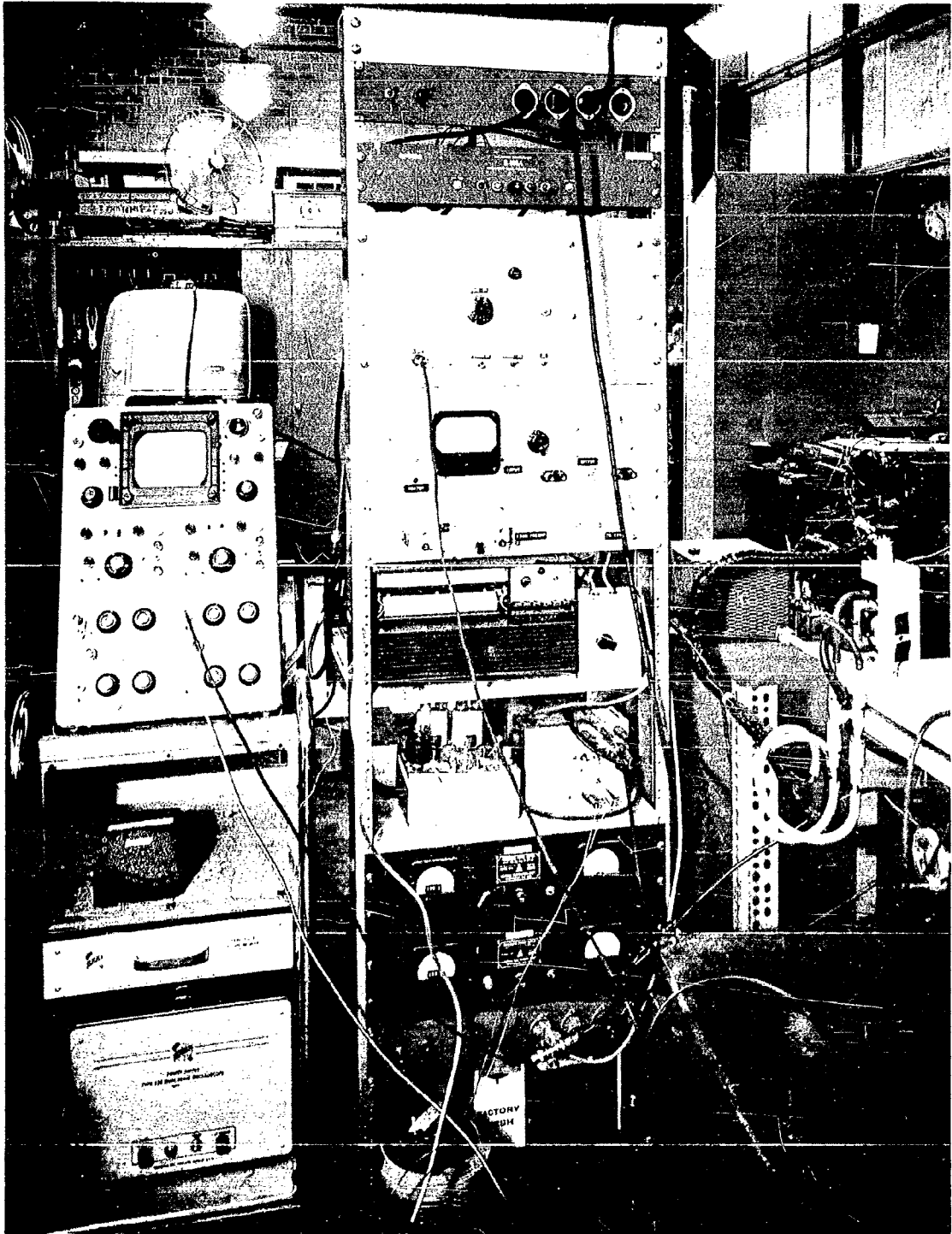


Fig. 44 VIEW OF INSTRUMENTATION SYSTEM

the circle view of Fig. 41. The heat sink housing is shown in back of the furnace in the large view of Fig. 43. The heat sink housing and drive is discussed below.

A portion of the protection tube is shown in Fig. 41. Two protection tube sections were suspended from the furnace ends, and were dovetailed around the central protection tube. The dovetail joint allowed for expansion of the protection tubes.

## 2. Heat Sink Details

Figure 42 shows the details of the heat sink, and heat sink mount. The heat sink was mounted between 10 bearings, two sets of four bearings each restricted the vertical movement of the sink; one set of bearings restricted the horizontal movement. The heat sink was driven by an air actuated double acting piston having a 10" stroke. The two microswitches shown mounted on either side of the heat sink were actuated by the sink when the sink was extended into the furnace. The signal produced by the microswitches was used to indicate the start of the temperature excursion. A cover was fitted to the rubber gasket shown in Fig. 42, so that an inert atmosphere could be maintained in the heat sink housing.

## 3. Optical Mount Details

The details of the optical system are shown in Fig. 43. The radiation from the sample was chopped by a chopper shown in the background of Fig. 43. The chopped radiation was focused by a spherical mirror shown in the left background of Fig. 43. The detector is shown in the left foreground of this figure. An optical nulling system was used to provide a zero output level at any temperature level. The null source was a 12 volt tungsten filament lamp located in the gray box, right foreground, Fig. 43. The radiation from the nulling lamp was inserted into the optical path by reflection from the back surface of the chopper. A series of optical mirrors is also shown in Fig. 43. These mirrors provided for folding of the optical path.

The detector was a photoconductive lead sulphide cell having dimensions 0.014" in width, 0.014" in height. The surface of the lead sulphide cell was cooled by blowing a stream of helium across the detector surface. The helium was cooled to a temperature of  $-120^{\circ}\text{F}$  by passing the gas through a copper coil immersed in a dry ice-acetone bath. Cooling the detector resulted in a large increase in sensitivity over operation at room temperature.

## 4. Measurement of Sample Temperature

The measurement of sample temperature was done by an optical pyrometer. The sample was observed by sighting down the axis of the graphite heater into a hole in the sample block. The graphite heater was plugged with a roll of carbon cloth, reducing the effective area for radiation from the furnace hot zone from a circle 3" in diameter, to a circle 1" in diameter.

A disappearing filament pyrometer was used for this purpose, the pyrometer was a model 8622 manufactured by the Leeds and Northrup Company.

b. Description of Instrumentation

The details of the instrumentation system are shown in Fig. 44. The detector signal was routed to a wide band low noise transistor amplifier, then to a narrow band amplifier having a fixed gain of 10. The narrow band amplifier had a fixed band width of 5 cps, centered at the chopper frequency of 150 cps. The signal was routed from the narrow band amplifier to a vacuum tube voltmeter. The latter instrument provided signal attenuation and detection. The detected signal was then routed to an oscillograph for readout. The oscillograph is shown in the center of the instrumentation stack, Fig. 44. The oscilloscope shown in the figure was used as an alternate readout device.

Signal nulling was achieved by control of current to the nulling lamp. A stabilized amplifier provided control of the current to the lamp, the lamp voltage source was a 12 volt wet cell. Lamp current was varied by means of a micropot providing very sensitive current control.

The signal from the vacuum tube voltmeter was recorded by the oscillograph on a roll of light sensitive paper. Simultaneously a timing system imprinted timing lines on the paper, the timing interval could be selected at 1.0, 0.10, or 0.01 second. The paper speed was variable at 1/4, 1, 4, 16, and 64 inches per second.

An oscillograph channel was also used for recording the entrance time of the heat sink over the exposed face of the sample. This circuitry consisted, simply, of a microswitch and a source of voltage, both in series with an oscillograph galvanometer. The microswitch is actuated by a small node on the moving heat sink, causing a momentary galvanometric deflection. The microswitch had a response time of three milliseconds.

A typical curve resulting from a temperature excursion is shown in Fig. 45. Time is determined as moving from left to right. The entrance time of the heat sink is determined by the abrupt galvanometer deflection (curve A). The decreasing temperature signal is shown in curve B.

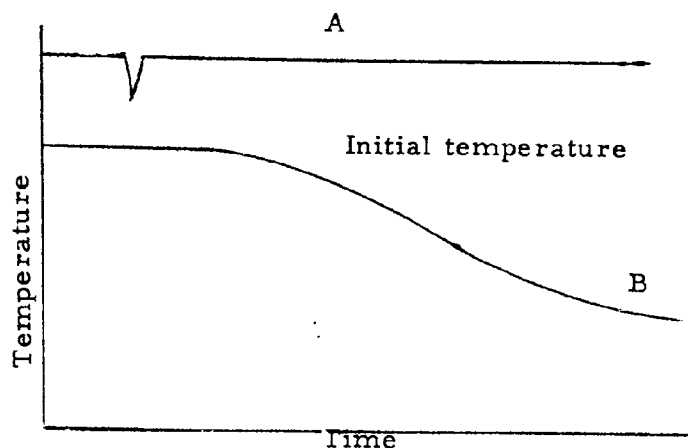


Fig. 45 TYPICAL TEMPERATURE-TIME TRACE

#### 4. Measurement Technique

The technique of measurement is described below:

i. The furnace temperature is brought to a steady state temperature level.

ii. The optical system was sighted on a hole drilled in the sample. The sample hole was 1" deep, and located 1/8" from the sample surface. The diameter of the sight hole varied from 0.055" at the surface of the sample, to 0.024" at the hole bottom. The optical system was mounted on a rotary table, the rotary table in turn was mounted on a vertical slide. It was possible then to achieve linear movement of the optical system in the XYZ directions, and rotational movements in horizontal and vertical planes. The detector output was at a maximum when the optical axis and sighting hole axis were in alignment, thus determining when the optical system was sighted down the hole.

iii The sample temperature was read with the optical pyrometer.

iv. The signal from the detector was nulled by varying the current to the nulling lamp to achieve a minimum reading on the vacuum tube voltmeter. Then the signal was switched to the oscillograph, and the latter instrument was started.

v. The air piston was actuated by a hand valve, moving the heat sink into the slab region. Then after a short pause, the heat sink was removed.

vi. The curves resulting from the test are shown typically in Fig. 45. All necessary data is now available for calculation of thermal diffusivity.

vii The steps ii through vi were repeated at the same sample temperature level.

viii The furnace temperature was changed, and steps i to vii were repeated.

## 5. Calculation of Thermal Diffusivity

The thermal diffusivity is calculated by the application of equation (9) to the data of Fig. 45. Equation (9) is rearranged:

$$\frac{\alpha^{1/2} \rho_c p (\theta_o - \theta)}{2\epsilon \sigma \theta_o^3} = \phi = t^{1/2} \text{ierfc} \frac{x}{2\sqrt{\alpha t}} \quad (11)$$

Equation (11) is integrated with respect to time:

$$\int_0^{\bar{t}} \phi dt = \zeta(\bar{t}) = 4\bar{t}^{3/2} i^3 \text{erfc} \frac{x}{2\sqrt{\alpha \bar{t}}} \quad (12)$$

The ratio of equation (12) to (11) is taken yielding:

$$\frac{\zeta(\bar{t})}{\phi(\bar{t})} = \frac{4\bar{t} i^3 \text{erfc} \frac{x}{2\sqrt{\alpha \bar{t}}}}{\text{ierfc} \frac{x}{2\sqrt{\alpha \bar{t}}}} \quad (13)$$

Dividing both sides of (13) by  $\bar{t}$ :

$$\xi(\bar{t}) = \frac{\zeta(\bar{t})}{\bar{t}\phi(\bar{t})} = \frac{4 i^3 \text{erfc} \frac{x}{2\sqrt{\alpha \bar{t}}}}{\text{ierfc} \frac{x}{2\sqrt{\alpha \bar{t}}}} \quad (14)$$

The term  $\xi(\bar{t})$  has significance relative to Fig. 45. The term  $\zeta(\bar{t})$  is proportional to the integrated area between the initial steady state temperature, and the temperature excursion. The term  $\bar{t}\phi(\bar{t})$  is proportional to the area of the rectangle having length  $t$ , and height  $\phi(\bar{t})$ , where  $\phi(\bar{t})$  is the temperature excursion. A calculation of the ratio of the measured, indicated areas gave a numerical value for (14). The right hand side of equation (14) was plotted as a function of  $x^2/4\alpha\bar{t}$  and given the numerical value for the area ratio of (14), the plot could be used to determine  $x^2/4\alpha\bar{t}$ ,  $t$  and  $x$  are known, consequently could be calculated.

Then equation (7) was used to obtain thermal conductivity, where  $c$  and  $\rho$  were determined by independent measurements, as discussed previously.

The resulting thermal conductivity values are listed in the following tables. The tables list the thermal conductivity for the temperature range 300°F to 1500°F as measured by the split block method. The thermal conductivity values calculated from measured thermal diffusivity are listed, along with measured specific heat and density. The thermal conductivities of the materials tested are presented in Figures 46 to 60. The thermal conductivities of Zirconium Nitride and Beryllia from References 2 and 3 are shown in Figures 48 and 49, respectively.

Table 36

## THERMAL CONDUCTIVITY OF BORON CARBIDE

Temperature °F	Thermal Diffusivity ft <sup>2</sup> /hr	Specific Heat Btu/lb °F	Density lb/ft <sup>3</sup>	Thermal Conductivity Btu/hr ft °F
385				14.3
510				12.9
775				11.0
1060				9.80
1405				9.00
1643	0.118	0.467	154	8.49
1905	0.111	0.502	153	8.53
2245	0.100	0.538	153	8.23
2790	0.095	0.581	152	8.46
3005	0.094	0.595	151	8.49
3283	0.096	0.603	151	8.74
3520	0.097	0.612	150	8.91
3765	0.098	0.623	150	9.18
3990	0.099	0.629	149	9.35
4185	0.101	0.633	149	9.53

Table 37

THERMAL CONDUCTIVITY OF SPINEL ( $\text{MgO-Al}_2\text{O}_3$ )

Temperature °F	Thermal Diffusivity $\text{ft}^2/\text{hr}$	Specific Heat $\text{Btu/lb-}^\circ\text{F}$	Density $\text{lb/ft}^3$	Thermal Conductivity $\text{Btu/hr-ft-}^\circ\text{F}$
180				4.50
450				3.30
730				2.60
1070				2.20
1380				2.10
1655	0.0392	0.313	160	1.96
1905	0.0365	0.321	159	1.86
2290	0.0362	0.332	158	1.90
2535	0.0352	0.339	157	1.87
2975	0.0354	0.350	156	1.93
3140	0.0363	0.353	155	1.99

Table 38

THERMAL CONDUCTIVITY OF ZIRCONIUM NITRIDE

Temperature °F	Thermal Diffusivity ft <sup>2</sup> /hr	Specific Heat Btu/lb-°F	Density lb/ft <sup>3</sup>	Thermal Conductivity Btu/hr-ft-°F
275				6.3
478				7.3
583				7.4
910				8.8
1260				10.5
1550	0.256	0.117	398	11.1
2010	0.274	0.121	395	13.1
2245	0.279	0.122	394	13.4
2490	0.282	0.127	392	14.0
2705	0.279	0.129	391	14.1
2930	0.278	0.131	390	14.2
3080	0.269	0.132	389	13.8
3175	0.265	0.132	388	13.6
3410	0.260	0.133	387	13.4
3570	0.256	0.134	386	13.2
3694	0.252	0.134	385	13.0

Table 39

## THERMAL CONDUCTIVITY OF BERYLLIUM OXIDE

Temperature °F	Thermal Diffusivity ft <sup>2</sup> /hr	Specific Heat Btu/lb-°F	Density lb/ft <sup>3</sup>	Thermal Conductivity Btu/hr-ft-°F
350				85.6
500				70.1
790				44.0
1120				27.5
1410				18.2
1790	0.150	0.479	174	12.5
2250	0.103	0.511	173	9.1
2770	0.0818	0.543	171	7.6
3130	0.0772	0.564	170	7.4
3500	0.0683	0.584	168	6.7

Table 40

THERMAL CONDUCTIVITY OF Cb-10W-1Zr-0.1C ALLOY

Temperature °F	Thermal Diffusivity ft <sup>2</sup> /hr	Specific Heat Btu/lb-°F	Density lb/ft <sup>3</sup>	Thermal Conductivity Btu/hr-ft-°F
210				30.5
550				32.7
830				34.5
1170				36.5
1360				37.7
1610	1.04	0.0692	552	39.8
1995	1.03	0.0730	549	41.3
2280	1.02	0.0762	548	42.5
2720	0.987	0.0810	543	43.4
3070	0.982	0.0858	540	45.5
3470	0.943	0.0912	537	46.2
3960	0.905	0.0990	531	47.6

Table 41

THERMAL CONDUCTIVITY OF Cb-5Mo-5V-1Zr ALLOY

Temperature °F	Thermal Diffusivity ft <sup>2</sup> /hr	Specific Heat Btu/lb-°F	Density lb/ft <sup>3</sup>	Thermal Conductivity Btu/hr-ft-°F
175				23.0
410				24.9
780				27.5
1020				29.1
1310				31.8
1525	0.802	0.0765	528	32.4
1868	0.826	0.0805	525	34.9
2180	0.837	0.0845	522	36.9
2530	0.835	0.0886	519	38.4
3000	0.862	0.0937	515	41.6
3555	0.847	0.0988	510	42.7
3860	0.840	0.101	508	43.1
4055	0.980	0.102	506	44.2

Table 42

THERMAL CONDUCTIVITY OF Cb-10W-5Zr ALLOY

Temperature °F	Thermal Diffusivity ft <sup>2</sup> /hr	Specific Heat Btu/lb-°F	Density lb/ft <sup>3</sup>	Thermal Conductivity Btu/hr-ft-°F
180				26.2
375				27.6
610				28.1
835				28.3
1230				30.5
1516	0.836	0.0655	562	30.8
2072	0.850	0.0718	557	34.0
2498	0.748	0.0783	554	34.6
3190	0.721	0.0928	547	36.6
3580	0.660	0.103	544	37.0
3970	0.639	0.113	540	39.0

Table 43

THERMAL CONDUCTIVITY OF Cb-10Ti-5Zr ALLOY

Temperature °F	Thermal Diffusivity ft <sup>2</sup> /hr	Specific Heat Btu/lb-°F	Density lb/ft <sup>3</sup>	Thermal Conductivity Btu/hr-ft-°F
155				16.6
482				18.0
823				19.6
1110				20.9
1436				22.7
1530	0.603	0.0801	476	23.0
2145	0.613	0.0885	472	25.6
2605	0.610	0.0952	468	27.2
2990	0.613	0.101	465	28.8
3435	0.609	0.109	461	30.6
3770	0.585	0.115	458	30.8
4010	0.577	0.120	456	31.6
4120	0.574	0.124	455	32.4

Table 44

## THERMAL CONDUCTIVITY OF Cb-15W-5Mo-1Zr-0.05C ALLOY

Temperature °F	Thermal Diffusivity ft <sup>2</sup> /hr	Specific Heat Btu/lb-°F	Density lb/ft <sup>3</sup>	Thermal Conductivity Btu/hr-ft-°F
270				30.1
444				31.7
815				32.6
1187				34.1
1550				35.8
1975	0.898	0.0709	584	37.2
2270	0.892	0.0743	582	38.6
2750	0.840	0.0825	577	40.0
3220	0.787	0.0918	573	41.4
3650	0.740	0.102	568	42.9
4010	0.715	0.110	557	43.8
4360	0.672	0.119	560	44.8

Table 45

THERMAL CONDUCTIVITY OF Cb-27Ta-12W-0.5Zr ALLOY

Temperature °F	Thermal Diffusivity ft <sup>2</sup> /hr	Specific Heat Btu/lb-°F	Density lb/ft <sup>3</sup>	Thermal Conductivity Btu/hr-ft-°F
235				26.5
495				27.0
820				28.1
1105				29.0
1420				29.9
1715	0.779	0.0621	655	31.7
2023	0.771	0.0651	651	32.7
2322	0.760	0.0678	648	33.4
2745	0.743	0.0717	644	34.3
3190	0.751	0.0760	638	36.4
3550	0.724	0.0792	635	36.4
3860	0.737	0.0819	631	38.1
4205	0.732	0.0847	624	39.0

Table 46

THERMAL CONDUCTIVITY OF Mo-0.5Ti-0.08Zr ALLOY

Temperature °F	Thermal Diffusivity ft <sup>2</sup> /hr	Specific Heat Btu/lb-°F	Density lb/ft <sup>3</sup>	Thermal Conductivity Btu/hr-ft-°F
160				73.5
310				72.0
600				70.0
945				67.5
1295				64.2
1520	1.44	0.0698	613	61.6
1915	1.28	0.0739	611	58.0
2230	1.17	0.0761	608	54.0
2605	1.05	0.0805	605	51.0
3065	0.896	0.0875	601	47.1
3570	0.748	0.0968	595	43.1
4180	0.606	0.110	588	39.2

Table 47

THERMAL CONDUCTIVITY OF Mo-29.83W-0.07Zr-0.012C ALLOY

Temperature °F	Thermal Diffusivity ft <sup>2</sup> /hr	Specific Heat Btu/lb-°F	Density lb/ft <sup>3</sup>	Thermal Conductivity Btu/hr-ft-°F
185				71.2
355				69.0
715				63.2
1050				57.4
1275				53.1
1540	1.27	0.0608	612	47.4
2018	1.09	0.0675	609	44.8
2445	0.905	0.0741	607	40.7
2658	0.708	0.0776	604	33.2
3170	0.551	0.0868	600	28.7
3665	0.454	0.0972	597	26.1
4075	0.365	0.109	588	23.4
4530	0.331	0.116	586	22.5

Table 48

THERMAL CONDUCTIVITY OF 90% TANTALUM-  
10% TUNGSTEN ALLOY

Temperature °F	Thermal Diffusivity ft <sup>2</sup> /hr	Specific Heat Btu/lb-°F	Density lb/ft <sup>3</sup>	Thermal Conductivity Btu/hr-ft-°F
324				31.0
559				33.0
1031				34.0
1428				34.9
1560	0.881	0.0406	1018	36.4
1905	0.851	0.0431	1014	37.2
2435	0.903	0.0462	1004	39.1
2870	0.832	0.0487	1000	40.5
3135	0.824	0.0501	998	41.2
3480	0.827	0.0518	992	42.5
3805	0.835	0.0533	988	44.0
4110	0.837	0.0548	983	45.1
4360	0.823	0.0568	973	45.5
4670	0.827	0.0573	975	46.2

Table 49

THERMAL CONDUCTIVITY OF Ta-8W-2Hf ALLOY

Temperature °F	Thermal Diffusivity ft <sup>2</sup> /hr	Specific Heat Btu/lb-°F	Density lb/ft <sup>3</sup>	Thermal Conductivity Btu/hr-ft-°F
190				25.0
450				27.1
730				29.0
1020				31.3
1250				32.9
1470				34.5
1650	1.02	0.0320	1039	34.0
1964	1.08	0.0340	1034	37.8
2385	1.09	0.0375	1032	42.3
2940	1.04	0.0420	1021	44.6
3255	1.06	0.0446	1016	48.1
3615	0.990	0.0475	1010	50.1
3910	1.02	0.0502	1007	51.4
4235	1.01	0.0530	1000	53.9
4585	0.980	0.0554	998	54.2

Table 50

## THERMAL CONDUCTIVITY OF Ta-30Cb-7.5V ALLOY

Temperature ° F	Thermal Diffusivity ft <sup>2</sup> /hr	Specific Heat Btu/lb-° F	Density lb/ft <sup>3</sup>	Thermal Conductivity Btu/hr-ft-° F
358				17.6
780				20.5
1090				22.6
1395				24.0
1783	0.539	0.0711	704	27.0
2255	0.516	0.0795	700	28.7
2730	0.529	0.0856	696	31.5
3065	0.539	0.0882	692	32.9
3390	0.542	0.0903	688	33.7
3775	0.548	0.0924	683	34.6
4060	0.553	0.0931	678	34.9

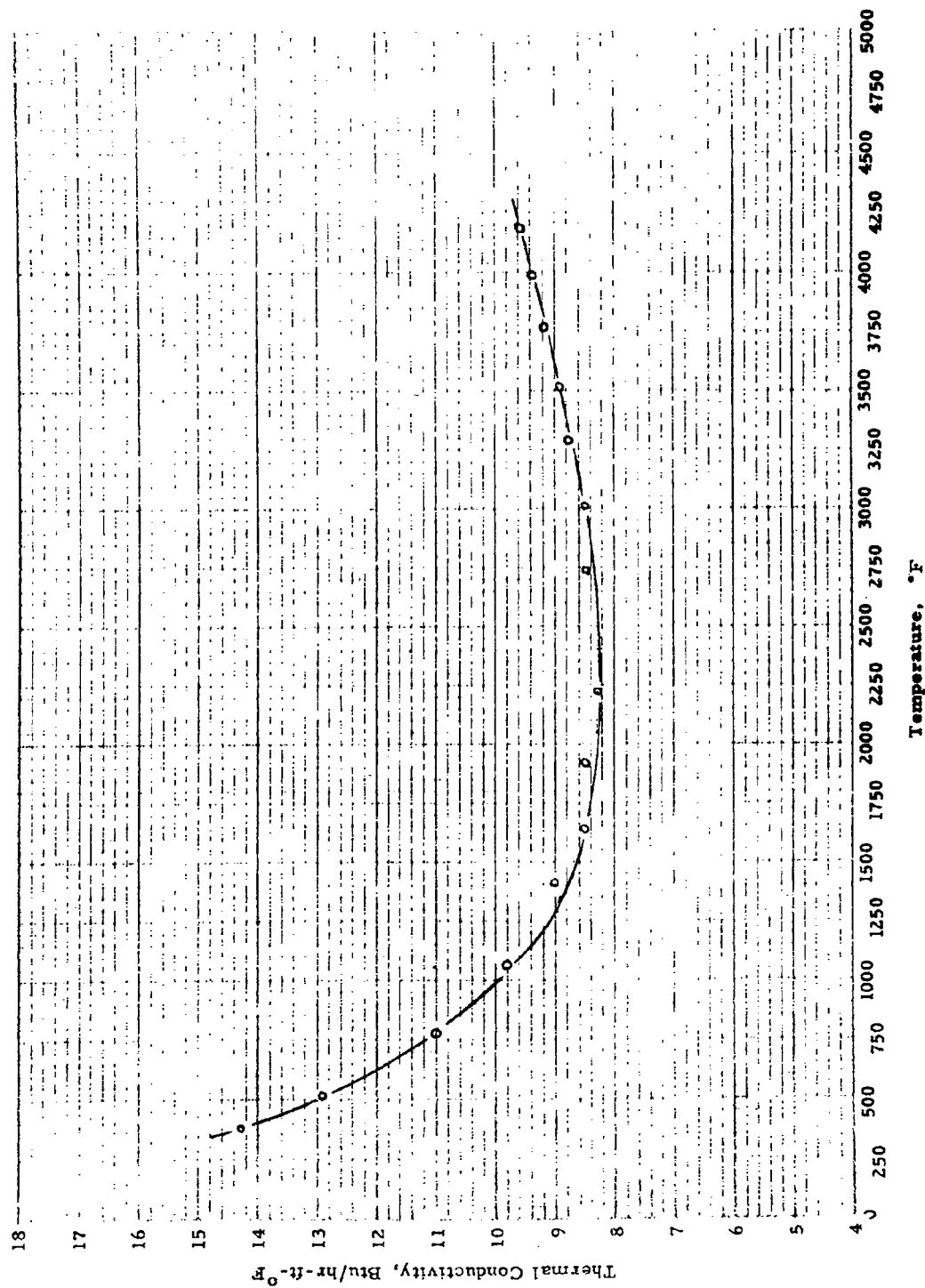


Fig. 46 THERMAL CONDUCTIVITY OF BORON CARBIDE.

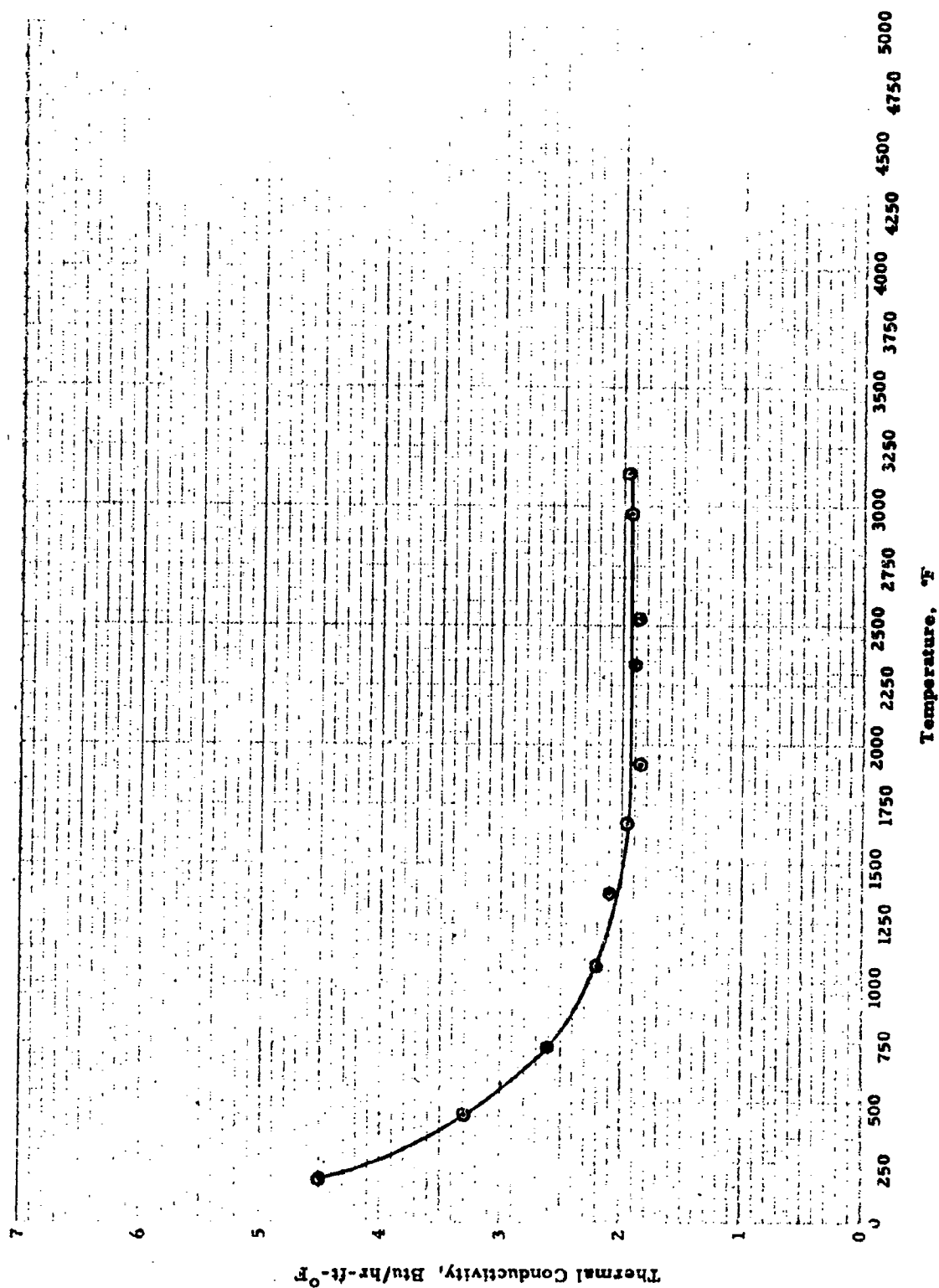


Fig. 47 THERMAL CONDUCTIVITY OF SPINEL ( $MgO-Al_2O_3$ )

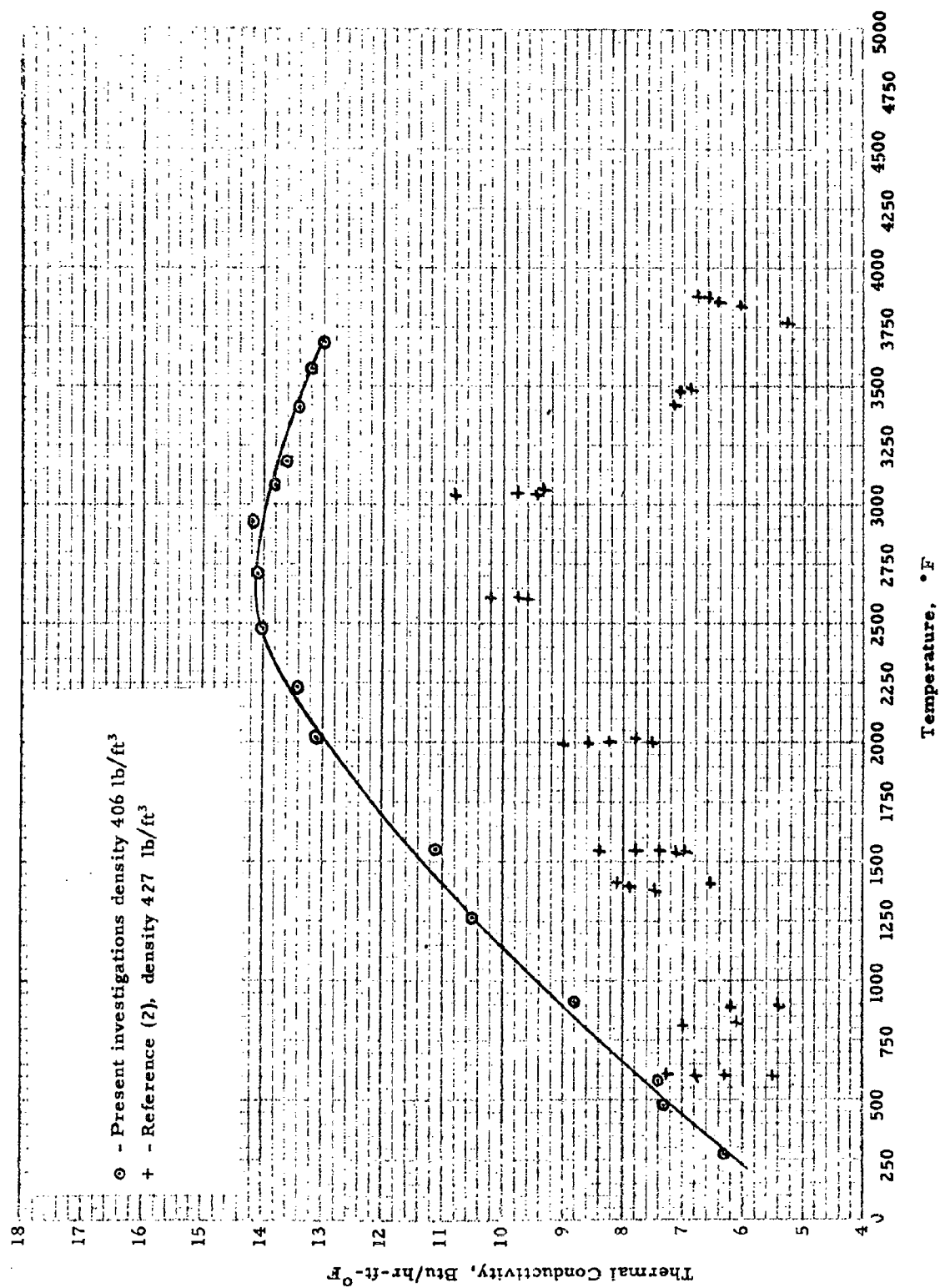


Fig. 48 THERMAL CONDUCTIVITY OF ZIRCONIUM NITRIDE

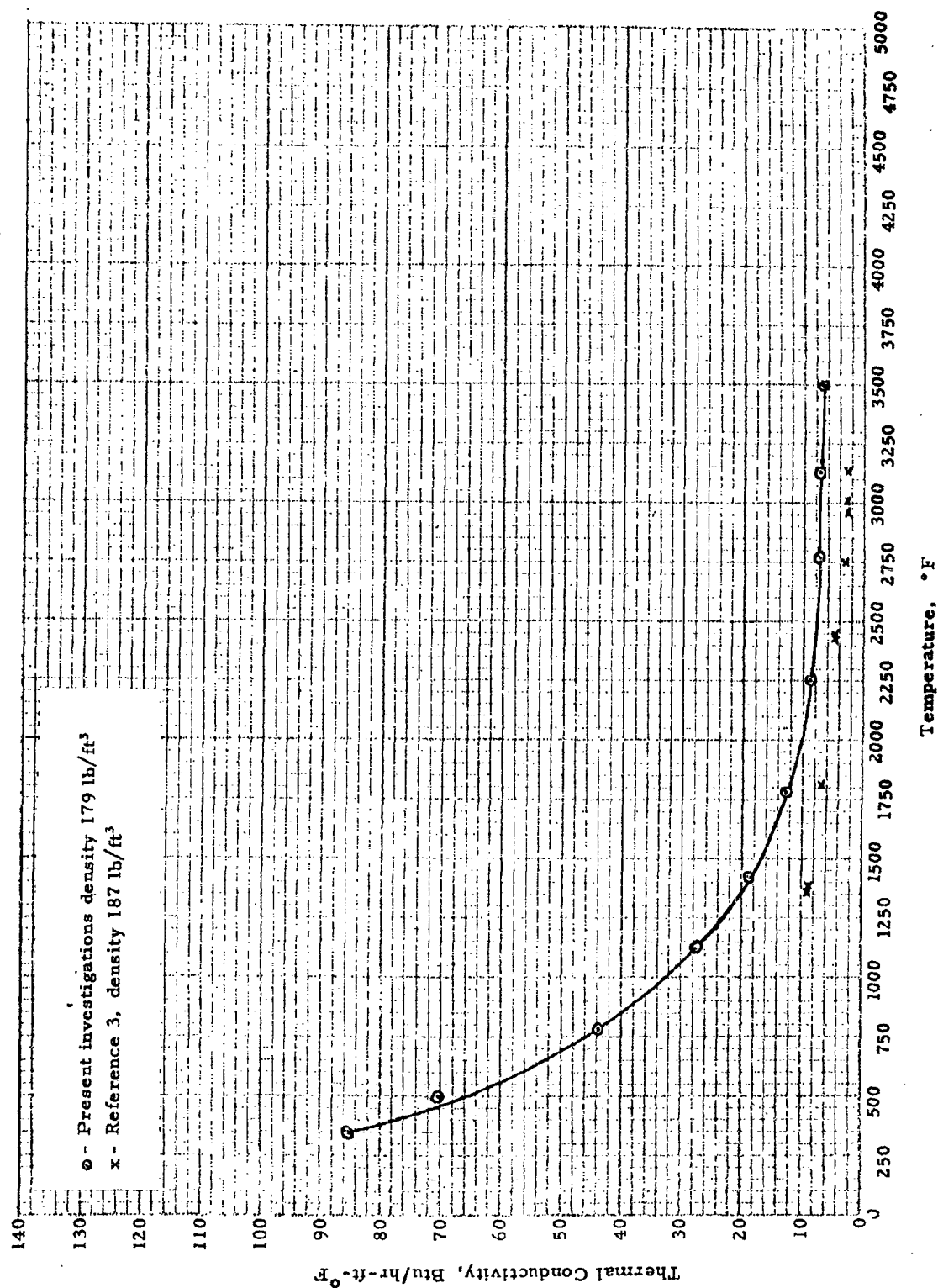


Fig. 49 THERMAL CONDUCTIVITY OF BERYLLIUM OXIDE

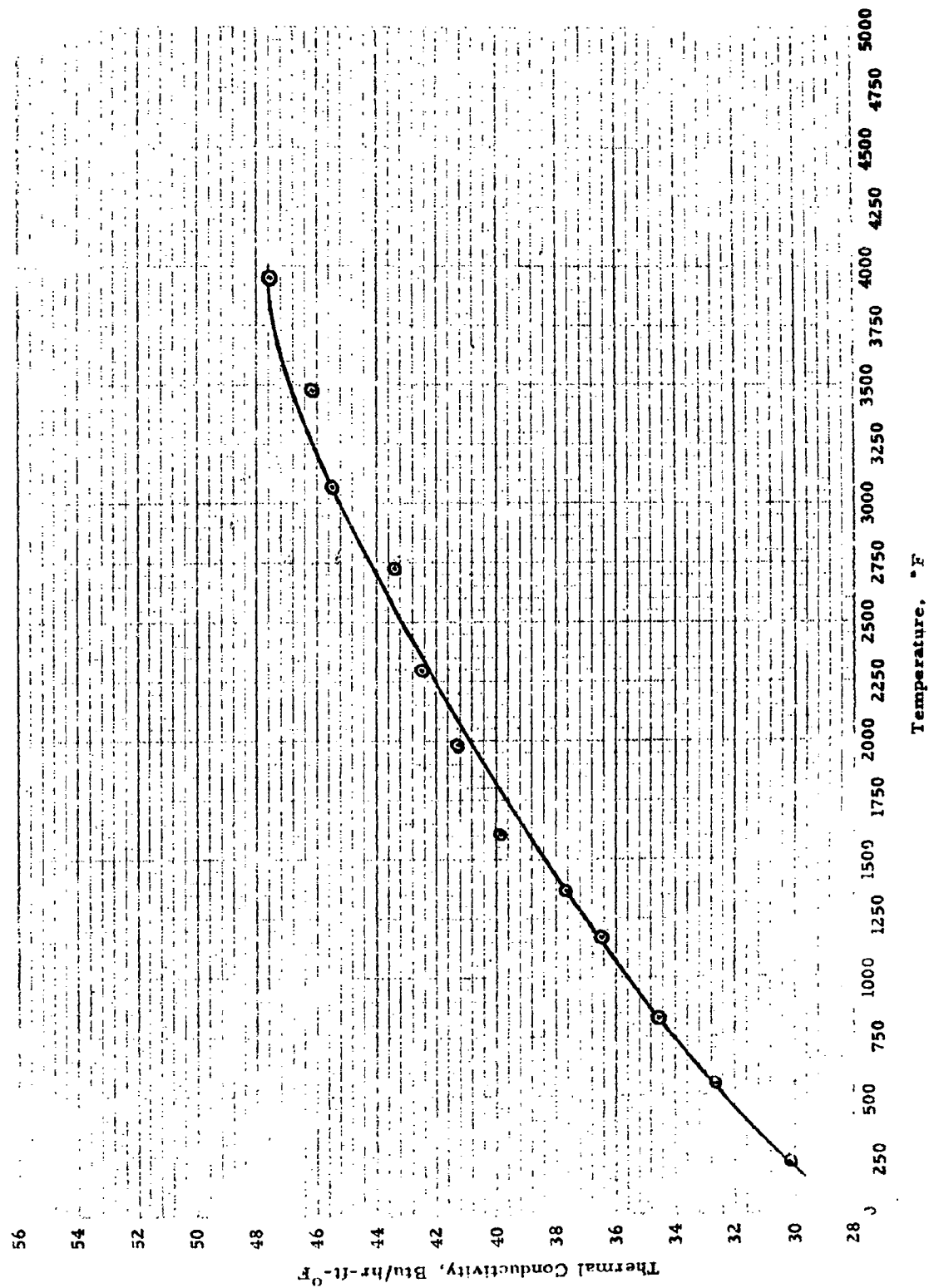


Fig. 50 THERMAL CONDUCTIVITY OF Cb-10W-1Zr-0.1C ALLOY

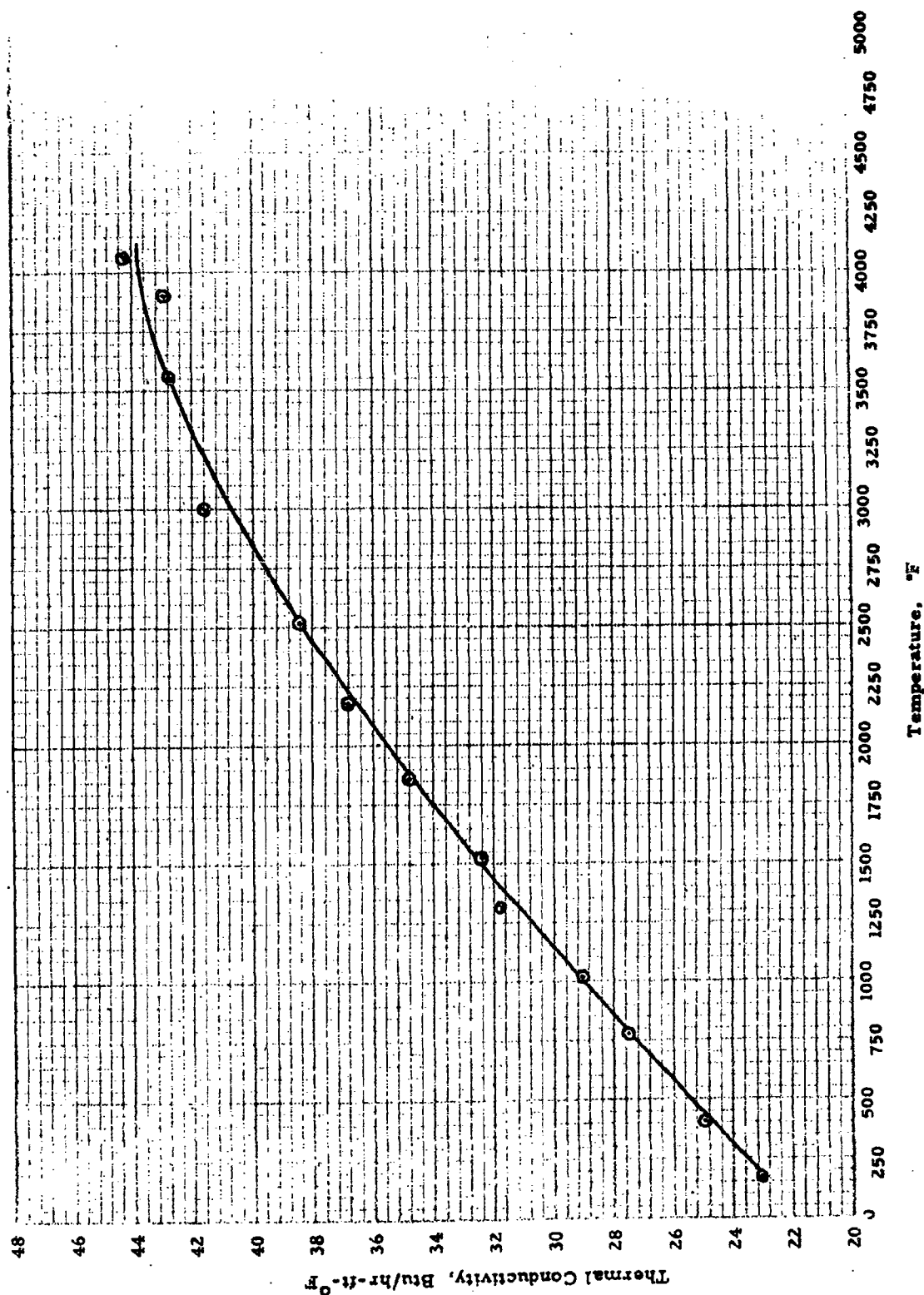


Fig. 51 THERMAL CONDUCTIVITY OF Cb-5Mo-5V-1Zr ALLOY

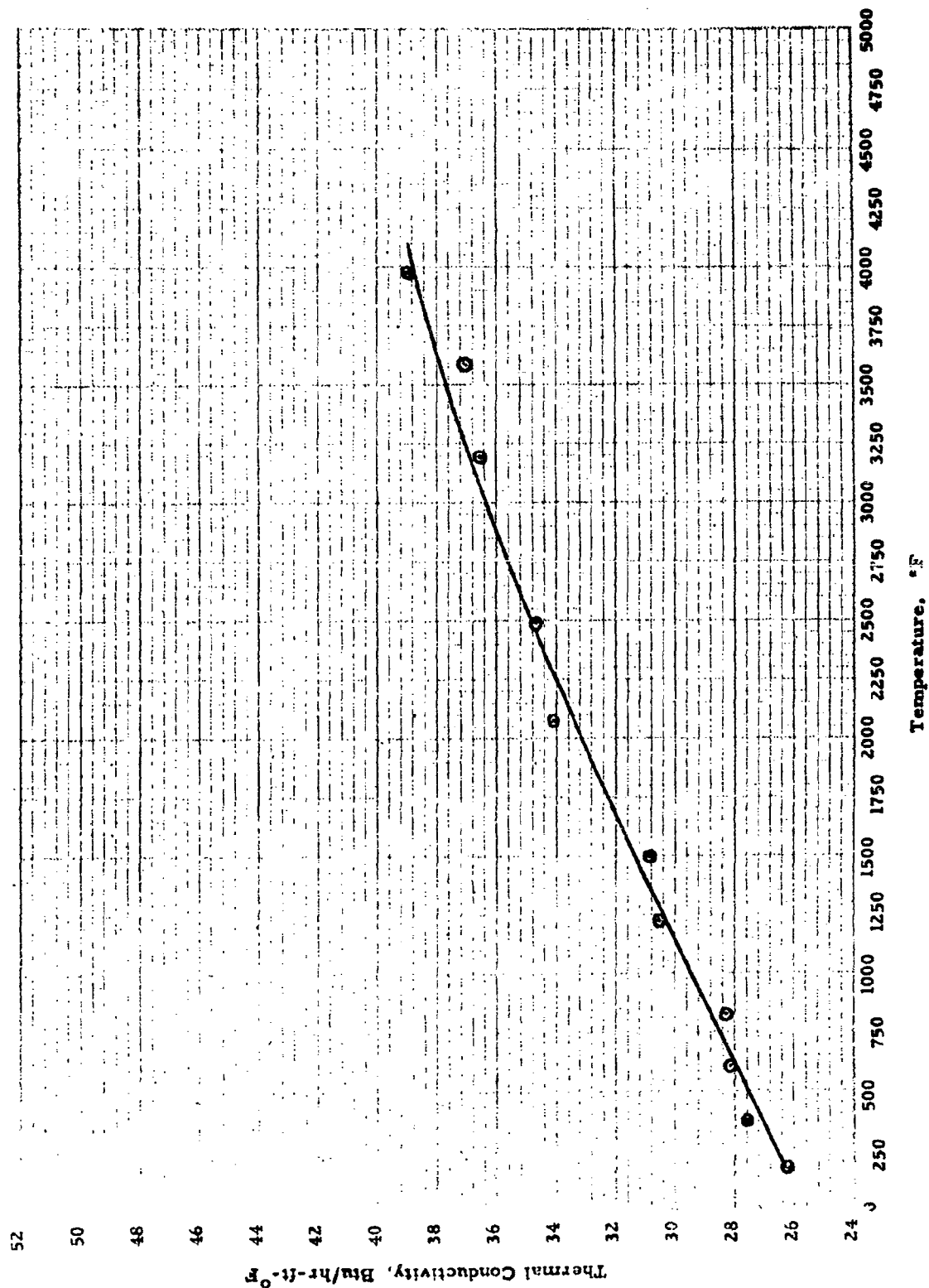


Fig. 52 THERMAL CONDUCTIVITY OF Cb-10W-5Zr ALLOY

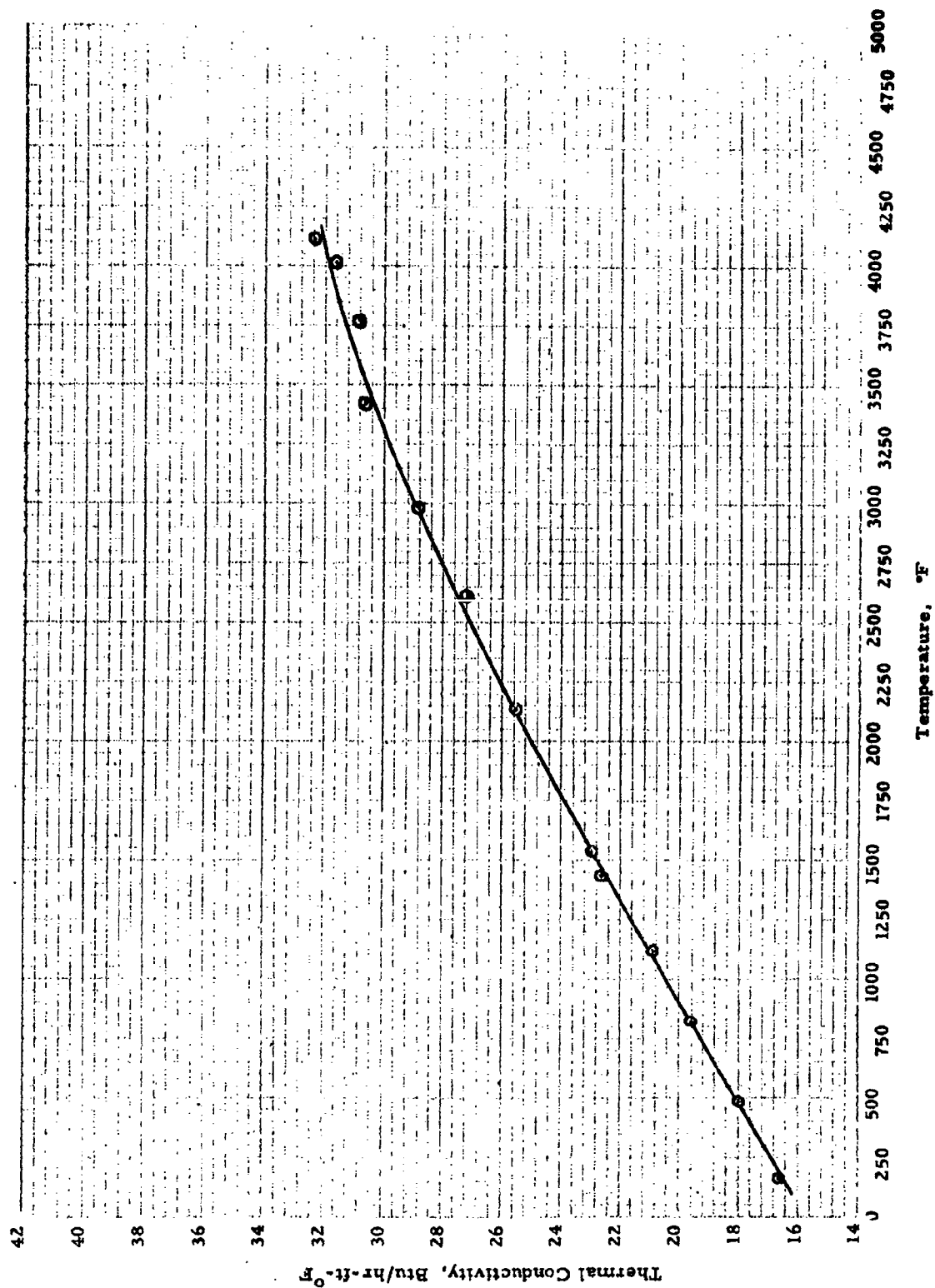


Fig. 53 THERMAL CONDUCTIVITY OF Cb-10Ti-5Zr ALLOY

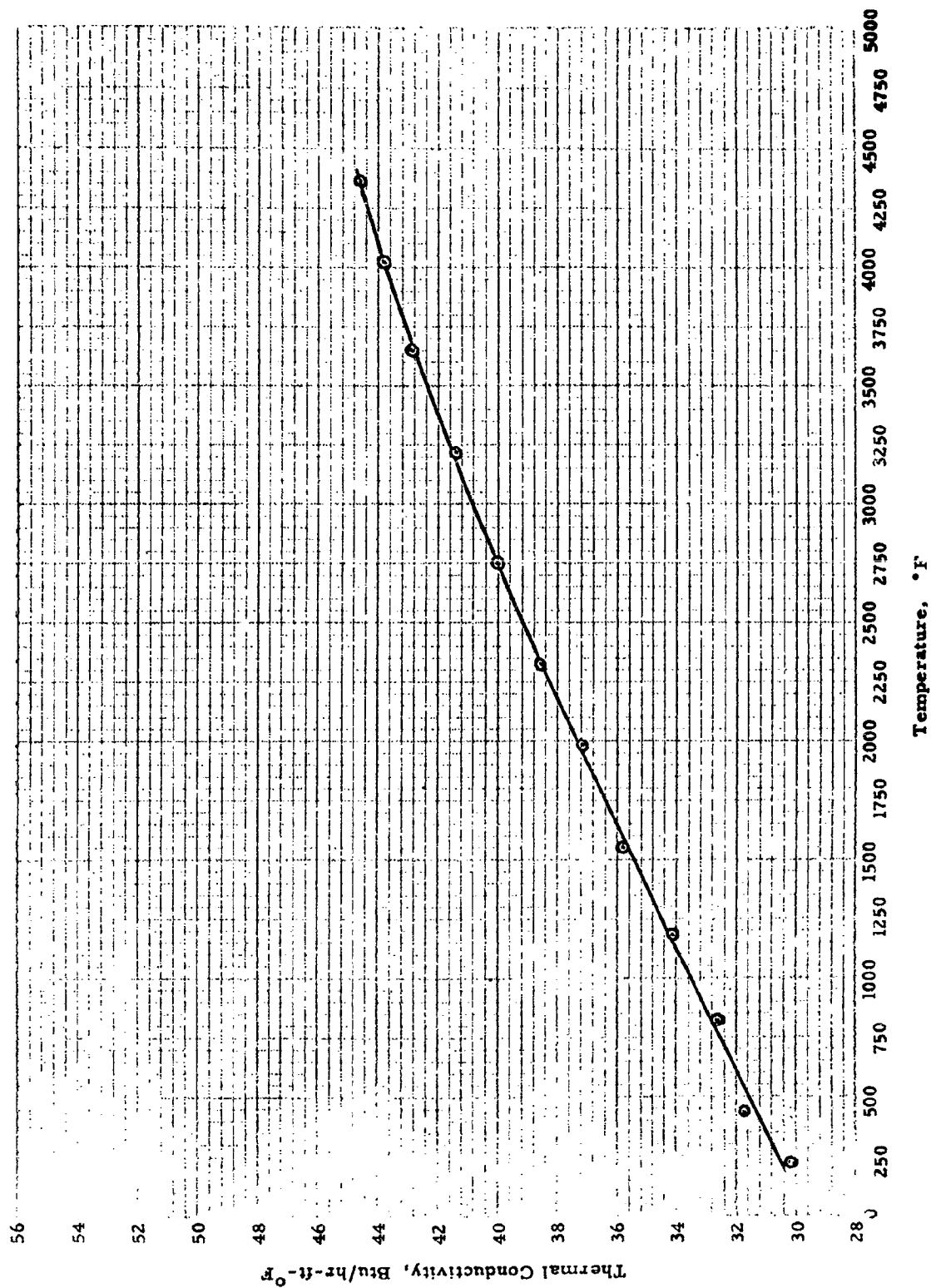


Fig. 54 THERMAL CONDUCTIVITY OF Cb-15W-5Mo-1Zr-0.05C ALLOY

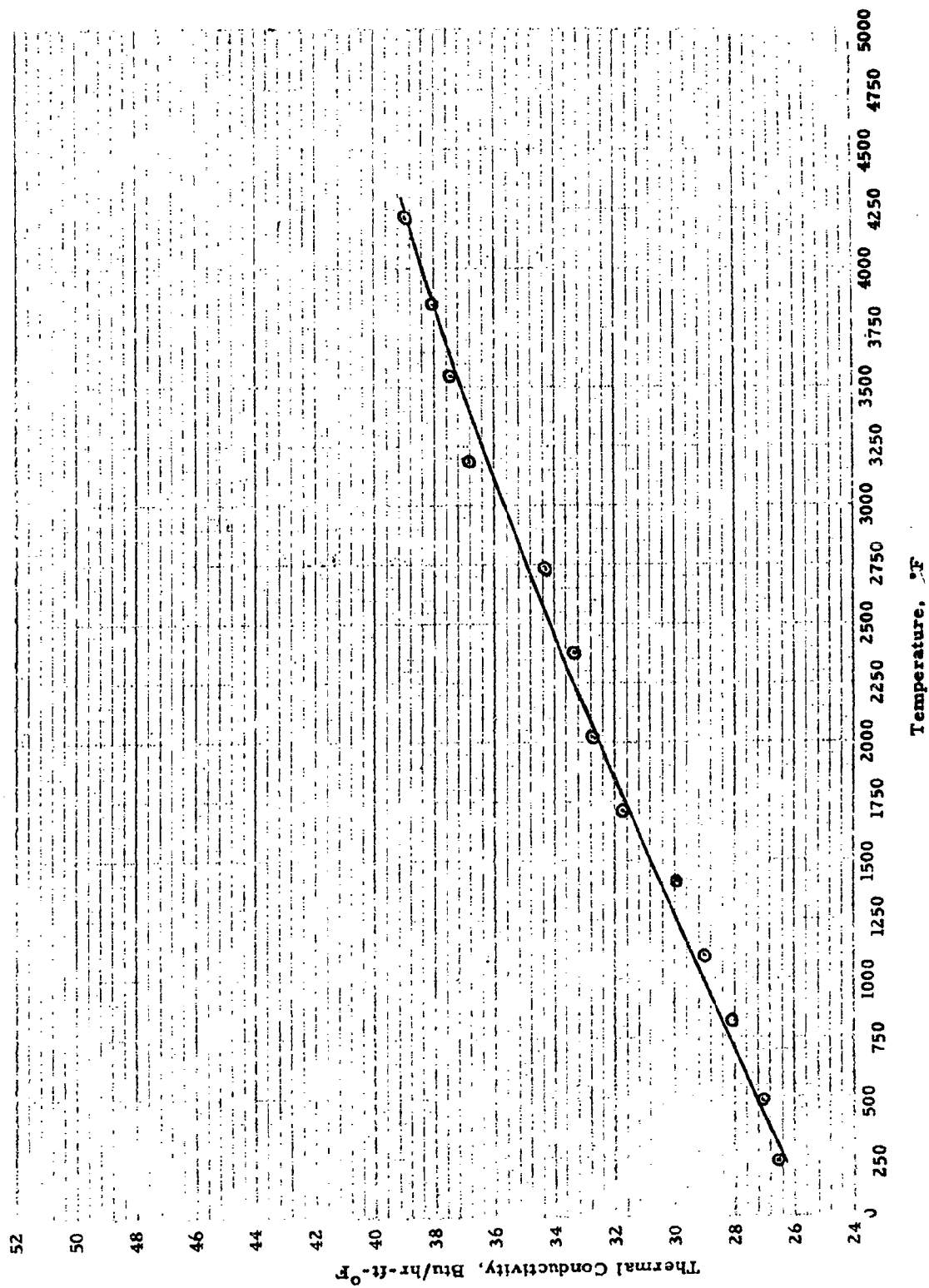


Fig. 55 THERMAL CONDUCTIVITY OF Cb-27Ta-12W-0.5Zr ALLOY

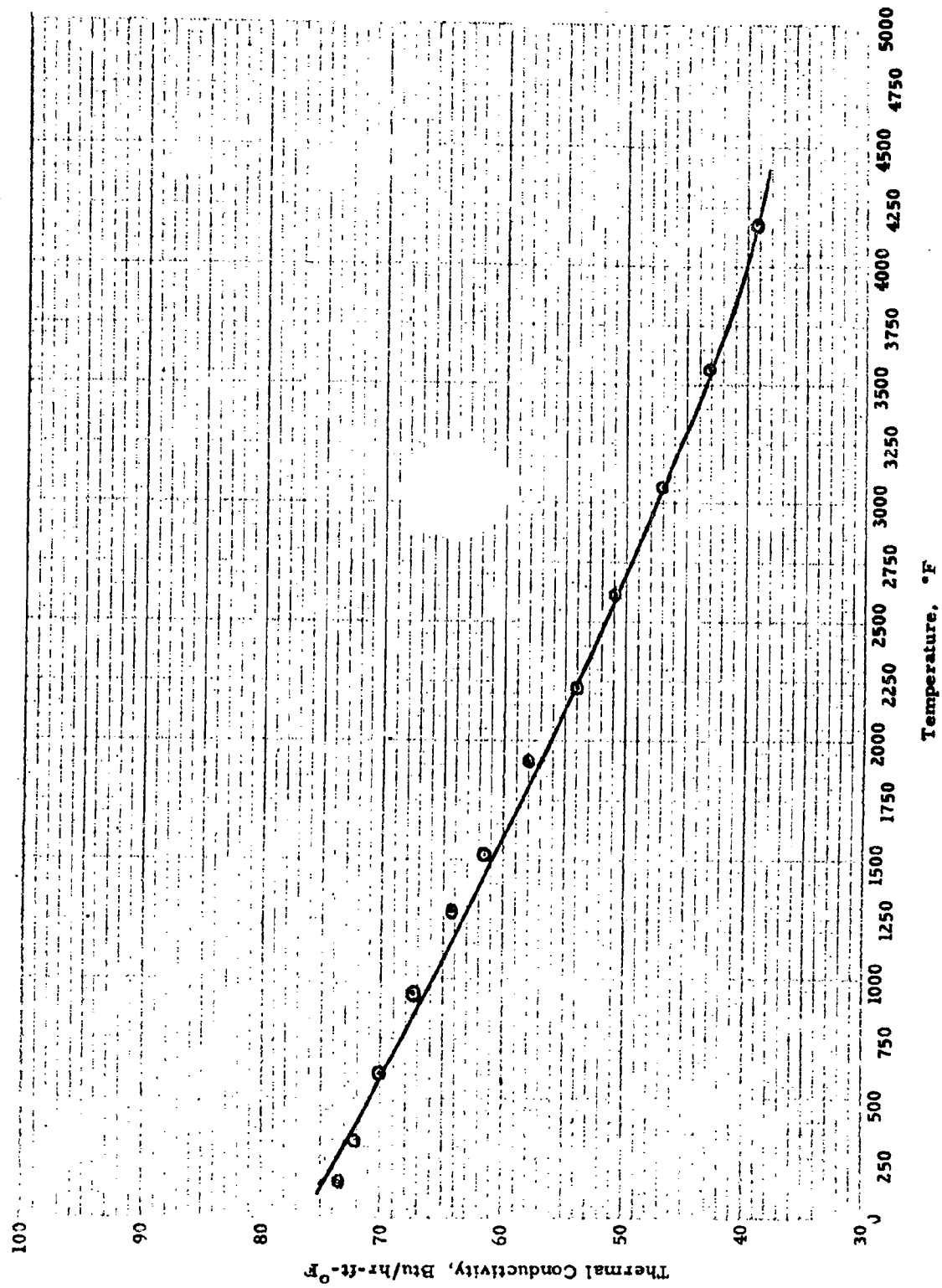


Fig. 56 THERMAL CONDUCTIVITY OF Mo-0.5Ti-0.08Zr ALLOY

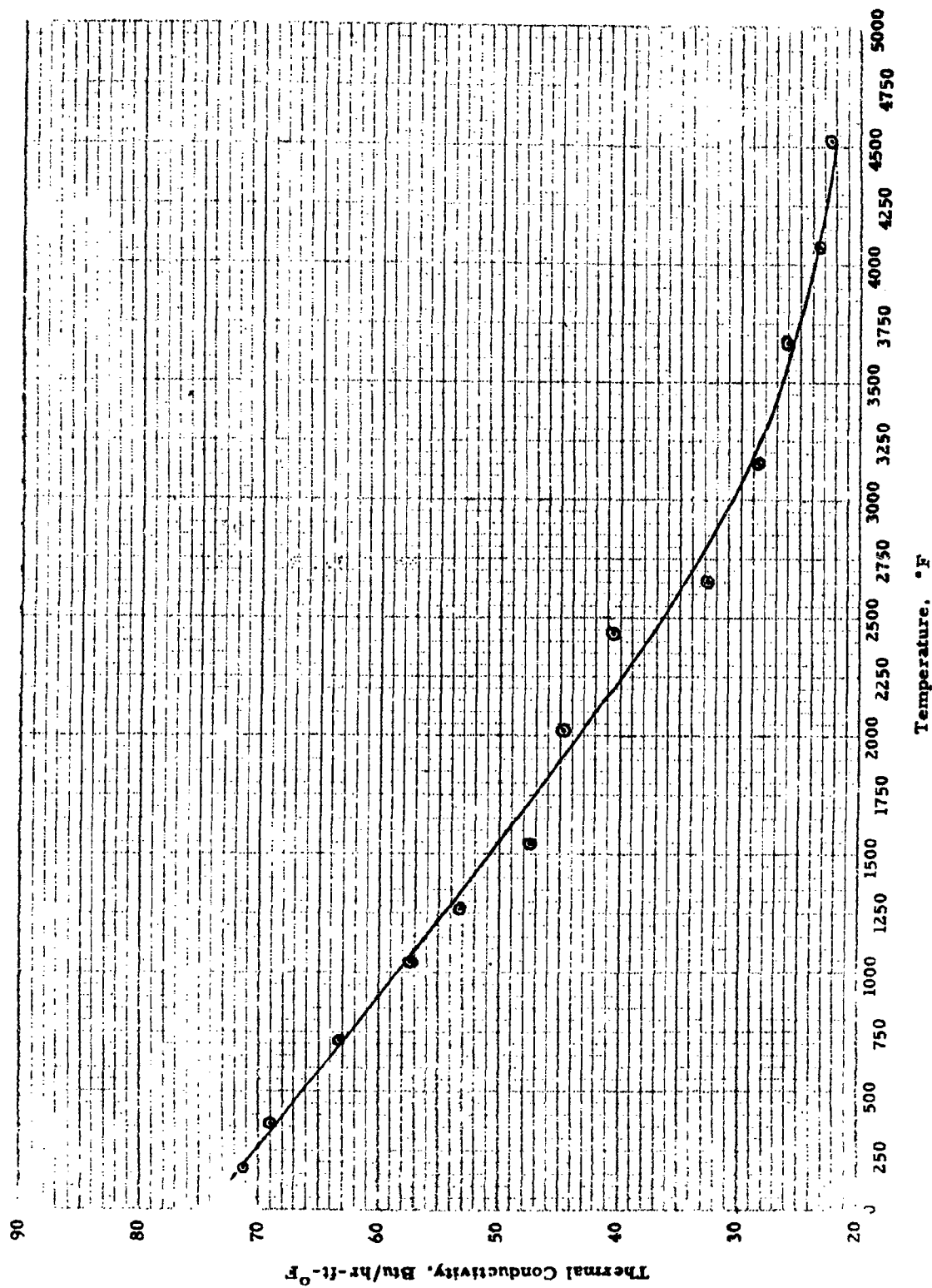


Fig. 57 THERMAL CONDUCTIVITY OF Mo-29.83W-0.07Zr-0.012C ALLOY

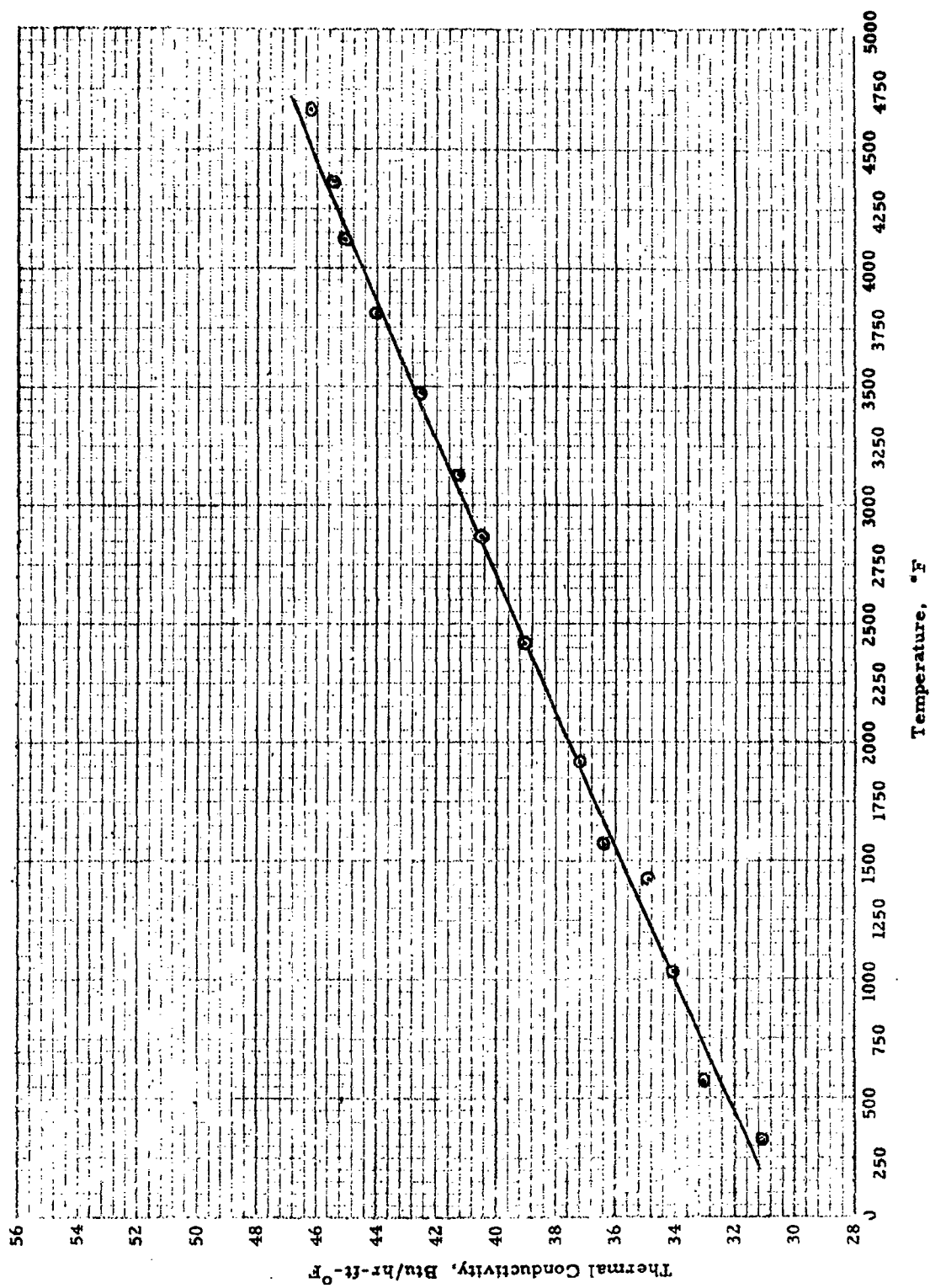


Fig. 58 THERMAL CONDUCTIVITY OF 90% TANTALUM-10% TUNGSTEN

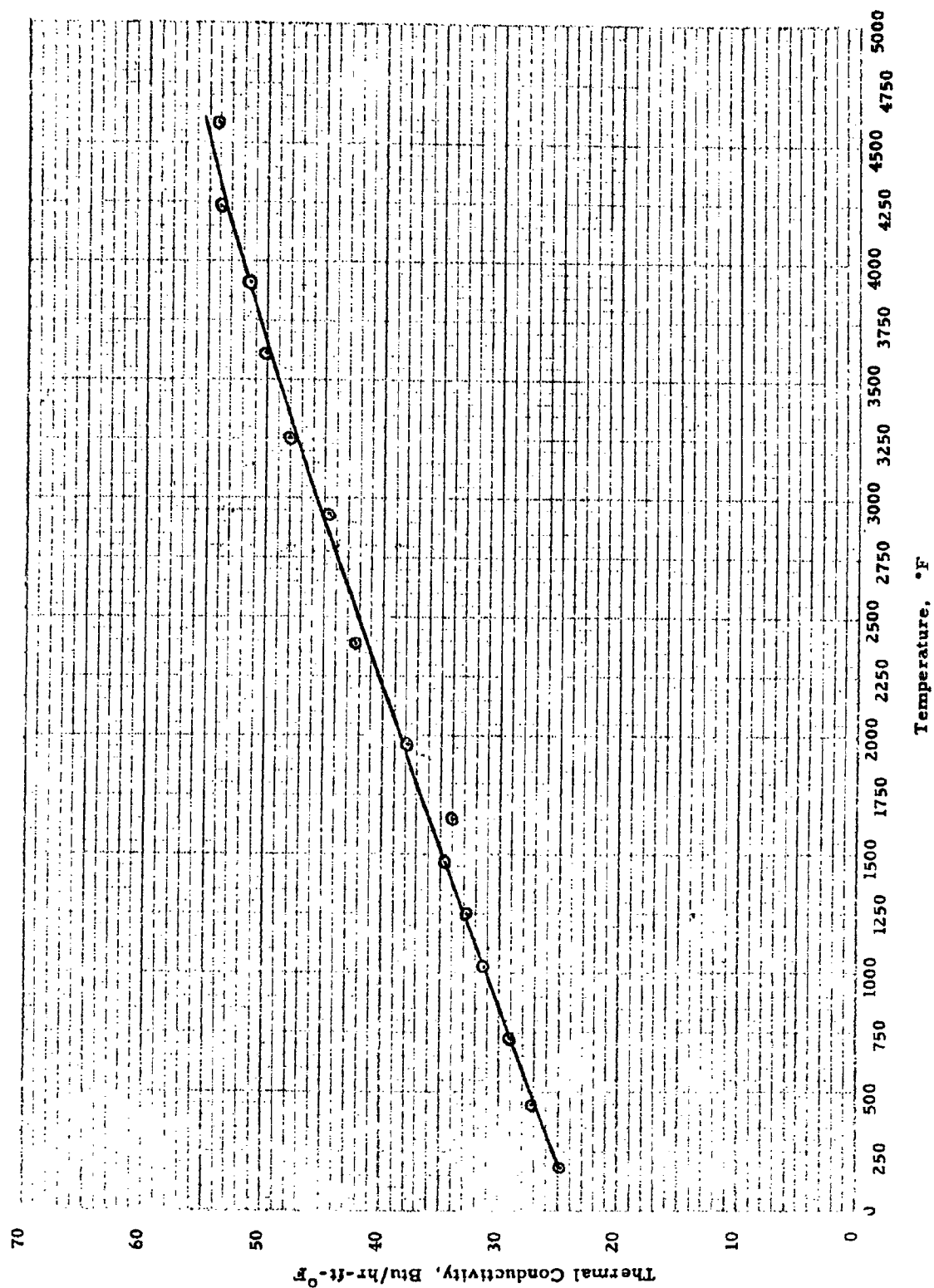


Fig. 59 THERMAL CONDUCTIVITY OF Ta-8W-2Hf ALLOY

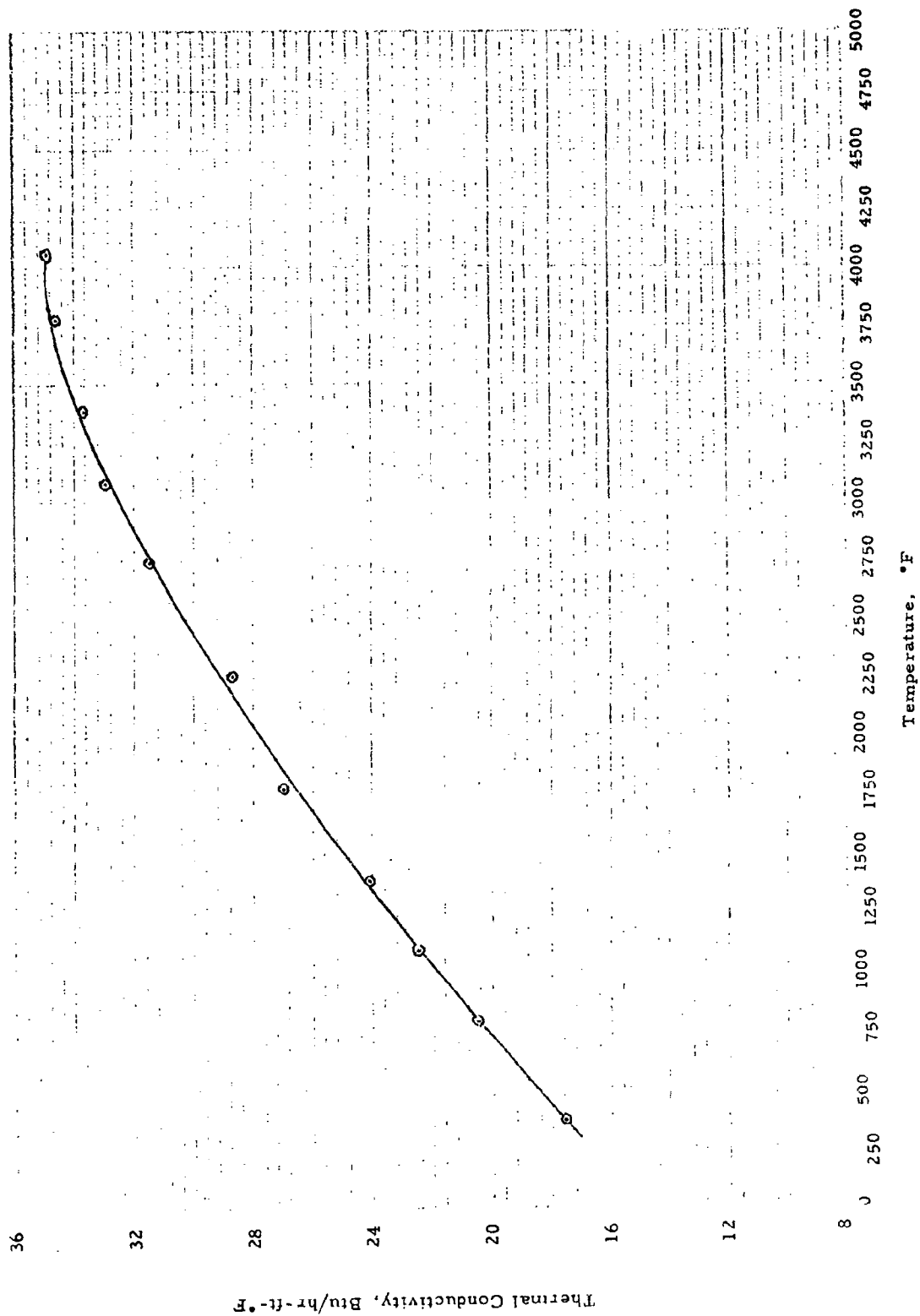


Fig. 60 THERMAL CONDUCTIVITY OF Ta-30Cb-7.5V ALLOY

## REFERENCES

1. Lowrie, R., "Research on Physical and Chemical Principles Affecting High Temperature Materials for Rocket Nozzles", Quarterly Progress Report, Contract No. DA-30-069-ORD-2787 under the Auspices of Advanced Research Projects Agency and U. S. Army Ordnance Missile Command prepared by Union Carbide Research Institute, Tarrytown, New York, June 30, 1962.
2. Neels, D. S., Pears, C. D., and Oglesby, S., "The Thermal Properties of Thirteen Solid Materials to 5000° F or Their Destruction Temperatures", Aeronautical Systems Division Technical Documentary Report No. WADD 60-924, Contract No. AF33(616)-6312 prepared by Southern Research Institute, Birmingham, Alabama, February, 1962.
3. Pears, C. D., Oglesby, S. and Others, "The Thermal Properties of Twenty-Six Solid Materials to 5000° F or Their Destruction Temperatures", Aeronautical Systems Division Technical Documentary Report No. ASD-TDR-62-765, Contract No. AF33(616)-7319 prepared by Southern Research Institute, Birmingham, Alabama, August, 1962.
4. Engberg, C. and Zehms, E., "Thermal Expansion of  $\text{Al}_2\text{O}_3$ ,  $\text{BeO}$ ,  $\text{MgO}$ ,  $\text{B}_4\text{C}$ ,  $\text{SiC}$ , and  $\text{TiC}$  Above 1000° C", J. Am. Ceram. Soc., 42 (6) pp. 300-305, 1959.
5. Taylor, R., "Thermal Conductivity and Expansion of Beryllia at High Temperatures", J. Am. Ceram. Soc., 45 (2) pp. 74-78, 1962.
6. Ginnings, D. C., Jour. of Res., NBS 38, Research Paper 1797, 1947.

<p>Aeronautical Systems Division AF Materials Laboratory, Wright-Patterson AFB, Ohio</p> <p>Rpt Nr ASD-TDR-63-597 THERMAL PRO- PERTIES OF REFRACTORY ALLOYS. Tech- nical Documentary Report, Jan 63, 128pp incl illus. and tables.</p> <p>Unclassified Report</p> <p>The objective of this program was the deter- mination of the thermal properties of fifteen selected refractory materials. The materials investigated were boron carbide, zirconium nitride, spinel, beryllium oxide, six colum- bium alloys, three tantalum alloys, and two molybdenum alloys. The thermal conductivity</p> <p>( over )</p>	<ol style="list-style-type: none"> <li>1. Refractory materials</li> <li>2. Thermophysical properties</li> <li>I. AFSC Project 7360, Task 736004</li> <li>II. Contract AF33(657)-8810</li> <li>III IIT Research Institute Chicago, Illinois</li> <li>IV. J. C. Hedge, J. I. Lang</li> <li>C. Kostenko</li> <li>V. Aval fr OTS</li> <li>VI. In ASTIA Collection</li> </ol>	<p>Aeronautical Systems Division AF Materials Laboratory, Wright-Patterson AFB, Ohio</p> <p>Rpt Nr ASD-TDR-63-597 THERMAL PRO- PERTIES OF REFRACTORY ALLOYS. Tech- nical Documentary Report, Jan 63, 128pp incl illus. and tables.</p> <p>Unclassified Report</p> <p>The objective of this program was the deter- mination of the thermal properties of fifteen selected refractory materials. The materials investigated were boron carbide, zirconium nitride, spinel, beryllium oxide, six colum- bium alloys, three tantalum alloys, and two molybdenum alloys. The thermal conductivity</p> <p>( over )</p>	<ol style="list-style-type: none"> <li>1. Refractory materials</li> <li>2. Thermophysical properties</li> <li>I. AFSC Project 7360, Task 736004</li> <li>II. Contract AF33(657)-8810</li> <li>III IIT Research Institute Chicago, Illinois</li> <li>IV. J. C. Hedge, J. I. Lang</li> <li>C. Kostenko</li> <li>V. Aval fr OTS</li> <li>VI. In ASTIA Collection</li> </ol>
<p>specific heat, and linear thermal expansion were measured from room temperature to the melting point, or 5000° F, whichever was lower.</p> <p>( over )</p>		<p>specific heat, and linear thermal expansion were measured from room temperature to the melting point, or 5000° F, whichever was lower.</p> <p>( over )</p>	

UNCLASSIFIED

UNCLASSIFIED